The Phenotypical Analysis Of *Mycobacterium Tuberculosis* Specific CD4 T Cells That Expand During Combined Antiretroviral Therapy In People With Latent Tuberculosis Infection

By

Ronnett Seldon

DVSRON003

A dissertation submitted to the University of Cape Town in fulfillment of the requirements for the degree of Master of Science (Med) in the Department of Medicine.

Faculty of Health Sciences

University of Cape Town

October 2009

DECLARATION

I, Ronnett Seldon, hereby declare that the work on which this dissertation is based is my original work (except where acknowledgements indicate otherwise) and that neither the whole work nor any part of it has been, is being, or is to be submitted for another degree in this or any other university.

I empower the university to reproduce for the purpose of research either the whole or any portion of the contents in any manner whatsoever.

Signature: ……

Date: ……

Abstract

The risk of tuberculosis infection in a healthy immuno-competent person is 10% per lifetime. This risk increases to 10% per annum in HIV infected persons due to a progressive decline in CD4 T cell numbers. In South Africa the estimated annual incidence of tuberculosis is 940 cases per 100,000 people. HIV infection is currently the greatest risk factor for developing tuberculosis in South Africa. The rate of HIV and tuberculosis co-infection in South Africa is estimated to be 53%.

Combination anti-retroviral treatment (cART), suppresses viral replication, resulting in an increase in the number of CD4 T cells as well as the restoration of antigen specific immune responses. In Cape Town, and elsewhere, the use of cART has been shown to reduce the incidence of tuberculosis in HIV infected people, by up to 80%. Since cART has no known anti-mycobacterial action, this reduction in incidence may be due to the restoration of MTB specific immune responses. cART reduces the risk of tuberculosis in HIV infected people. Therefore a novel approach to gain insight into protection against tuberculosis is to analyse the T cells that expand in people sensitised by MTB during cART.

The objectives of this dissertation was to longitudinally analyse CD4 T cell subsets during the first year of cART, from the time of starting cART (day 0), in HIV infected, MTB sensitised adults. Peripheral blood mononuclear cells were obtained on day 0, weeks 2, 4, 12, 24, 36 and 48 of cART and were stimulated with Purified Protein Derivative (PPD), followed by flow cytometry to analyse surface markers and intracellular cytokines.

$CD4^+$ T cell numbers and proportions significantly increased during follow up and the viral load fell to undetectable levels in each patient, indicating successful immune restoration. Central memory $CD27^+CD45RA^-$ and $CD27^+CCR5^-$ $CD4^+$ cells expanded by 12 weeks ($p<0.02$) followed by naïve $CD27^+CD45RA^+$ cells at 36 weeks ($p=0.02$).

Terminally differentiated effector $CD4^+CD27^-CCR7^-$ cells decreased by 12 weeks (p=0.02), paralleled by a proportional decline of PPD specific $CD4^+IFN\text{-}\gamma^+$ cells (p=0.02). However the absolute numbers of PPD specific IFN-γ producing cells, determined by ELISpot, increased (p=0.02).

Rapid effector responses are often measured when evaluating immunity. This study shows that while cART is associated with an absolute increase in effector function, the proportional response decreased and the strongest correlate of increased cART mediated immunity was the central memory response.

Acknowledgements

Dr. Katalin Wilkinson, my supervisor, designed the study and performed the optimisation of the concentration of antigens used in the ELISpot assay. She also performed the assays for the early study time points of the first participants recruited. I joined our group in February 2005 and started doing the assays in April 2005. Dr. Wilkinson also made a significant contribution to the final data analysis.

Professor Robert Wilkinson, our Group Leader, provided laboratory space, equipment, the study reagents, and intellectual support. He also designed the concept diagram presented in **Figure 35, Chapter 4**.

Professor Willem Hanekom provided the use of the SATVI flow cytometry facility.

Dr. Graeme Meintjies, Dr. Molebogeng Rangaka, and Priscilla Mouton facilitated the recruitment and follow-up of the participants.

Thank you.

I am sincerely grateful for the support and encourgement received from my husband Wayne, my children Daniel and Rebecca, my parents Mr. and Mrs. Davies, Dr. Katalin Wilkinson, Professor Robert Wilkinson, the staff at the postgraduate office as well as my colleagues in the mycobacterial immunology group and the Division of Medical Microbiology.

Contents

Tables

Chapter 1

Chapter 2

Appendix 3

Figures

Chapter 1

Chapter 3

Chapter 4

Abbreviations

˚C	degrees Celsius
%	percent
3TC	lamivudine
ACR	α-crystallin
ACR1	Rv2031c
ACR2	Rv0251c
ALP	alkaline phosphatase
APC	allophycocyanin
APC	antigen presenting cells
B cells	B Lymphocytes
BCG	Bacillus Calmette- Guerin
BFA	Brefeldin A
BSA	bovine serum albumin
Ca	Calcium
cART	combination antiretroviral therapy
CC	β-chemokines
CCR	chemokine receptor
CD	Cluster of differentiation
CD45R	CD45 receptor
CD40L	CD40 ligand
CD62L	L- selectin
CFP-10	culture filtrate protein-10
CO_2	carbon dioxide
d4T	stavudine
DC	dendritic cells
DC-SIGN	dendritic cell-specific intercellular adhesion molecule-3-grabbing non-intergrin
DMSO	Dimethyl Sulfoxide
DOT	directly observed therapy

EFZ	efavirenz
ELISA	enzyme linked immunosorbent assay
ELISpot	ezyme-linked immunospot
ER	endoplasmic reticulum
ESAT-6	early-secretory antigenic target-6
Esx	*esat-6 gene*
FACS	fluorescence-activated cell sorting
FITC	fluorescein isothiocyanate
FL	flow cell
FSC	forward scatter
g	centrifugal force
H_2O_2	hydrogen peroxide
HI FCS	heat-inactivated foetal calf serum
HIV	human immunodeficiency virus
IFN-γ	interferon gamma
IFN-γR	IFN-γ receptor
IgG	immunoglobulin gamma
IL	interleukin
IL-2-R-α	IL-2- receptor-α
iNOS	nitric oxide synthase
IQR	inter-quartile range
LTBI	latent tuberculosis infection
LPA	lymphocyte proliferation assay
mAbs	monoclonal antibodies
Mg	magnesium
mRNA	messenger ribonucleic acid
M.bovis	*Mycobacterium bovis*
MHC	Major Histocampatibility
mls	milliliters
MTB	*Mycobacterium tuberculosis*
MDR-TB	multi-drug resistant TB

Myd 88	myeloid differentiation protein 88
NaN_3	sodium azide
NO	nitric Oxide
NF-KB	nuclear Factor KB
NK	natural killer
NKT	natural killer T cells
NVP	nevirapine
$O2^-$	superoxide anion
OH	hydroxyl radical
PAMP	pathogen-associated molecular patterns
PBMC	peripheral blood mononuclear cells
PBS	posphate-buffered saline PBS
PCR	polymerase chain reaction
PE	phycoerythrin
PerCp	peridinin chlorophyll protein
PHA	phytohaemagglutin
PMT	photomultiplier tubes
PPD	purified protein derivative
PRR	pattern-recognition receptors
RD1	*region of difference-1*
ROI	reactive oxygen intermediates
rpm	rotations per minute
SEB	staphylococcal enterotoxin B
SFC	spot forming cells
SOP	standard operating procedures
SSC	Side scatter
TB	tuberculosis
TB10.3	Rv3109c
T cells	T Lymphocytes
T_{EM}	effector memory T cells
T_{CM}	central memory T cells

TCR	T cell receptor complex
TLRs	Toll like receptors
Th	helper T cells
Th1	type 1 Helper T cells
Th2	type 2 Helper T cells
TNF	tumour necrosis factor
TST	tuberculin skin test
µg	microgram
µl	microliter
µm	micrometer
XDR-TB	Extensively drug resistant TB

Chapter 1. Introduction

1.1. Tuberculosis

1.1.1. Epidemiology

Mycobacterium tuberculosis (MTB) DNA has been amplified from the tissues of Egyptian mummies more than 5000 years old (1). Despite being an old, treatable and curable disease, the 2008 WHO-Stop TB partnership fact sheet reports 1.7 million deaths due to Tuberculosis (TB) and 9.2 million new cases of TB in 2006 (2). It is estimated that more than 2 billion people, about one-third of the worlds population, have been exposed to MTB (3).

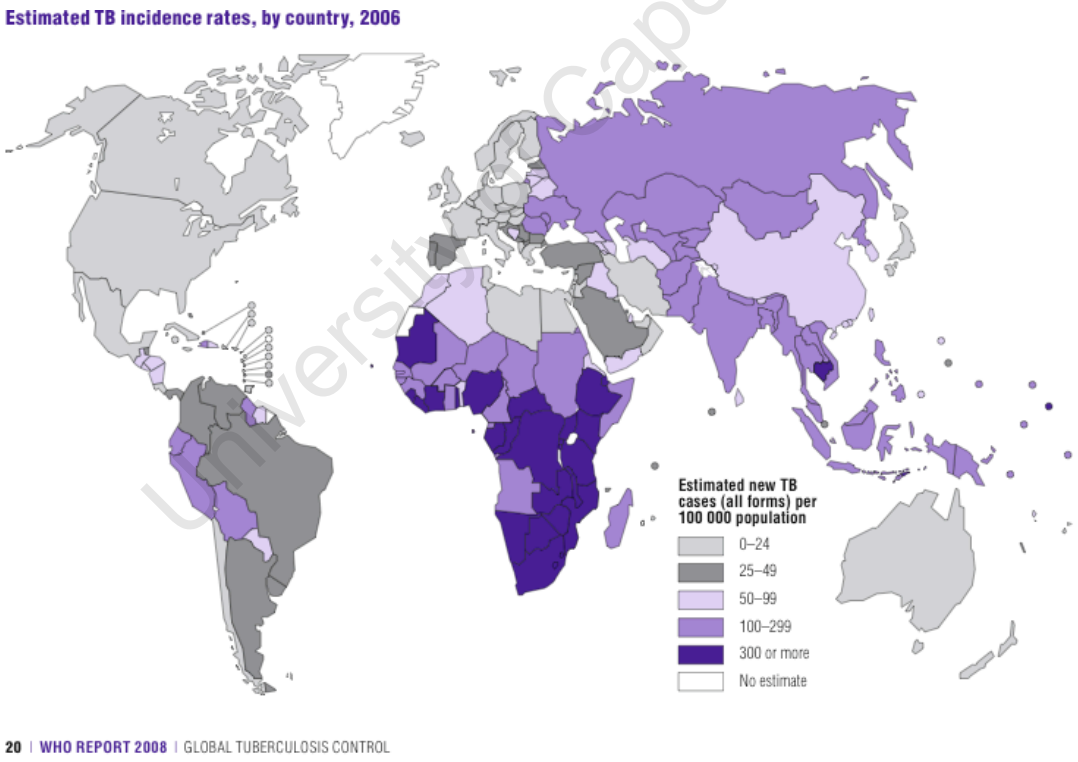

Figure 1. Global Tuberculosis Incidence (5).

A 2006 report by the Health Systems Trust indicated the national prevalence in South Africa to be 930 per 100 000 population (4).

Of the 22 countries defined as being high burden, and responsible for 80% of global TB, South Africa is ranked as number 7 globally and number 4 in Africa. Of the global cases of human immunodeficiency virus (HIV)-TB co-infection, 85% occurred in Africa in 2006. Of those, 28% occurred in South Africa (5). In South Africa the risk of developing active TB in HIV-TB co-infected people was shown to be 10.4% per annum and exceeding 30% per annum in people with WHO stage 3 and 4 disease (6). A study in a cohort of mine workers found that the risk of TB infection doubled within a year of acquiring HIV infection (7). A recent report on cause of death in South African miners showed TB to be the leading cause of death in HIV infected persons who had died of natural causes (8).

1.1.2. The organism

The bacterium, MTB, was first isolated by Robert Koch and established as the causative organism of TB humans in 1882. MTB is a rod shaped, aerobic, obligatory intracellular organism with an acid-fast cell wall. It is a slow growing organism with a doubling time of about 20 hours (1).

The composition of the MTB wax-rich cell wall includes highly cross-linked peptidoglycan and glycolipids, especially mycolic acids, the latter accounting for more than 60% of the cell wall. Polysaccharides such as glucan, mannan, arabinomannan, and arabinogalactan are attached to the lipids. The lipid content of the cell wall results in the hydrophobic nature of the bacillus which is associated with resistance to acidic and alkaline compounds, resistance to antibiotics, long term drug treatment, resistance to injury by human immune mechanisms, chronic infection and disease, impermeability to stains, acid fastness and difficulty in laboratory identification (9).

1.1.3. Pathogenesis

TB is an infectious disease acquired via the inhalation of MTB in airborne droplet nuclei. People with active pulmonary tuberculosis disease produce the airborne droplet nuclei during sneezing, talking and coughing, the latter generating about 3000 droplet nuclei.

The droplet nuclei, 1-5um in diameter, remain airborne for minutes to hours and facilitates transmission of the organism via the airborne route (10).

After inhalation into the lung, resident phagocytic cells engulf MTB, which includes alveolar macrophages, dendritic cells (DC), and neutrophils. Thus a local infection is established (11). The events that follow allows for the description of various stages of TB infection.

In the first stage, MTB avoids intracellular destruction and multiplies within the infected cells. Growth and multiplication of the bacilli causes death and disruption of the infected cells and subsequently the bacilli are spilled into the immediate vicinity. The bacilli and necrotic cellular debris initiate an inflammatory response, attracting phagocytic immune cells to the site of infection (12).

These infiltrating cells engulf the bacilli, leading to further multiplication and increase in the bacillary load. Macrophages and DC bearing MTB antigens migrate to regional lymph nodes and stimulate the generation of MTB recognising lymphocytes. Migration of these lymphocytes to the site of infection results in activation of infected, as well as, infiltrating macrophages to kill the bacilli or inhibit its intracellular growth (13).

This marks the start of the second stage, which results in the formation of a granuloma at the site of infection and the reduction of the bacillary load. A granuloma is a well-organized structure of cells characterized by a solid causeous center consisting of necrotic debris and infected cells (14).

Giant multinucleated cells typically surround this center as well as a layer consisting of lymphocytes, fibroblasts, and blood-monocyte derived macrophages. Live bacilli in the centre are deprived of oxygen and nutrients and enter into an altered state of metabolism in which they remain viable but may not be replicating. The granuloma thus restricts the infection as well as its spread and dissemination (15).

Within the first one to three years of infection, about 5% of infected people experience impaired granuloma formation and the solid caseous centre begin to soften and liquefy resulting in a rich environment suitable for the extracellular growth and replication of MTB. The infection spreads via the intrapulmonary lymphatic channels and enlarged lymph nodes can rupture into the adjacent airways causing tuberculous bronchopneumonia (16).

This is referred to as an Acute Primary infection and symptoms include chronic fatigue, progressive weight loss, and the production of a chronic and contagious cough. In the lung, extensive tissue damage occurs as a result of the host's inflammatory response. The infection can range from self-limiting tuberculosis pleuritis to more severe hematogenous dissemination of the infection throughout the body known as miliary TB (17).

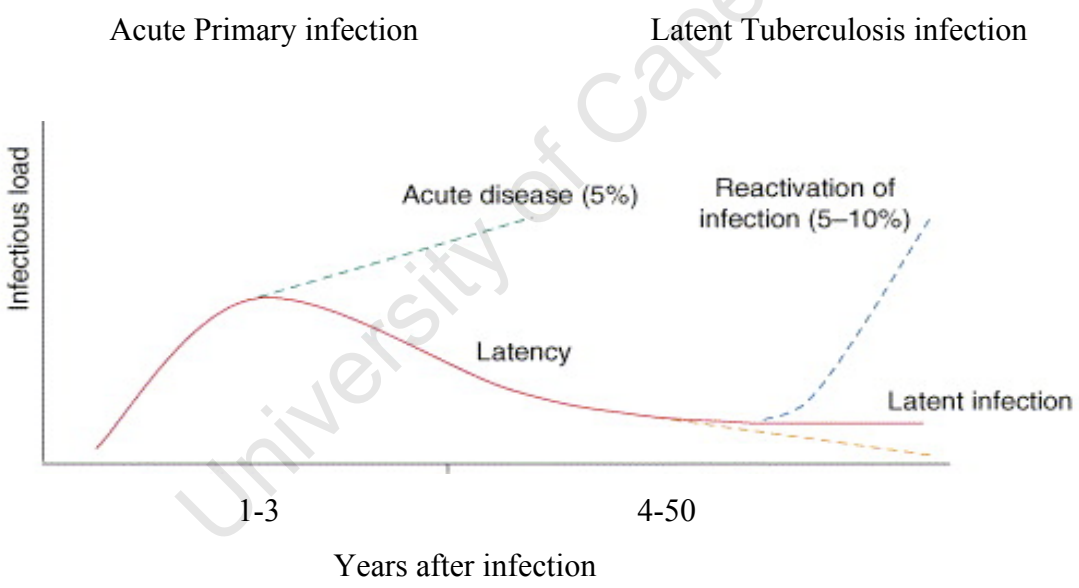

Figure 2. Stages of tuberculosis infection, adapted from PeterAnderson (18).

Active disease develops in about 10% of infected people (19). The rest will contain the infection, developing a latent form of the disease, Latent Tuberculosis Infection (LTBI). LTBI is defined as the existence of an immune response to the bacilli without the signs and symptoms of active tuberculosis disease. This state of infection can be maintained for the rest of the infected persons life (20).

In about 5-10% of latently infected people, a third stage of TB infection occurs when the host's immune status changes, leading to the loss of granuloma maintenance, reactivation, growth and dissemination of the bacilli and the development of active disease. This is referred to as secondary acute infection and can occur due to immunosuppressive therapy, old age, malnutrition, and HIV infection (21).

The risk of developing reactivation tuberculosis in the immunocompetent host is about 10% per lifetime as compared to an approximate 10% per annum risk in HIV co-infected people (22)(23).

1.1.4. Treatment

Treatment of active TB by the administration of anti-tuberculous drugs is associated with cure rates of up to 82% (24). However, antibiotic regimes used for treatment of active TB, requires a treatment length of at least six months. The necessity for long-term treatment has contributed to poor treatment adherence, which may be compounded by other factors such as re-treatment, poor medical supervision, irregular supply of drugs and inappropriate drug dosage. All together these factors have contributed to the emergence of TB drug resistance and thereby, as a countermeasure, to the implementation of directly observed therapy (DOT), which ensures that the patient is seen to be swallowing the medication in the presence of a trained supervisor (25).

Multi-drug resistant TB (MDR-TB) is described as resistance to at least isoniazid and rifampicin, considered as two of the most powerful anti-tuberculous drugs available (26).

In 2003 the WHO estimated that globally, 50 million people may be infected with drug resistant strains of MTB. It also reported that 79% of MDR-TB was resistant to three or more drugs (27). The authors of a survey, based on 9 880 383 new and previously treated cases notified in 184 countries in 2004, showed that 4.3% (424 203) of these cases were MDR-TB. They found a positive correlation between the proportion of patients who had been previously treated (40%), and the proportion of MDR-TB among new cases (28).

Extensively drug resistant TB (XDR-TB) is described as MDR-TB plus resistance to one of the injectable drugs used in TB treatment regimes (Kanamycin, Amikacin, and Capreomycin), as well as resistance to one of the quinolones (Ofloxacin, Ciprofloxacin), used in TB treatment regimes (26). Based on this definition of XDR-TB, South Africa had reported more than 300 cases of XDR-TB by December 2006. In September 2006, a new strain of XDR-TB in Tugela Ferry, in the province of Kwazulu-Natal, South Africa was reported. In 2005, 221 of 544 people in the area had MDR-TB. Of the 221 MDR-TB cases, 53 were identified as MDR-TB plus resistance to at least three of six classes of second-line anti-tuberculous agents. All 53 cases were HIV infected. Of the 53 cases, 52 died with a median survival time of 16 days from the time of sputum collection (29).

The current statistics on TB drug resistance emphasises the need for the development of new and effective anti-tuberculous drugs that will shorten the length of treatment (30).

1.1.5. Vaccination

In 1921, Albert Calmette and Camille Guerin developed a vaccine against TB using a live attenuated strain of *Mycobacterium bovis* (M.bovis) the cause of bovine TB. The vaccine, Bacillus Calmette- Guerin (BCG) was first tested in infants in 1921 and has since been administered to about 3 billion people to date. However, the analysis of numerous clinical trials showed that the protection afforded by BCG vaccination has ranged from as much as 82% to as little as 7%. In 46-100% of cases, BCG vaccination has protected against severe forms of TB in childhood, such as TB meningitis and disseminated TB (31).

However this protective efficacy varies dramatically during adolescence and adulthood in which pulmonary TB is the more prevalent form of TB and ranges from as much as 80% protection in the United Kingdom to as little as 5% in India. Factors thought to contribute to these discordant results include route of administration, vaccine dose, vaccine strain, as well as exposure to environmental non-pathogenic Mycobacteria (32).

It is estimated that BCG vaccination has prevented only 5% of deaths due to TB. The availability of the genome sequence of MTB as well as *M.bovis*, has increased the identification of new genes and antigens which has facilitated the development of various new vaccine candidates, some of which have already entered Phase I and II clinical trials (33).

The successful development of a vaccine requires understanding of the protective immune response as well as correlates of protection. Neither the immune response to MTB nor reliable correlates of protection thereof, have been completely defined. In addition, it is not clearly understood why BCG vaccination has failed in some populations. As a result, current estimates of the time required to develop a new vaccine against TB is about 20 years. The development of vaccines effective in all populations, especially the immunocompromised, will be facilitated by further studies aimed at unraveling the complexity of the interactions that take place in the host-pathogen relationship (34).

1.2. The immune response to MTB infection

The human immune response is composed of the innate and acquired elements. The two elements are distinct but function in a synergistic manner (35).

The cells of both the compartments originate from pluripotent hematopoietic stem cells in the bone marrow from which lymphoid and myeloid progenitors arise. Lymphoid progenitors differentiate into lymphocytes of the acquired response as well as the natural killer (NK) cells of the innate response. Myeloid progenitors differentiate into the granulocytes of the innate response, i.e. neutrophils, monocytes, macrophages, DC, and mast cells (36).

The specificity of the innate cell receptors are genetically predetermined, as they are germ-line encoded, and recognise highly conserved, invariant structures that are shared by microbial pathogens.

These microbial structures are referred to as pathogen-associated molecular patterns (PAMP) and include bacterial lipopolysaccharide, peptidoglycan, mannans, and bacterial DNA. The complimentary receptors on human cells of the innate system are called pattern-recognition receptors (PRR). The effector responses of the innate system are therefore non-specific and available immediately irrespective of the number of times the same pathogen is encountered (37).

The specificity of the receptors of the acquired response is generated by somatic gene rearrangement, which produces a vast repertoire of antigen specific receptors, about $1014\text{-}1018 \times 10^6$, enabling the recognition of a wider range of antigens and increased ability to detect pathogens. After encountering and recognizing pathogenic antigen presented by antigen presenting cells (APC), naïve (antigen inexperienced) lymphocytes generate effector cells by clonal expansion and differentiation, which requires two to three weeks. This process also produces memory cells, which allows a more rapid response on subsequent re-exposure to the same antigen (38).

Immune recognition and uptake of MTB by the phagocytic cells of the innate system leads to the initiation of the inflammatory response as well as the induction and activation of the acquired response. Phagocytosis is mediated by binding of PAMP to endocytic PRR including the macrophage mannose receptor, complement receptors, scavenger receptors as well as the dendritic cell-specific intercellular adhesion molecule-3-grabbing non-intergrin (DC-SIGN) receptor, **Figure 3** (39).

In the immunocompetent host, this process takes place within hours after the inhalation of MTB, via the interaction of the innate receptors on macrophages and DC and various MTB components (12)(39).

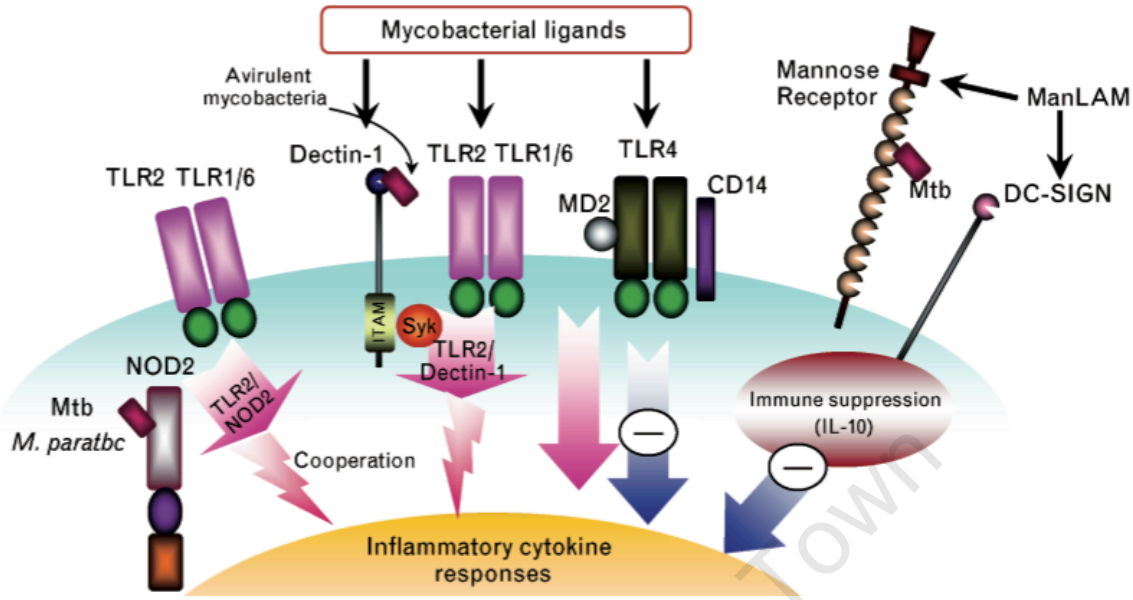

Figure 3. Recognition of MTB by the innate immune response, adapted from Eun- Kyeong Jo (39).

Phagocytosis induces innate killing mechanisms, which include phagosomal acidification and fusion with lysosomes containing microbicidal enzymes, proteins and peptides that are released into the phagosome. Nitric Oxide (NO), a toxic anti-mycobacterial product, is produced by the induction of nitric oxide synthase (iNOS) in activated macrophages. Another mechanism is the respiratory burst, which generates toxic products via the generation of superoxide anion ($O2^-$), which is further converted to hydrogen peroxide (H_2O_2). H_2O_2 is further processed into additional toxic chemicals including the hydroxyl radical (OH). Collectively these toxic products are referred to as reactive oxygen intermediates (ROI) (40).

However, MTB has evolved strategies to overcome and inhibit these macrophage effector functions and survives within the phagosomes of infected macrophages via mechanisms that block phagosome acidification as well as mechanisms that avoid oxidative killing (41).

The Toll like receptors (TLRs) are mammalian homologues of the Drosophila Toll protein, which was first identified as a component of the embryonic development of the fly and later as a key component of the immune response of the adult fly . At least 10 mammalian TLRs have been identified to date. Binding of TLRs, present on the surface of macrophages and DC, to various mycobacterial components, induces a common signaling transduction pathway. This takes place via the cytosolic adaptor protein, myeloid differentiation protein 88 (Myd 88), and leads to the activation of transcription factors for the Nuclear Factor KB (NF-KB) family, which moves into the nucleus (37).

This results in the macrophage and DC expression of cytokines, chemokines and co-stimulatory molecules required to initiate and activate components of the acquired immune response, as well as innate killing mechanisms.
Figure 4 presents a diagrammatic summary of key innate generated molecules and cytokines that contribute to the initiation and activation of acquired immune responses, following MTB phagocytosis (39)(40).

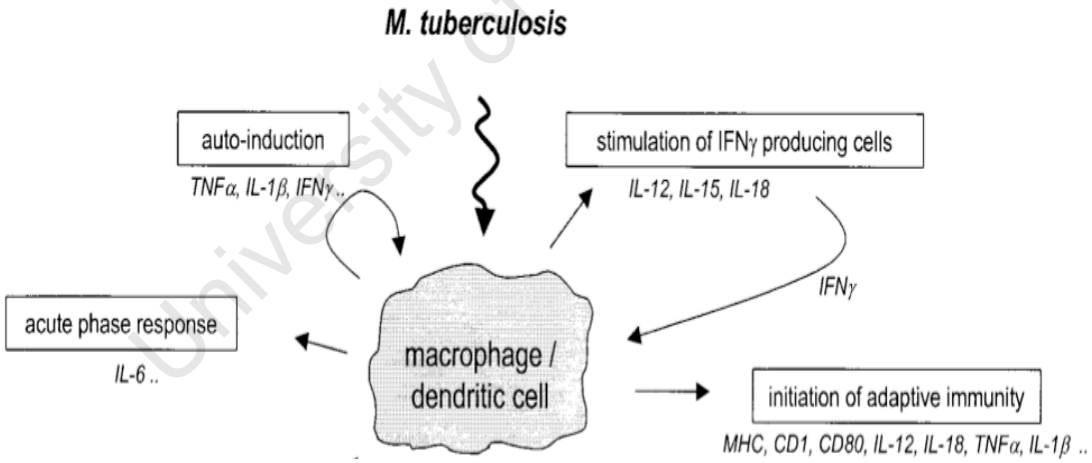

Figure 4: Immune activation following MTB/phagocyte binding, adapted from van Crevel *et al* (14).

Within the APC, degradation of phagocytosed MTB antigens into peptides, takes place via the action of proteases inside endosomes. Fusion of the endosomes with the Golgi apparatus allows the binding of the peptides to newly synthesised Major Histocampatibility (MHC) class II molecules, which are retained in the Golgi apparatus. The MHC class II-peptide complex is transported to the surface of the APC, which migrates to the regional lymph nodes to present antigen to T cells. Newly synthesised MHC class I molecules are retained within the Endoplasmic Reticulum (ER). Peptides formed from the degradation of antigens present in the cell cytoplasm are transported into the ER where they bind to MHC class I molecules, forming MHC class I-peptide complexes, which are transported to the cell surface to facilitate antigen presentation to T lymphocytes (T cells) (42).

MTB antigens confined in phagosomes are secluded from transport to the ER and classical MHC class I binding. However, recent studies have revealed that apoptosis of MTB infected APC, allows the delivery of MTB antigen to non-infected bystander APC, via apoptic vesicles, in a process referred to as cross priming. This process subsequently allows the binding of MTB peptides to MHC class I molecules, and subsequent presentation to T cells (43)(44).

In the lymph nodes, naïve T cells (antigen inexperienced) are stimulated via interaction with the MHC-peptide complex and co-stimulatory signals provided by the expression of Cluster of differentiation (CD) molecule 80 and CD86 on the APC. $CD4^+$ and $CD8^+$ T cells bind to MHC-peptide complexes via the αβ T cell Receptor Complex (TCR). Co-stimulation takes place via the binding of the CD28 molecule expressed on the T cell surface to the co-stimulatory molecules expressed on the surface of the APC. Stimulation results in proliferation by clonal expansion and differentiation into antigen specific effector cells, which migrate to the site of infection and exert effector function (38).

$CD4^+$ T cells function as helper T cells (Th) via the secretion of cytokines (45). $CD4^+$ T cells are classically differentiated into type 1 helper T cells (Th1) and type 2 helper T cells (Th2) on the basis of distinct cytokine secretion.

Th1 $CD4^+$ T cells secrete the cytokines, tumour necrosis factor (TNF), interferon gamma (IFN-γ), and interleukin (IL)- 2. IL-10 and Transforming Growth Factor β (TGFβ) are regulatory cytokines also secreted by T cells. Th2 $CD4^+$ T cells secrete IL-4, IL-5, and IL-13 (46). A novel group of IL-17 secreting, Th17 T cells have been identified recently (47).

Activated $CD4^+$ T cells express CD40 ligand (CD40L), which binds to CD40 expressed on B cells and activates antibody production (48). DC and macrophages also express CD40 (49). Binding to CD40L stimulates the secretion of TNF, IL-12, MHC molecules, as well as co-stimulatory molecules (50)(51).

$CD8^+$ T cells have a cytotoxic function, and kill infected cells via activation of enzyme-mediated apoptosis, as well as through their production of cytotoxic mediators such as granzyme, perforin, and granulysin (52).

NK cells do not express an antigen specific TCR and use non-specific receptors to identify and kill infected cells in an innate cytotoxic manner. NK cells also secrete IFN-γ and are considered to be an important source of IFN-γ in early infection (53). Natural killer T cells (NKT) bind to glycolipid antigen via CD1 antigen presentation, resulting in the secretion of IL-4 and IFN-γ (53).

Studies have revealed the involvement of various T cell subtypes and cytokines in the immune response to MTB (54). $CD4^+$ IFN-γ secreting T cells have been shown to be essential for the maintenance of a protective response to MTB in mice and humans. $CD4^+$ T cell knockout mice are unable to control MTB infection despite the presence of large volumes of IFN-γ (55). Deficiency of the IFN-γ receptor (IFN-γR) in humans is associated with an increased susceptibility to non-tuberculous mycobacterial infection (56). The role of $CD4^+$ T cells in the protective response to MTB in humans is further emphasized by the increased risk of active TB infection in HIV co-infected people (6).

IFN-γ activates killing mechanisms in infected macrophages and regulates the expression of MHC and co-stimulatory molecules, which is essential for the stimulation and activation of the acquired immune response (57). Despite the established role of IFN-γ in the protective response to MTB, studies investigating the IFN-γ response as a marker of protection found a lack of correlation, stressing the need for identification of more reliable correlates (58)(59).

TNF is involved in the induction of the inflammatory response (60). The role of TNF in the induction of MTB specific T cells and activation of innate mechanisms is best demonstrated by the reactivation of TB in people with LTBI, who had received anti-TNF (Infliximab) therapy for autoimmune disease (61).

IL-10 has been associated with suppression of macrophage function (60). The over expression of IL-10 in mice has been associated with the reactivation of chronic pulmonary TB (62). In humans, the expression of IL-10 in response to Purified Protein Derivative (PPD) re-stimulation was associated with anergy and the absence of IFN-γ secretion (63).

IL-2 induces T cell proliferation (60). A study that investigated the effect of HIV infection on the expression of IL-2 and the IL-2- receptor-α (IL-2-R-α) found that TB in HIV infected people was associated with substantially reduced serum IL2-R-α levels, compared to HIV uninfected people with TB (64).

The cytotoxic effect of $CD8^+$ T cells has been demonstrated in mice in which the knockout of β2-microglobulin resulted in a high susceptibility to MTB. This was probably due to iron overload (65). In humans, the presence of IFN-γ secreting, antigen specific $CD8^+$ T cells have been shown to participate in the maintenance of LTBI in adults (66). $CD8^+$ IFN-γ secreting T cells have been identified in BCG vaccinated newborns (140).

In studies performed by Vankayalapati *et al*, NK cells were shown to regulate $CD8^+$ T cells by contributing to IFN-γ secretion and priming of $CD8^+$ T cells to lyse MTB infected monocytes and alveolar macrophages (67).

A recent study by Sutherland *et al*, 2009, documents a significant decrease in the percentage of B and NKT cells in adults with active TB as compared to their LTBI house hold contacts (68).

T cells expressing a γδTCR have been shown to secrete IFN-γ and lyse MTB infected macrophages (69). They have also been associated with the restriction of mycobacterial growth (70).

The immune response to MTB infection, which can result in active TB or LTBI, is determined by the interaction of a wide range of MTB molecules and cells of both the innate and acquired immune response. The final outcome is a reflection of the balance created as a result of these interactions. The development of new vaccines and the identification of reliable correlates of immune protection against MTB infection will be influenced by the unraveling of these complex interactions (54).

1.3. Measuring the MTB specific immune response

1.3.1. Techniques

Antigen stimulated whole blood assays have allowed secreted protein and messenger ribonucleic acid (mRNA) levels to be measured by the use of techniques such as the enzyme linked immunosorbent assay (ELISA) and the polymerase chain reaction (PCR), which allows the detection of bioactive protein as well as very low levels of message. Lymphocyte proliferation assays (LPAs) are suitable for analysis of large numbers of samples; however, they do not provide information on the phenotype of antigen specific cells (71) (72).

Achieving the objectives of this dissertation, as presented in **Section 1.4**, required the use of techniques that allowed qualitative and quantitative analyses at the level of the single cell, as well as the detection of antigen specific cytokine secreting cells that were present in low numbers.

Another relevant consideration was that the chosen techniques could be efficiently performed within the scope of the environment in which the study would be taking place. Thus, Flow Cytometry in conjunction with intracellular cytokine staining and the ezyme-linked immunospot (ELISpot) technique were the chosen assays.

1.3.1.1. Flow cytometry and intracellular cytokine staining

Immunophenotyping requires the description of molecules expressed on the cell surface, as well as inside the cell. Flow cytometry enables the simultaneous measurement of multiple cell surface antigens at a single cell level.

It also enables the measurement of the proportion of specific subtypes within a population of cells and the absolute number of cells in a volume of whole blood. Flow cytometry in conjunction with fluorescent conjugated monoclonal antibodies (mAbs) are used to characterise distinct cell types and activation states (73).

The basic principle of a flow cytometer is the measurement of scattered and fluorescent light emitted as cells pass through the intersection of a light source, via a fluid stream. Laser beams at specific wavelengths provide the light source. Scattered light is derived from the size and granularity of cells and fluorescent light is derived from the fluorochromes conjugated to mAbs (73)(74)(75).

Cells for immunophenotyping are prepared by incubation with fluorochrome-labeled mAbs. The cell suspension is drawn up into a sample port on the flow cytometer and injected into a stream of isotonic saline solution to form a laminar flow. The containment of the sample stream by the carrier stream creates a hydrodynamic focus that allows the cells to pass through the intersection of the laser light source in single file.

This process takes place inside a flow cell (FL). As the cells pass through the light source, detectors collect the scattered and fluorescent light (73)(74)(75).

The detector collecting forward scatter (FSC) is placed directly in the path of the light source. The remaining side scatter (SSC), and fluorescent light is collected at 90˚ from the light source, and is directed to the fluorescent detectors via fiber optic cables. Optical filters direct specific wavelengths of light to the appropriate filters. The detectors are photomultiplier tubes (PMT) that convert electrical signal to a voltage pulse. The voltage output is quantified and digitised by a computer system (73)(74)(75).

The size of the voltage output is determined by the amount of light reaching the PMT as well as the voltage setting of the PMT, and therefore optimisation of the voltage setting is an important aspect of machine setup.

Each fluorescent detector is setup to collect light from a particular fluorochrome, however light from other fluorochromes may also be detected. Fluorescent spillover is referred to as spectral overlap and requires removal in a process referred to as fluorescent compensation. The separation of small less granular lymphocytes from other leukocytes is achieved on the basis that larger cells scatter more light, in a process called scatter gating (73)(74)(75).

The analysis of flow cytometry generated data starts with the assessment of the quality of the lymphocyte gate as well as the establishment of negative and positive analysis regions using isotype controls. **Figure 5** presents the basic design of a flow cytometer set up (73).

The use of anti-cytokine antibodies in a staining technique that allows the intracellular detection of cytokines and cell surface molecules, without the separation of cells, has greatly enhanced the use of flow cytometry to determine immunophenotype in human cells (76)(77)(78)(79).

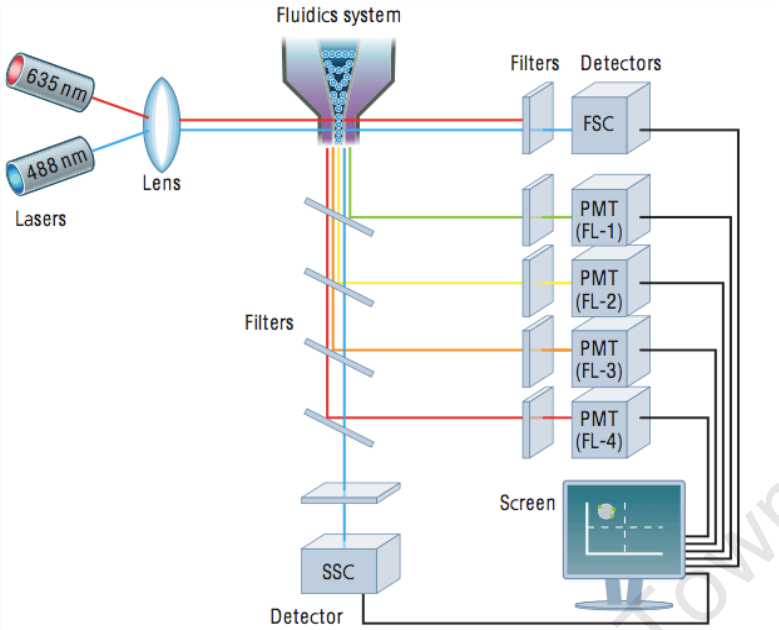

Figure 5. Schematic diagram of a typical flow cytometer set up, adapted from Micha Rahman (74).

1.3.1.2. Detecting antigen specific T cells by ELISpot

In 1983, the ELISpot was described as an alternative for the detection of antibody secreting cells (80). The use of nitrocellulose membranes and anti-cytokine mAbs modified the assay for the detection of antigen specific T cells. The assay was shown to have an estimated sensitivity of detecting 50 or fewer antigen specific T cells per 10^6 lymphocytes. This represents an increased sensitivity of at least 1 $\log_{10}$ more than the LPA (71).

Cytokine secreting T cells are detected as coloured spots via staining with an enzyme linked anti-cytokine mAb. The spots can be enumerated with the naked eye, however the development of ELISpot readers have automated the enumeration of spot forming cells and facilitated the ongoing development of standardised protocols (81).

The technique has been successfully used in the detection of antigen specific T cells in a range of infectious diseases (82)(83)(84). **Figure 6** is a diagrammatic presentation of the technique.

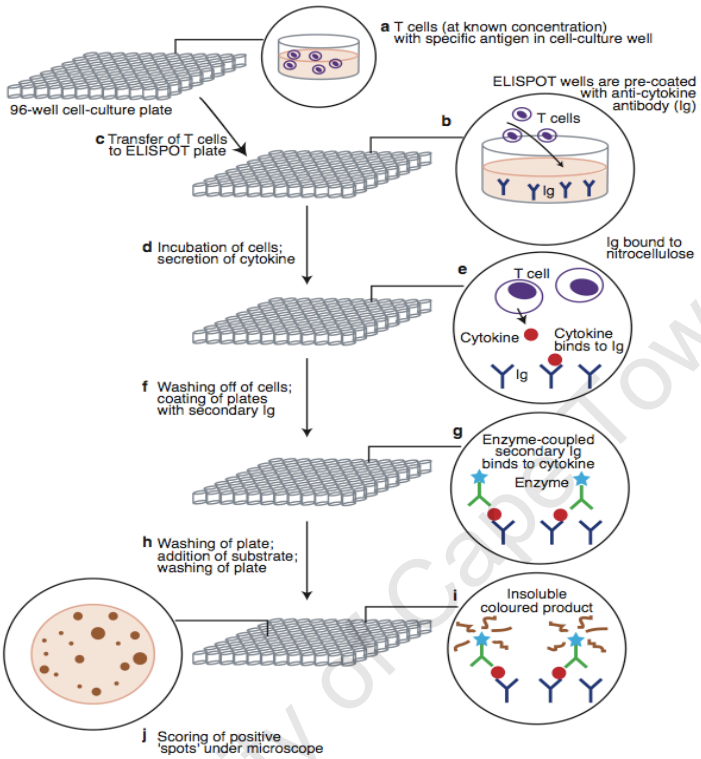

Figure 6. Diagrammatic presentation of the ELISpot technique adapted from Julian K. Hickling (71).

1.3.2. MTB specific antigens

The detection of prior sensitisation to MTB has traditionally been achieved via the tuberculin skin test (TST). The TST is performed by the intradermal administration of PPD. The induration of a delayed-type hypersensitivity reaction is measured 48-72 hours later. A positive skin test response may be an indication of LTBI, however PPD is a crude mixture of MTB proteins, which are shared amongst MTB, *M. Bovis* BCG and many other environmental mycobacteria. False positive TST results could therefore develop as a result of cross reactivity to prior BCG vaccination and exposure to environmental mycobacteria (85).

The search for non cross reactive antigens and the sequencing of the MTB genome have revealed MTB specific antigens that are potential candidates in the development of new vaccines, and the search for reliable correlates of immune protection. Thus it is necessary to investigate the ability of these antigens to induce a measurable T cell response as well as to determine the quality of the response to these novel antigens in people who are already sensitised by MTB (86)(87).

Early-secretory antigenic target-6 (ESAT-6), and culture filtrate protein-10 (CFP-10), are encoded by the MTB genomic segment, *region of difference-1* (RD1).
This region is absent from the BCG vaccine and most environmental mycobacteria (88). ESAT-6 and CFP-10, in conjunction with ELISA and ELISPOT, have been shown to be immunodominant targets of the acquired immune response to MTB. Both antigens are used in approved diagnostic test kits to detect the existence of an IFN-γ secreting T cell response to TB antigens as a measure of prior sensitisation to MTB (89)(90)(91).

The *esat-6 gene* (Esx*)* family has revealed a number of immunogenic proteins that are recognised by the acquired immune response in both humans and cattle. *M. bovis* and MTB share genetic homology of 99.9% (92). Rv3109c (TB10.3), a member of the Esx family, was shown to induce a significant IFN-γ response in BCG vaccinated cattle (93).

Other MTB antigens investigated for immunogenic ability include Rv2031c (ACR1) and Rv0251c (ACR2). ACR1 and ACR2 are both members of the α-crystallin (ACR) family of molecular chaperones. ACR1 has been associated with the persistence of bacteria in a non-replicating state. The infection of mice with a mutant ACR2 gene has been associated with a reduction in the recruitment of T cells and macrophages to the lungs of mice infected with MTB (94)(95).

1.3.3. Measuring T cell memory to MTB infection

The identification of molecules involved in the cellular activity of the immune response has facilitated the identification of T cell phenotype and function (36).

Naïve T cells do not migrate (home) to peripheral tissues. Following homing from the thymus to the lymph nodes, naïve T cells proliferate and differentiate into effector T cells capable of homing to peripheral tissues. Effector T cells are mostly short-lived; although a few antigen experienced cells remain long-lived and give rise to a population of memory T cells. Memory T cells are differentiated on their migratory ability. Central memory T cells (T_{CM}) preferentially migrate to the lymphoid tissues whereas effector memory T cells (T_{EM}) migrate to peripheral tissues (96)(97). CD45 is a phosphatase enzyme involved in the activation of T cells. The CD45 receptor (CD45R) occurs in different isoforms. The isoforms, CD45RA and CD45RO differentiate naïve from memory cells respectively (98). The CD45RA molecule can also be used in the

β-Chemokines (CC), are chemoattractant molecules that induce the migration of lymphocytes. Selectins are molecules that facilitate the movement of cells (38). The homing of naïve and T_{CM} cells to lymph nodes are assisted by the expression of chemokine receptor (CCR) 7 and the receptor for L- selectin (CD62L) (97). The homing of T_{EM} to sites of infection in peripheral tissues is assisted by the expression of CCR5. The expression of CCR5 can differentiate $T_{EM,}$ from T_{CM}. Terminally differentiated effector T cells do not require co-stimulation on activation. The lack of expression of the co-stimulatory molecule CD27 differentiates terminally differentiated effectors from naïve cells, T_{CM} and T_{EM} (99). Terminally differentiated effector $CD4^+$ T cells are also associated with a lack of CCR7 expression and re-expression of the CD45RA molecule (99).

The phenotype of T cells can be identified on the basis of expression, or lack of expression, of these and other molecules. **Table 1** presents a scheme used in the phenotyping of memory T cells in the present study.

Table 1. Scheme used to characterise $CD4^+$ T cell subtypes by phenotype and function, adapted from Elisabeth Amyes *et al* (99), and Frederica Sallusto *et al* (97).

Subtype	**Naive**	**Central memory (T_{CM})**	**Effector memory (T_{EM})**	**Terminally differentiated effector**
Surface molecules	$CD27^+$ $CD45RA^+$ $CD62L^+$ $CCR7^+$ $CCR5^-$	$CD27^+$ $CD45RA^-$ $CD62L^+$ $CCR7^+$ $CCR5^-$	$CD27^+$ $CD45RA^-$ $CD62L^-$ $CCR7^-$ $CCR5^+$	$CD27^-$ $CD45RA^+$ $CD62L^-$ $CCR7^-$ $CCR5^+$
Homing capacity to lymphoid organs	++	+	-	-
Homing capacity to site of disease	-	-	+	++
IFN-γ producing capacity	-	+	++	+++
Proliferative capacity and IL-2 production	+++	++	+	-

1.3.4. The effect of HIV on the immune response to MTB infection

HIV gains entry to cells via CCR5 and α-chemokine receptor (CXCR) 4, which are expressed on activated CD4 T cells. HIV also uses the CD4 molecule. HIV infection and replication leads to excessive cell death, alterations in antigen presentation, alterations in T cell migration patterns and damage of thymic function (100)(101). The acute phase of the HIV infection is associated with a profound decline in the $CCR5^+$ $CD4^+$ T cells, which represent a memory and effector T cell subset, and this depletion is maintained throughout all stages of the disease (102)(103).

HIV infection causes a progressive loss and decline in $CD4^+$ T cell numbers which is emphasised by the increase in risk of developing TB to 10% per annum in HIV infected people, as compared to 10% per life time in HIV uninfected people (20)(23)(6)(7)(8). Antiretroviral treatment acts by blocking viral entry to cells and preventing replication, which decreases infection of $CD4^+$ T cells by the virus and has been associated with an increase in $CD4^+$ T cell numbers.

Combination antiretroviral therapy (cART) has been shown to reduce the incidence of tuberculosis. A study performed in Cape Town, and others, showed that cART was associated with a reduction in the incidence of TB, in HIV-TB co-infected people, of more than 80% (104)(105)(106)(107)(108). Studies performed in the late 1990's document the restoration of immune function during antiretroviral therapy. This was largely due to the restoration of $CD4^+$ memory T cells by 4 weeks after treatment, which was sustained up to 12 months, as well as the restoration of naive $CD4^+$ T cells by 4 months after antiretroviral therapy, also sustained up to 12 months of therapy (109)(110)(111)(112)(113).

Antiretroviral therapy has no known anti-mycobacterial activity, which leads to the question of 'How is the protection mediated'. Detailed in vitro analysis of MTB antigen specific T cell subsets that expand during cART in persons with latent tuberculosis will contribute toward a better understanding of the nature of the MTB specific memory response as well as contribute to the need for the identification of more reliable correlates of protection. This study was therefore performed to investigate the hypothesis of the dissertation as stated in **Section 1.4.**

1.4. Hypothesis of the study

MTB specific $CD4^+$ T cell subsets that expand during cART in people with LTBI, mediate protection.

1.5. Aim of the study

To characterise, in a longitudinal analysis, MTB specific T cell subsets that expand during cART, in order to determine protective mechanisms in TB and thus contribute to the identification of novel correlates of protection.

1.6. Objectives of the study

1. To determine the phenotype of the $CD4^+$ T cell subsets, as well as other cell types, that respond to stimulation by MTB specific antigens, particularly the $CD4^+$ memory subtypes, from the time of starting cART, over a period of 48 weeks using flow cytometry in conjunction with intracellular cytokine staining.

2. To quantitate IFN-γ production in response to a range of MTB specific antigens, from the time of starting cART, over a period of 48 weeks using the ELISpot technique.

Chapter 2. Materials and Methods

All tissue culture procedures were performed using strict aseptic techniques, under sterile conditions.
All manipulations with unfixed cells took place inside Class II bio-safety cabinets.
All reagents were used and stored according to the manufacturers instructions.
All laboratory equipment was regularly serviced according to the manufacturers instructions and temperature ranges were monitored on a daily basis.
All waste generated were disposed of according to the bio-hazardous waste disposal protocols of the University of Cape Town.
Materials used, manufacturers details and product numbers are presented in the form of tables at the end of each section.

2.1. Study site and participants

The study received approval from the Research Ethics Committee of the University of Cape Town: REC REF 336/2004. Study participants were identified and recruited on enrollment into the antiretroviral treatment program at GF Jooste Hospital, Manenberg, and Cape Town whose catchment area includes the townships of Khayelitsha, Gugulethu, and Nyanga. Eligibility was based on a CD4 count of 200 cells/µl or less, and/or WHO stage 4 disease according to South African national guidelines. Antiretroviral treatment prescribed was the standard first line combination of stavudine (d4T), lamivudine (3TC) and either nevirapine (NVP) or efavirenz (EFZ).

All participants provided informed consent and a copy of the consent form was given to each participant. Exclusion criteria were age under 18 years, active TB, and pregnancy. A total of 28 study participants were recruited and enrolled between April 2005 and September 2007. The study baseline was the day on which cART started (d0) and follow up time-points were at 2,4,12,24,36 and 48 weeks into cART.
A 30 ml sodium heparinised whole blood sample was aseptically obtained via venepuncture for immunological analysis.

A 5 ml clotted blood sample for serum separation was also obtained. All blood samples were transported to the laboratory site and processed according to the study's experimental standard operating procedures (SOP) within 4 hours of collection.

Twelve HIV uninfected, MTB sensitised adults (as determined by either a positive tuberculin skin test or a positive response to either ESAT-6 or CFP-10 in the ELISpot assay) were recruited from the same community (5 females, 7 males, median age 25 years) and served as controls in parts of the study.

2.2. Isolation and cryopreservation of the peripheral blood mononuclear cells (PBMC) and Serum

2.2.1. Method

PBMC were isolated from the heparinised whole blood sample, drawn at each study time point, using density gradient separation (114). Whole heparinised blood was diluted 1:2 with sterile phosphate-buffered saline (PBS) to a total volume of 30 mls, in a sterile 50 ml centrifuge tube. The diluted whole blood was aspirated and gently layered onto 10 mls of Ficoll-Paque in a 50 ml centrifuge tube. The layered, diluted whole blood was centrifuged at 700g for 20 minutes with the centrifuge brakes off, so as not to disturb the cell layers formed. The layer of PBMC was carefully aspirated and transferred to a new 50 ml tube containing 10 mls PBS. After aspiration and transfer of the PBMC, more PBS was added so that the total volume equaled 40 mls.

The PBMC were pelleted by centrifugation at 600g for 10 minutes, with the centrifuge brakes on. The pellet was re-suspended and washed twice, in 10 ml RPMI 1640 culture medium containing 10% Heat-Inactivated Foetal Calf Serum (HI FCS), that was filtered through a 0.22 μm low protein-binding filter, prior to use.

A 20-μl aliquot of the washed and re-suspended PBMC was used to perform a cell count, using 0.4% Trypan blue dye and a disposable cell counting chamber (115). Cells that excluded the dye were counted as viable.

The following formula was used to determine the number of cells per ml:

$$\text{Count/ml} = \frac{\text{total count}}{\text{Number of 4 x 4 grids counted (1 grid equals 16 squares)}} \times 10^4 \times \text{sample dilution}$$

Freshly isolated PBMC were used for the flow cytometry assay. Remaining cells were re-suspended at a concentration of $10x10^6$ cells/ml in a cell freezing solution consisting of 45% RPMI, 45% HI FCS and 10% Dimethyl Sulfoxide (DMSO) (116). This cell suspension was transferred to 1.8 ml cryotubes. The cryotubes were placed into a Nalgene Mr. Frosty freezing apparatus, and frozen at -80˚C overnight (117). The next day the frozen cells were transferred to the vapour phase of a liquid nitrogen tank, where they were stored for use in the ELISpot assay. Serum was isolated from the 5ml clotted blood sample by centrifugation at 3000g for 10 minutes. The serum was aspirated and transferred to 1.8 ml cryotubes. All sera were stored at -80˚C for future use.

2.2.2. Materials and reagents

Table 2. Materials and reagents used in the isolation and cryopreservation of PBMC.

Product	**Supplier and product number (#)**
10 ml BD Vacutainer®, glass Sodium Heparin, plasma tube	BD Diagnostics, 1 Becton Drive Franklin Lakes, NJ USA 07417 #368480
5 ml BD Vacutainer® SST II Plus, plastic serum tube	BD Diagnostics, 1 Becton Drive Franklin Lakes, NJ USA 07417 #367955
BD Falcon™ 50ml centrifuge tubes	Becton Dickson Biosciences, Pharmingen, San Diego, CA, USA #352070
Phosphate Buffered Saline	Sigma-Aldrich, South Africa #D8537

Ficoll-Paque™ PLUS	GE Healthcare Biosciences, Sweden #17-1440-03
RPMI 1640	Sigma-Aldrich, South Africa #R8758
Fetal calf serum, endotoxin free	Delta Bioproducts, Highveld Biological, Lyndhurst, South Africa #14-501-BI
500µl Filter System 0.22um CA (Cellulose Acetate), Low Protein Binding membrane	Corning, NY 14831, USA #430769
Dimethyl Sulfoxide	Sigma-Aldrich, South Africa #D5879
Trypan blue 0.4%	Sigma-Aldrich, South Africa #T8154
Fast-Read 102, disposable counting chambers	Immune Systems LTD, United Kingdom #BVS100
NUNC™, 1.8ml Cryotubes, sterile, external thread	Thermo Fisher Scientific, Roskilde, Denmark #375418
5100 Cryo 1˚C Freezing Container, "Mr. Frosty"	Nalgene ® Labware, Thermo Fisher Scientific, AEC-Amersham, South Africa

2.3. The Flow Cytometry Assay

The flow cytometry assay was used to determine PBMC phenotype and cytokine secretion. The *in vitro* re-stimulation and staining of molecules for surface phenotyping, and intracellular cytokine expression, were performed consecutively on the same sample aliquot (118)(119).

2.3.1. Method

2.3.1.1. Re-stimulation and surface phenotype staining

The staining and re-stimulation of the cells were performed in a round-bottomed 96 well micro-titre plate. Freshly isolated PBMC were inoculated into duplicate wells on a micro-titre plate at a minimum concentration of 200 000 cells per well and a maximum of 500 000 cells per well, depending on availability, in a volume of 200 µl RPMI 1640 culture medium containing 10% HI FCS. PPD was used as a stimulant to determine the MTB specific memory responses, at a final concentration of 10 µg/ml. Co-stimulating molecules were not used (120).

The superantigen, Staphylococcal Enterotoxin B (SEB), was used as a stimulant in the positive control wells, at a final concentration of 5 µg/ml (121). No stimulant was added to the negative control wells. After addition of the stimulant, the cells were incubated for 2hrs at 37˚C with 5% CO_2, to allow antigen presentation to take place. The plate was removed from the incubator after 2hrs and the cytokine secretion inhibitor, Brefeldin A (BFA), was added to each well intended for intracellular cytokine staining (118)(119). The final concentration of BFA was 5 µg/ml. The cells were returned to incubation at 37˚C in 5% CO_2 for a further 18hrs, following which, the cells were pelleted by centrifugation at 1200 rotations per minute (rpm) for 5 minutes.

The supernatant was gently removed, using a multi-channel pipette, and the pellet loosened by gently vortexing the closed plate. The cells were then washed with Fluorescence-activated cell sorting (FACS) wash buffer (PBS, 2% HI-FCS and 0.1% Sodium Azide (NaN_3), 100 µl per well, and re-pelleted as described.

Surface staining was performed using predetermined, optimal volumes of fluorescent conjugated mAbs at 4˚C for 20 minutes. After staining, the cells were washed in FACS buffer, 100 µl per well, re-pelleted, and loosened as described. The cells used for surface staining only were then re-suspended in FACS FIX buffer (PBS/2%HI- FCS/0.1% NaN_3 and 1.6% paraformaldehyde), 200 µl per well. These cells were transferred to 5 ml round bottomed polystyrene tubes, and stored at 4˚C in the dark, until the rest of the protocol was completed.

2.3.1.2. Intracellular cytokine staining

The cells intended for intracellular cytokine staining were re-suspended in 100 µl per well of BD Cytofix/Cytoperm™ solution for 20 minutes at 4˚C, to allow for fixation and permeabilisation of the cell membrane. The cells were then washed in 100 µl per well of 1x BD Perm/Wash™ buffer, re-pelleted and loosened as described. Intracellular staining was performed using predetermined optimal concentrations of fluorescent conjugated monoclonal antibodies, for 30 minutes at 4˚C. Thereafter a final wash was performed in 100 µl per well of 1x BD Perm/Wash™ buffer. The cells were re-pelleted and loosened as described, and were re-suspended in 200 µl per well of FACS wash buffer. All stained samples were acquired immediately on a BD FACSCalibur™ Flow Cytometer (Serial number E3530), using the BD Cellquest™ Pro Programme. A total of 150 000 events, within the lymphocyte gate, were acquired per tube. Results were analysed using Flowjo Cytometry Analysis software, Version 7 (Tree star Inc Stanford University, Flowjo Africa Scheme).

The combination of fluorescent conjugated mAbs was restricted to the use of four fluorescent dyes as shown in **Table 3**.

Table 3. Combinations of fluorescent conjugated monoclonal antibodies used to Investigate surface phenotype and cytokine producing cells.

Tube no.	Stimulant	Allophycocyanin (APC) Conjugated Antibodies FL4	Peridinin Chlorophyll Protein (PerCp) Conjugated Antibodies FL3	Fluorescein Isothiocyanate (FITC) Conjugated Antibodies FL1	Phycoerythrin (PE) Conjugated Antibodies FL2
1	PPD	anti-IFN-γ	anti-CD4	anti-CD27	anti-CD62L
2	PPD	anti-IFN-γ	anti-CD4	anti-CD27	anti-CCR5
3	PPD	anti-IFN-γ	anti-CD4	anti-CD27	anti-CCR7
4	PPD	anti-IFN-γ	anti-CD4	anti-CD27	anti-CD45RA
5	PPD	anti-IFN-γ	anti-CD4	anti-CD69	anti-CD45RO
6	PPD	anti-TNF	anti-CD4	anti-IL-2	anti-IL-10
7	PPD	anti-IFN-γ	anti-CD8	anti-CD27	anti-CD62L
8	PPD	anti-CD3	anti-CD4	anti-CD25	anti-IL-10
9	PPD	anti-CD3	anti-CD19	anti-CD69	anti-CD56

2.3.2. Determination of optimal antibody concentrations

Using the method described in **Section 2.3.1**, antibody titrations were performed in order to determine the concentration of antibody that would result in maximum positive staining and minimum non-specific staining under the conditions of the study method (119). Optimal volumes, as shown in **Table 4**, were determined and applied throughout the study.

Table 4. Optimal volumes of fluorescent conjugated monoclonal antibodies used.

Fluorescent conjugated monoclonal antibody used	Volume per well
All surface phenotype antibodies	3 µl
anti-IFN-γ	0.5 µl
anti-TNF	3 µl
anti-IL-10	5 µl
anti-IL-2	3 µl

2.3.3. Validation of the flow cytometry assay parameters

This section describes the optimisation of the Flow Cytometer instrument settings, sensitivity, and fluorescent compensation. It includes a description of the controls used to adjust for auto-fluorescence, non-specific background staining and the controls used to study the PBMC response to *in vitro* re-stimulation. All the PBMC controls were prepared using the study methods described in **Sections 2.3.1 and 2.3.2**. Parallel experiments were performed when preparing the PBMC controls, one using un-stimulated PBMC as well as PPD re-stimulated PBMC, in order to identify any component of the methods and reagents that could contribute to non-specific fluorescence.

2.3.3.1. Instrument optimization

The Flow Cytometer instrument settings, sensitivity and fluorescent compensation settings were optimised and monitored on a routine basis using the BD CaliBRITE™ bead system in conjunction with FACSComp™ software, according to the manufacturer's instructions (119). The BD CaliBRITE™ bead system uses two tubes, one containing an unlabeled bead suspension and another containing a mixture of fluorescent labeled beads, each present in equal amounts.

The software positions the unlabeled bead suspension at predetermined target positions, following which the individual PMT voltages are adjusted until the mean values correspond to predetermined target value.

The software programme then uses the mixed-bead suspension to achieve optimal fluorescent compensation following which it performs an instrument sensitivity test. The software generates a visual report for each test performed. The routinely generated reports were also used to monitor the stability of the instrument over time.

When any failed parameters or alterations in the stability of the instrument were detected, the required procedures and interventions, as recommended by the manufacturers, were performed and the above measures repeated until acceptable reports were generated. When all the parameters were passed, the generated instrument sensitivity, PMT voltages and fluorescent compensation settings were validated and adjusted for use on the study PBMC, as described in the following section.

2.3.3.2. PBMC controls

The beads used in the BD CaliBRITE^{TM} bead system possess optical properties different to that of human cells, thus PMBC controls, as shown in **Table 5**, were prepared, in order to validate and optimize the settings generated as described in **Section 2.3.2.1**, for the purpose of analysing the study PBMC (122,123). To ensure that the study PBMC were placed within the gates and analysis regions of the various plots formatted, the software generated PMT voltage settings were validated and optimised first, and the subsequent settings saved. The saved settings were then applied to the validation and optimisation of the instrument generated fluorescent compensation settings.

Table 5. PBMC controls used in the Flow Cytometry Assay.

Tube Label	Stimulant	APC Conjugated Antibody	PerCp Conjugated Antibody	FITC conjugated antibody	PE conjugated antibody	Frequency
Unstained	Nil					All time points
Unstained	PPD					Monthly
Isotype 1	Nil			anti-IgG1		Monthly
Isotype 1	PPD			anti-IgG1		Monthly
Isotype 2	Nil				anti-IgG1	Monthly
Isotype 2	PPD				anti-IgG1	Monthly
Isotype 3	Nil				anti-IgG2	Monthly
Isotype 3	PPD				anti-IgG2	Monthly
Isotype 4	Nil	anti-IgG1				Monthly
Isotype 4	PPD	anti-IgG1				Monthly
Isotype 5	Nil		anti-IgG2			Monthly
Isotype 5	PPD		anti-IgG2			Monthly
Four colour	NIL	anti-IFN-γ	anti-CD4	anti-CD27	anti-CD45RA	Monthly
Four colour	PPD	anti-IFN-γ	anti-CD4	anti-CD27	anti-CD45RA	Monthly
Positive Positive	SEB SEB	anti-IFN-γ anti-TNF				All time points Occasionally

Following validation of the unstimulated PBMC controls the re-stimulated PBMC controls were used to verify that re-stimulation did not alter the position of the study PBMC. The unstained PBMC control was used to optimize the resolution of the PBMC and lymphocyte populations, evaluate possible auto-fluorescence as well as to confirm that the unstained, un-stimulated lymphocyte population was placed in the correct acquisition region (123).

The isotype-matched controls were then used to evaluate possible non-specific staining and to set the negative and positive analysis regions, using quadrant markers (123).

The four colour stained control was used to determine that appropriate separation between the negative and positive analyses regions were achieved and to adjust the fluorescent compensation settings as required (123). SEB was used as a stimulant in the positive control to validate cytokine release (121). The final instrument settings, compensation settings, gates, negative and positive analysis regions were saved and applied to the analysis of the study PBMC.

2.3.4. Gating strategies

2.3.4.1. Acquisition of data

The BD Cellquest^{TM} Pro Programme was used to design an acquisition template. Scatter dot plots were chosen to display the data acquired. The acquisition of data was restricted to the $CD4^+$, $CD8^+$, $CD3^+$, and $CD3^-$ T cells, which were identified using the FSC and SSC parameters, and isolated by drawing a gating around it. These gates were set to acquire all positive events. The template was designed to display the acquisition of the gated T cells and subsets using combinations of the SSC, FL1, FL2, FL3, and FL4 parameters. The template was applied during the acquisition of the control PBMC as well as the study PBMC, in order to monitor the quality of the events displayed.

2.3.4.2. Analyses of data

The gating strategies used to analyse the subsets within the T cell populations are shown in the individual results in **Chapter 3.**

2.3.5. Materials and Reagents

Table 6. Material and reagents used in the Flow Cytometry Assay.

Product	**Supplier and product number (#)**
Costar round bottomed 96 well micro-titre plates	Corning Incorporated, Corning, New York #14831
RPMI 1640	See Table 2
Tuberculin Purified Protein Derivative (PPD)	Statens Serum Institut, DK-2300, Copenhagen S, Denmark #2391
Epstein Barr Virus infected cell extract East Coast Bio, Inc, USA	East Coast Bio, Inc, USA
Staphylococcal Enterotoxin B	Sigma-Aldrich, South Africa #S-4881
Brefeldin A	Sigma-Aldrich, South Africa #B-7651
Phosphate Buffered Saline	See Table 2
Fetal calf serum, endotoxin free	See Table 2
Sodium Azide	Sigma-Aldrich, South Africa #S-2002
Paraformaldehyde, 16% w/v aqueous solution, methanol free	Alfa Aesar, The Right Chemicals, 30 Bond Street, Ward Hill, MA 01835, 800-343-0660 #CAS-#30525-89-4
BD Falcon™ Polystyrene round bottomed tubes, 5ml, 12x75mm style	Becton Dickson Biosciences, Pharmingen, San Diego, CA, USA #352054
BD Cytofix/Cytoperm™	Becton Dickson Biosciences, Pharmingen, San Diego, CA, USA #51-2090KZ

BD Perm/Wash™	Becton Dickson Biosciences, Pharmingen, San Diego, CA, USA #51-2091KZ
BD CaliBRITE™ 3 three-color-kit	Becton Dickson Biosciences, Pharmingen, San Diego, CA, USA #340486
BD CaliBRITE™ APC Beads	Becton Dickson Biosciences, Pharmingen, San Diego, CA, USA #340487

Table 7. BD Pharmingen™ fluorescent conjugated antibodies used in the Flow Cytometry Assay.

Supplier	**BD Biosciences, 2350 Qume Drive, San Jose, CA USA 95131**
Fluorescent conjugated antibody	**Product number**
BD Pharmingen™ CD3 APC	555335
BD Pharmingen™ CD4 PERCP	345770
BD Pharmingen™ CD27 FITC	555440
BD Pharmingen™ CD62L PE	341012
BD Pharmingen™ CD195 PE (CCR5)	555993
BD Pharmingen™ CCR7 PE	552176
BD Pharmingen™ CD5RA PE	555489
BD Pharmingen™ CD69 FITC	555530
BD Pharmingen™ CD45RO PE	555492
BD Pharmingen™ CD8 PerCP	345774
BD Pharmingen™ CD25 FITC	555431
BD Pharmingen™ CD19 PerCP	345778
BD Pharmingen™ CD56 PE	555516
BD Pharmingen™ IFN-γ APC	554702

BD Pharmingen™ TNF APC	340534
BD Pharmingen™ IL-2 FITC	340448
BD Pharmingen™ IL-10 PE	559330
BD Pharmingen™ IgG_1 FITC	349041
BD Pharmingen™ IgG_1 PE	349043
BD Pharmingen™ IgG_{2a} PE	340459
BD Pharmingen™ IgG_1 APC	550874
BD Pharmingen™ IgG_{2a} PerCP	349054

2.4. The ELISpot Assay

The ELISpot assay was used to measure IFN-γ production in response to re-stimulation by a range of MTB antigens, during the study period (81). The assay was always performed using batched cryopreserved study PBMC (124).

2.4.1. Preparation of the PBMC

The PMBC were thawed and rested overnight as follows (116). The cryotubes were removed from the vapour phase in the liquid nitrogen storage tank and immediately transferred to dry ice within a sealed styrofoam container inside a fume cabinet. Immediately after transfer the screw caps were loosened to allow any vapour to escape and thereafter were transferred to a 37˚C incubator to defrost.

When just a small bit of ice remained in the vial, it was transferred to the bio-safety cabinet; the outside surface wiped with 70% ethanol and the contents of the vial added, drop wise, to 10 mls of warm RPMI/10% HI FCS. The cells were pelleted by centrifugation at 600g for 10 minutes. The supernatant fluid was decanted and the pellet re-suspended in 10 mls of RPMI/10% HI FCS.

A cell count was performed using 0.4% Trypan blue, to establish viability, as described in **Section 2.2.1**. The cells were re-pelleted and re-suspended to a final concentration of $2x10^6$ cells per 1 ml of RPMI/10% HI FCS. The cells were incubated and rested overnight in a 37˚C incubator with 5% CO_2. The following morning the cells were re-pelleted, the cell count repeated and the PBMC were re-suspended in RPMI/10% HI FCS to the concentration of cells per ml required. The rested PBMC were re-suspended at a minimum concentration of $2x10^6$ cells/ml and a maximum concentration of $3x10^6$ cells/ml, depending on availability.

2.4.2. Inoculation and development of the ELISpot assay

The ELIspot assay was performed on a sterile, high protein binding, multi-screen, 96 well plate. The membranes inside the wells were pre-wetted with 50µl PBS. The PBS was removed and an anti-human IFN-γ monoclonal coating antibody, 1-D1K, was added to each well at a final concentration of 15µg/ml in 100µl. The plate was covered and incubated overnight at 4˚C to allow for binding of the coating antibody to the membrane. Following overnight incubation the coating antibody was carefully removed using a multi-channel pipette and the wells were washed 5 times with 100µl RPMI, per wash. The wells were blocked using RPMI/10% HI FCS, 100µl per well, for 2 hours at 37˚C with 5% CO_2. After removing the blocking medium, the PMBC (thawed the day before and rested overnight) were added at a minimum of 200 000 cells/100µl per well, and a maximum of 300 000 cells/100µl per well.

The following endotoxin free, MTB antigens were used as stimulants at predetermined concentrations (one stimulant per well):

1. ESAT-6 (Rv3875), a secreted species-specific antigen, at a final concentration of 5µg/ml.
2. CFP-10 (Rv3874), a secreted species-specific antigen, at a final concentration of 2.5µg/ml.
3. ACR1 (Rv2031c), a cytoplasmic heat shock protein, at a final concentration of 1µg/ml.

4. ACR2 (Rv0251c), a cytoplasmic heat shock protein, at a final concentration of 20µg/ml.
5. TB10.3 (Rv3019c), a homologue of the ESAT-6 family, at a final concentration of 2.5µg/ml
6. PPD, a MTB culture filtrate extract, at a final concentration of 5µg/ml.

After addition of the stimulants the plates were covered and incubated at 37˚C with 5% CO_2 for 18-24 hours. Following incubation, the supernatant was gently removed, using a multi-channel pipette, after which the wells were washed 5 times each, with 100µl of PBS per well. A biotinylated, anti-IFN-γ detection antibody, 7-B6-1-Biotin, was added to each well at 50µl per well at a concentration of 1µg/ml in PBS. The plates were incubated at room temperature for 2 hours. After incubation the plates were washed 5 times with PBS and a Streptavidin-alkaline phosphatase (ALP) antibody was added at 50µl per well at a dilution of 1:1000 in PBS. The plates were incubated at room temperature for 1 hour and then washed 5 times with 100µl of PBS per well. An ALP substrate solution was added to each well at 50µl per well. The plate was left to develop for 5-15 minutes, until the formation of spots was clearly visible. The reaction was stopped by washing the wells with tap water after which the plates were air-dried by the airflow in the bio-safety cabinets.

All the ELISpot plates were read on an Immunospot Series 3B Analyzer (Cellular Technology, Cleveland, OH).

2.4.3. Positive and negative controls used in the ELISpot assay

The ability of the study PBMC to release cytokine was validated by the inclusion of a positive control well at each time point. The PBMC used in the positive control were stimulated using the mitogen, Phytohaemagglutin (PHA) at a concentration of 5µg/ml. A negative, unstimulated control well, used to verify non-specific background staining, was also included at each point .

2.4.4. Verification of the ELISpot $CD4^+$ T cell IFN-γ response

In order to validate that the IFN-γ measured in the ELISpot assay were due to $CD4^+$ T cell re-stimulation, a control experiment was performed on PBMC (n=4) from which the $CD4^+$ T cells were depleted using Dynabeads CD4®. Dynabeads CD4® contains anti-CD4 coated, super paramagnetic polystyrene beads in suspension (125)(126).

2.4.4.1. Preparation of PBMC

The PBMC were thawed, rested, and re-suspended as described in **Section 2.4.1**, to a concentration of $2.5x10^6$ cells/ml. A 1ml aliquot of the re-suspended cells was aspirated and transferred into a sterile closed tube for use as an un-depleted control. The remaining PBMC were re-pelleted by centrifugation at 600g for 10 minutes, and re-suspended in wash buffer (PBS without (w/o) Calcium (Ca) and Magnesium (Mg) and 0.1% Bovine serum albumin (BSA)), at a concentration of 10^7 cells/ml, in a volume determined by the post-resting cell count. The re- suspended PBMC was placed on ice till further processing.

2.4.4.2. Preparation of the Dynabeads CD4®

Dynabeads CD4® were supplied at a concentration of $4x10^8$ beads per ml in buffer consisting of PBS pH 7.4, 0.1% BSA and 0.02% NaN_3. The vial of Dynabeads CD4® was gently mixed to ensure even distribution of the beads in suspension. The concentration of Dynabeads CD4® used was 55µl per 10^7 cells/ml. A 55µl aliquot of the beads was transferred to a 2ml screw-capped, sterile tube. The NaN_3 was removed by washing the beads in 1ml of wash buffer (PBS w/o Ca, Mg/ 0.1% BSA).

After addition of the wash buffer to the tube, the tube was gently mixed and then placed in a Dynal Magnetic Particle Concentrator ® (Dynal MPC®), which draws the beads to the wall of the tube via a magnetic field. After 1 minute, the wash buffer was gently removed from the tube in the Dynal MPC™, using a pipette, and discarded.

The bead containing tube was removed from the Dynal MPC™ and the beads were re-suspended in 55µl of wash buffer.

2.4.4.3. Depletion of $CD4^+$ T cells

The 55µl of washed beads was added to the PBMC suspension, which had been kept on ice, gently mixed and further incubated on ice to prevent phagocytosis of the beads. The mixture was incubated for a total of 30 minutes on ice, during which, the tube was gently mixed every 5-10 minutes to prevent the beads from settling on the bottom of the tube. After the incubation, the tube was placed in the Dynal MPC™ for 1 minute, the supernatant was gently removed, using a pipette, and transferred to a sterile tube.
The tube containing the bead-bound $CD4^+$ T cells was removed from the Dynal MPC™ and discarded.

The $CD4^+$ T cell depleted fraction was re-pelleted at 600g for 10 minutes and re-suspended in at a concentration of $2.5x10^6$ cells per ml in a volume determined by the post-resting cell count. Using the ELISpot assay as described **in Sections 2.4.2 and 2.4.3**, the $CD4^+$ T cell depleted cells and the aliquot of undepleted PBMC were set up, in order to validate the effect of $CD4^+$ T cell depletion on the secretion of IFN-γ. Depletion efficiency was verified by the flow cytometry assay using, a combination of anti-CD3, anti-CD4 and anti-CD8, as described in **Section 2.3.1.1**.

2.4.5. Interpretation of the ELISpot assay results

Results were expressed as spot forming cells (SFC) per million PBMC.
A negative result was defined as <5 spots per well.
A positive result was defined as >5 spots per well and twice the background value.
The SFC for the negative wells was subtracted from the antigen re-stimulated wells.

2.4.6. Materials and reagents

Table 8. Materials and reagents used in the Elispot assay.

PRODUCT	SUPPLIER AND PRODUCT NUMBER (#)
RPMI 1640	See Table 2
Fetal calf serum, endotoxin free	See Table 2
Trypan blue 0.4%	See Table 2
Fast-Read 102, disposable counting chambers	See Table 2
Multiscreen® 96-Well Plates	Millipore Ireland BV, Tullagreen, Carrantuohill, Country Cork, Ireland #MAIP N45 10
ELSIPOT ASSAY FOR HUMAN INTERFERON-γ: Coating mAb (1-D1K) Detection mAb, biotinylated (7-B6-1-Biotin) Streptavidin-ALP	Mabtech, Sweden #3420-2A
Recombinant ESAT-6 (Rv3875)	Proteix, Prague, Czech Republic
Recombinant CFP-10 (Rv3874)	Proteix, Prague, Czech Republic
Recombinant ACR1 (Rv2031c)	Proteix, Prague, Czech Republic
Recombinant ACR2 (Rv0251c)	Proteix, Prague, Czech Republic
Recombinant TB10.3 (Rv3019c)	Proteix, Prague, Czech Republic
Tuberculin Purified Protein Derivative (PPD)	See Table 6
BCCP/NBT (PLUS), Alkaline phosphatase substrate	Moss Inc P.O. Box 189, Pasadena, Maryland 21123-0189, U.S.A. #NBTM-500
PHA	Sigma-Aldrich, South Africa #L4144

Phosphate Buffered Saline	See Table 2
Bovine Serum Albumin	Sigma-Aldrich, South Africa #A9418
2.0ml Graduated Free Standing Screw Cap Micro tube, Sterile with O-ring	Quality Scientific Plastics (QSP), Whitehead Scientific (Pty) Ltd., Brackenfell 7561, South Africa #520-GRDS
Dynabeads CD4®	Invitrogen Dynal AS, Oslo, Norway #111.45D
Dynal MPC®	Invitrogen Dynal AS, Oslo, Norway #120-01D
BD Pharmingen™ CD3 FITC	BD Biosciences, 2350 Qume Drive, San Jose, CA USA 95131 #345763
BD Pharmingen™ CD4 APC	BD Biosciences, 2350 Qume Drive, San Jose, CA USA 95131 #345771
BD Pharmingen™ CD8 PerCP	See Table 7

2.5. CD4 counts and viral loads

The blood samples drawn for the CD4 count and viral load, per time point, were submitted to the accredited National Health Laboratory at Groote Schuur Hospital for analysis. The results were obtained using internationally approved and validated standard diagnostic techniques.

2.6. Statistical Analysis

All statistical analysis of data was performed using Graph Pad Prism, Version 5.0a, for Mac OS X. The data were tested for normality using the D'Agostino and Pearson normality test. Data that were normally distributed were analysed using analysis of variance (one way ANOVA) and Dunnett's post-test for multiple comparisons, or the paired t-test. These results are shown as means ± standard deviation.

Data that were not normally distributed were analysed using the Kruskal Wallis test and Dunn's post-test correction, or Wilcoxon matched pairs test, for paired observations and the Mann Whitney U test for unpaired observations. These results are shown as medians plus the inter-quartile range (IQR).

Chapter 3. Results

3.1. Study participants, CD4 counts, and viral loads

A total of 28 participants were recruited and enrolled to the study.
Nine participants were excluded from the final analysis due to the following reasons:

1. Two developed active tuberculosis during the study
2. Three relocated to a different treatment centre
3. One defaulted cART
4. One withdrew from the study
5. One died in a car accident
6. One died prior to starting cART

The remaining 19 participants, who completed the study, were included in the final analysis. They participated as follows:

1. Thirteen attended all follow up visits
2. Five missed one follow up visit
3. One missed two follow up visits

None of the 19 participants developed active TB or opportunistic infections caused by non-tuberculous Mycobacteria during the study period. Nine participants had documented evidence of previous TB. The baseline characteristics and follow up results discussed are presented in **Table 9**.

The median age of the 19 participants was 35 years (IQR 32-39). Of the 19, 7 were males and 12 females. 9/19 participants had documented evidence of previous TB disease in the years preceding cART. While this adds a degree of heterogenecity to the study cohort, there was no significant difference between the median age, 34 and 36 years respectively, of the group who had previous TB (n=9, 8 females) and the group who did not (n=10, 4 females).

The median baseline viral load was 103,419 copies/ml (IQR 11,000-250,000). The viral load declined to low or undetectable levels by the 24th week of cART. The median baseline viral load for the group who had no previous TB was 67,710 copies/ml. The median baseline viral load for the group who had previous TB was 179,759 copies/ml. Although the latter is higher, the difference is not statistically significant (p=0.6).

CD4 counts were not available for all the participants at all the time points (individual results are presented in tables in **Appendix 3**). Thus comparisons could not be made between all the time points. A comparison made between week 0 (n=19), and week 48 (n=18), revealed a highly significant (p<0.0001) increase in absolute CD4 count over the 48 weeks of the study period. The median count increased from a baseline of 93 (IQR 40-131) at week 0, to 313 (IQR 236-434) at week 48. A comparison of the median CD4 counts at baseline, and the median CD4 counts at 24 weeks, between the group who had previous TB and the group who had no previous TB, revealed no significant difference.

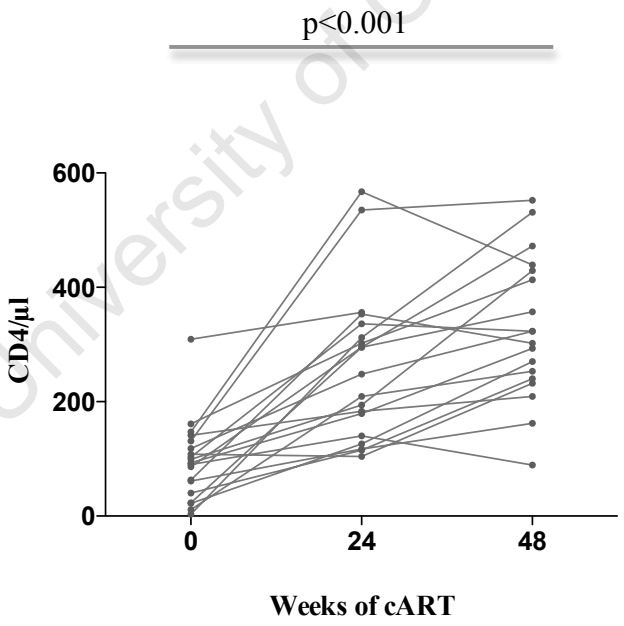

Figure 7. Changes observed in the median expansion of the absolute CD4 count during cART. A significant increase (one way ANOVA, p<0.001) occurred between weeks 0 and 48 **(**n=19).

Table 9. Baseline characteristics, CD4 counts and Viral loads.

Study number	Age (years)	Previous TB	Viral Load (copies/ml)		CD4 count (cells/µl)		
			Baseline	24 week	Baseline	24 week	48 week
1	41	YES	1,030	LDL *	141	183	209
2	35	NO	32,000	230	161	302	413
3	46	YES	21,000	LDL	63	353	302
4	25	YES	180,000	LDL	23	295	472
5	44	YES	NA§	280 **	147	567	439
6	37	NO	500,000	<50	22	126	270
7	32	YES	250,000	LDL	309	356	NA
8	38	YES	102,888	<50	93	179	293
10	35	NO	2,400	LDL	108	104	232
11	30	YES	500,000	<50	131	535	552
13	38	NO	11,000	<50	86	295	357
14	40	NO	103,419	52	103	336	323
17	32	NO	NA	LDL	61	117	162
20	39	NO	380,000	<50	118	248	323
21	38	NO	140,000	20,000 **	99	194	429
22	30	NO	2,400	LDL	90	140	89
24	26	NO	NA	LDL	11	209	253
25	32	YES	179,759	87	40	115	240
28	34	YES	NA	LDL	3	312	531
MEDIAN	**35**		**103,419**		**93**		**313**

*** Lower than detectable level**

§ not available

**** LDL at the 48-week time point**

3.2. T cell phenotype and function

T cell phenotype and function were analysed using the Flow Cytometry methods described in **Sections 2.2 and 2.3** and the combinations of antibodies shown in **Table 3.**

3.2.1. Instrument settings and controls

A representative FACSComp ^{TM} software generated report and a representative report of final settings used, following PBMC optimization, are presented in **Appendix 1** and **2**, respectively.

3.2.2. Antibody titrations

Antibody titrations were performed on surface phenotype and cytokine molecules. **Figure 8** presents a representative result. The volumes of antibody providing optimal fluorescence as presented in **Table 3,** were used.

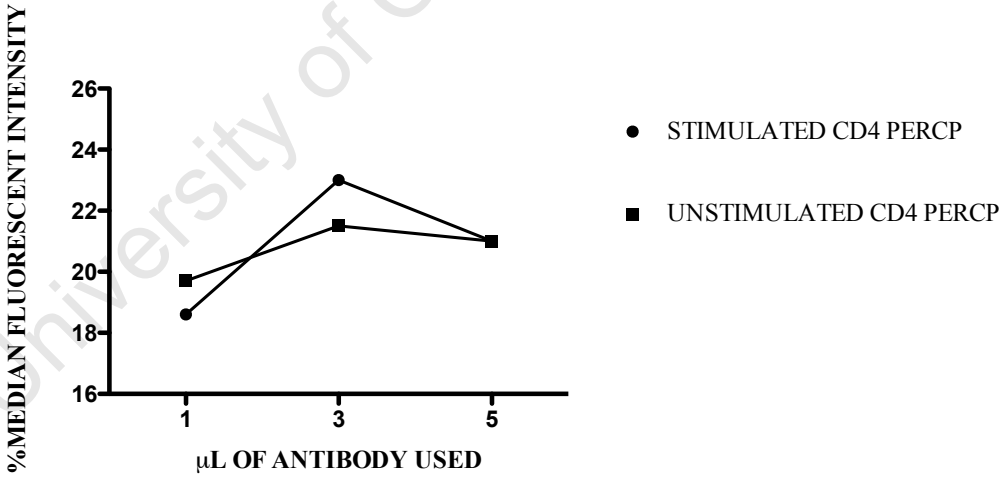

Figure 8. **Anti-CD4 titration**. Representative graph, (n=1), showing median fluorescent intensity on the Y-axis and volume of antibody used on the X-axis. The % of $CD4^+$ T cells detected was the same for each titration (24%).

3.2.3. PBMC controls

The unstained, unstimulated negative control, performed at all time points, showed nil fluorescence throughout the study (<0.3% = nil), and thus was not subtracted from the stained study PBMC results. The routine isotype controls also showed nil fluorescence (not shown).

The SEB stimulated positive control, **Figure 9**, performed at all time points, showed a median IFN-γ response of 5.7% throughout the study.

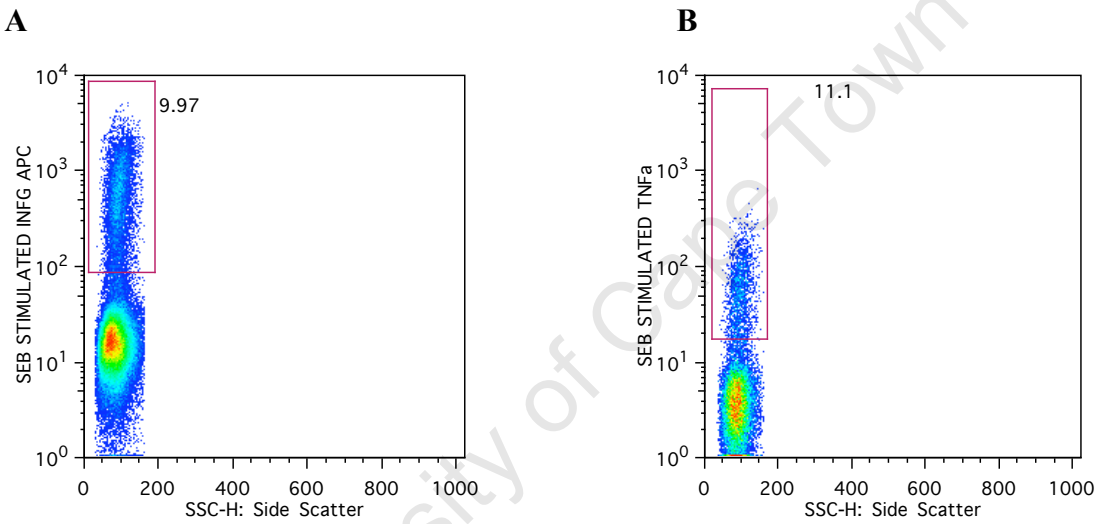

Figure 9. Representative responses for the SEB stimulated controls. Scatter dot plots, (n=1), showing representative responses for the SEB stimulated controls. Plot **A** shows IFN-γ staining and Plot **B** shows TNF staining.

In addition to the schedule of PBMC controls presented in **Table 5**, the effect of incubation time on non-specific staining, auto-flourescence and up-regulation of surface molecules was assessed (127). PPD stimulated and un-stimulated PBMC were tested at 0,2,4,6, and 18 hours for each control. The isotype and unstained negative controls showed nil fluorescence throughout the experiment (<0.3% = nil), **Table 10** presents representative results for the negative control. The 4-colour control showed that overnight incubation did not result in up-regulation of surface molecules; **Figure 10** presents representative results for the 4-colour and isotype controls.

Table 10. The effect of incubation time on the negative unstained controls.

Negative unstained controls recorded as percentage of PBMC negative										
	PPD stimulated					**Unstimulated**				
Hours incubated	**0**	**2**	**4**	**6**	**18**	**0**	**2**	**4**	**6**	**18**
FL1-FL2-	100	100	100	100	100	100	100	100	100	100
FL1-FL3-	100	100	100	100	100	100	100	100	100	100
FL1-FL4-	100	100	100	100	100	100	100	100	100	100
FL2-FL3-	100	100	100	100	100	100	100	100	100	100
FL2-FL4-	100	100	100	100	100	100	100	100	100	100
FL3-FL4-	100	100	100	100	100	100	100	100	100	100

Table 10. Representive results, (n=1), for the PPD stimulated and un-stimulated negative, unstained control at 0,2,4,6 and 18 hours, which remained negative all the time points (<0.3%-nil).

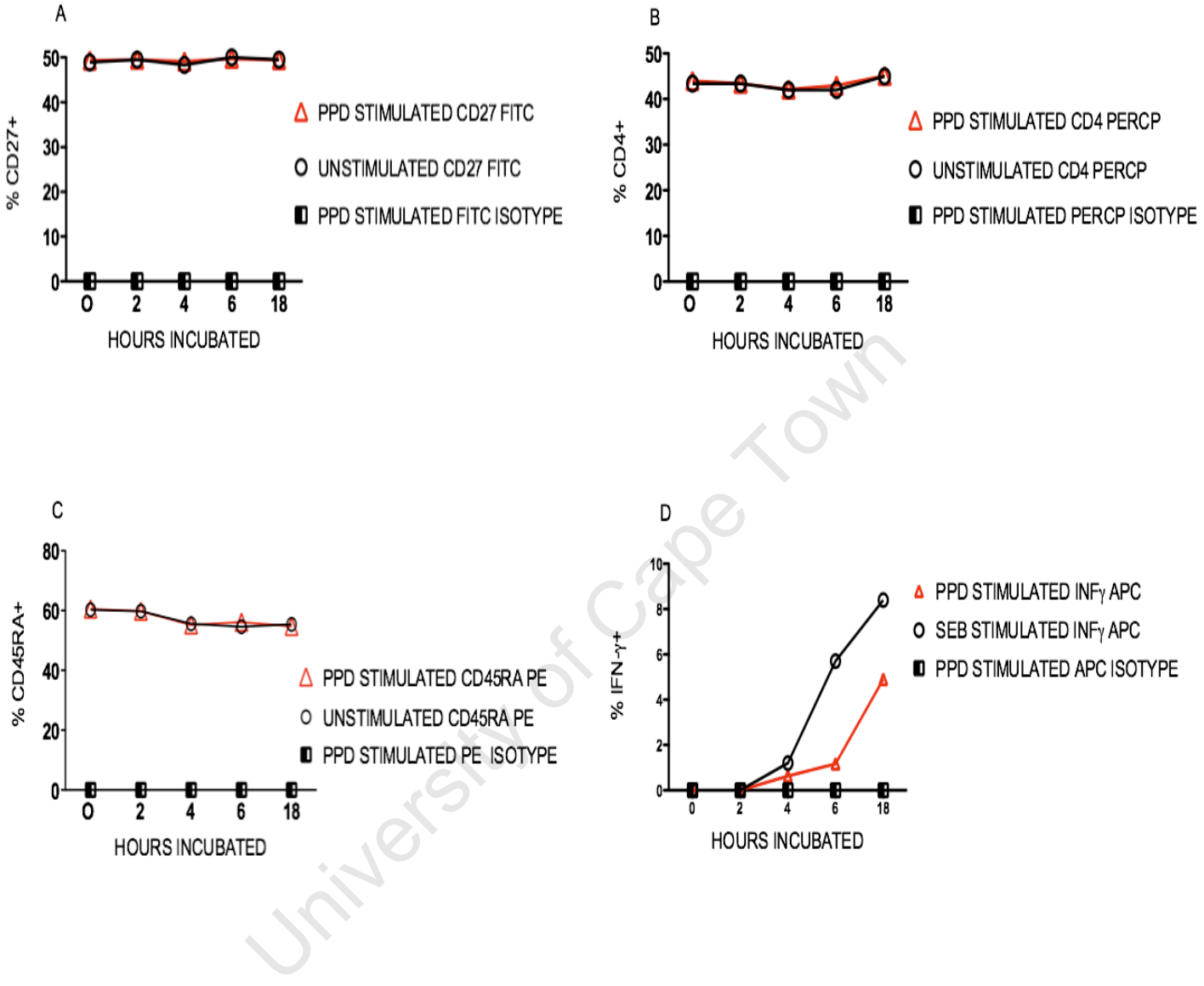

Figure 10. **The effect of incubation time on the stained positive controls.** Graphs **A**, **B** and **C** show representative results, (n=1), for the PPD stimulated and un-stimulated responses observed at 0,2,4,6, and 18 hours for the surface molecules CD4, CD27, and CD45RA, respectively as well as the PE, FITC and PERCP isotype controls.
In the same manner, Graph **D** shows the responses observed for the cytokine, IFN-γ and compares the PMBC, APC isotype, and SEB controls. The unstimulated, stained isotype controls, as well as a SEB stimulated, unstained control showed nil responses (not shown).

3.2.4. $CD4^+$ T cells

$CD4^+$ T cells were identified using the SSC and FL3-CD4 PerCP parameters, and selected by gating. The percentage of $CD4^+$T cells increased significantly from a baseline of 7.3±4.8%, to 17.4±7.1% ($p<0.0001$, **Figure 11**) by 48 weeks of cART. This parallels the increase observed in the absolute CD4 count.

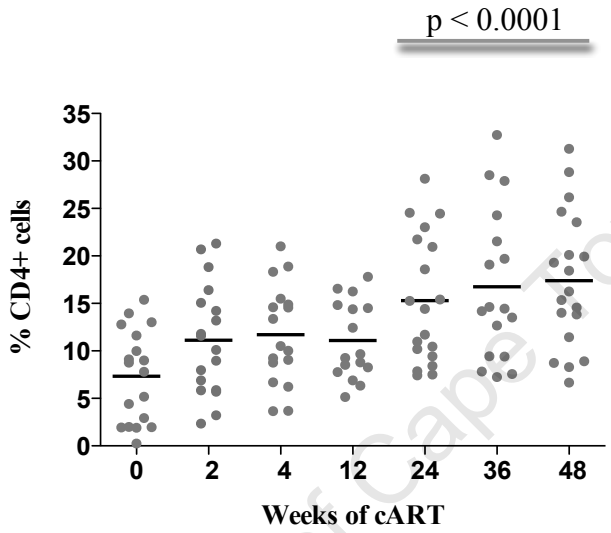

Figure 11. The mean expansion of the $CD4^+$ T cells. Scatter dot plot showing the mean expansion of $CD4^+$ T cells (n=19), as determined by flow cytometry during the 48-week study period, which increased significantly over time ($p<0.0001$).

The $CD4^+$ population was further analysed on the basis of surface expression, or lack of surface expression, of the molecules presented in **Table 1, Section 1.3.3**. Scatter dot plots, representative of the gating strategy used, are presented in **Figure 12.**

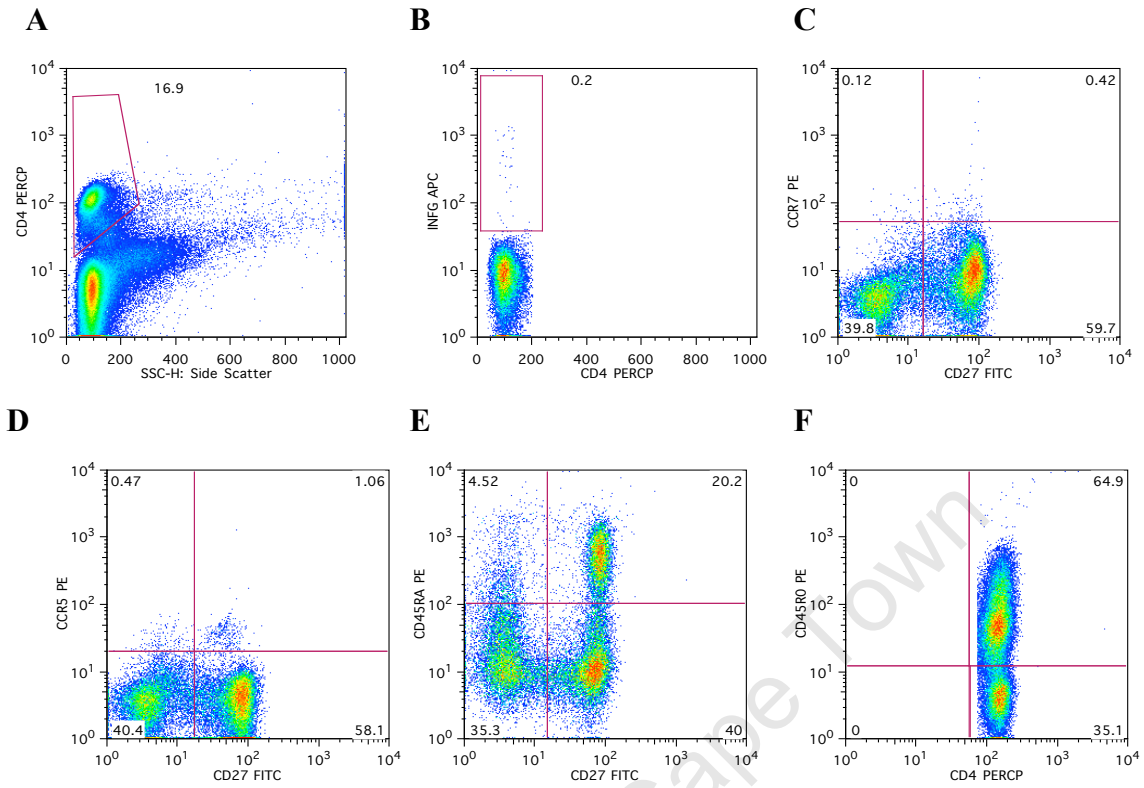

Figure 12. The gating strategy used for the CD4$^+$ T cells. Representative scatter dot plots showing the gating strategy used for CD4$^+$ T cells (n=1). CD4$^+$ T cells were identified and gated using the SSC and FL3-PERCP parameters as shown in Plot **A**. The CD4$^+$ population was further analysed as shown in Plots **B**, **C**, **D**, **E,** and **F**. Plot **B** shows the CD4$^+$ INFγ$^+$ T cell gating using the FL3-PERCP and the FL4-APC parameters. A similar strategy was applied to the identification of the CD4$^+$IL2$^+$, CD4$^+$IL10$^+$, and CD4$^+$TNF$^+$ populations (not shown). Plots **C**, **D**, **E** and **F** shows the gating strategy using the FL1 and FL2 parameters, to determine the expression of CD27, CCR5, CCR7, CD45RA, and CD45RO. A similar strategy was used to determine CD69 and CD25 expression.

3.2.4.1. Naïve $CD4^+$T cells

Naïve cells were identified by the co-expression of the CD27 and CD45RA molecules. At the time of starting cART, the mean proportion of the $CD4^+CD27^+CD45RA^+$ population was 16.1±12.8%. A significant change occurred at week 36, when it increased to 25.2±15.3% (p= 0.0017, **Figure 13**). This increase was sustained at week 48 (27±15.4%, p=0.008).

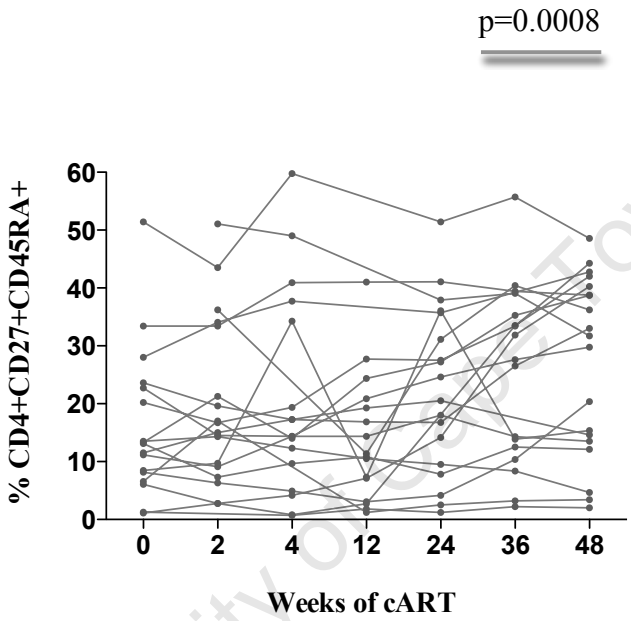

Figure 13. Changes observed in the mean expansion of the$CD4^+CD27^+CD45RA^+$ population during cART. Before and after plot showing the mean expansion of the $CD4^+CD27^+CD45RA^+$ population, which showed a significant increase at week 36, sustained at week 48, (n=19).

3.2.4.2. Central memory $CD4^+$ T cells

Central memory cells were identified by the expression of the CD27 molecule and the lack of expression of either the CD45RA or the CCR5 molecule. The mean percentage of the $CD4^+CD27^+CD45RA^-$ population at week 0 was 34.2±17.8. It increased significantly to 47.8±14.6% (p=0.0001, **Figure 14A**) at week 12, and remained significantly higher until week 48 (46.3±12.1%, p=0.002). This increase was paralleled by the change observed in the $CD4^+CD27^+CCR5^-$ population, which increased from a mean of 52.3±29.5% at week 0, to a mean of 58±22.2% at week 12 and continued to increase until week 48 (67.1±20.1%, p=0.02, **Figure 14B**).

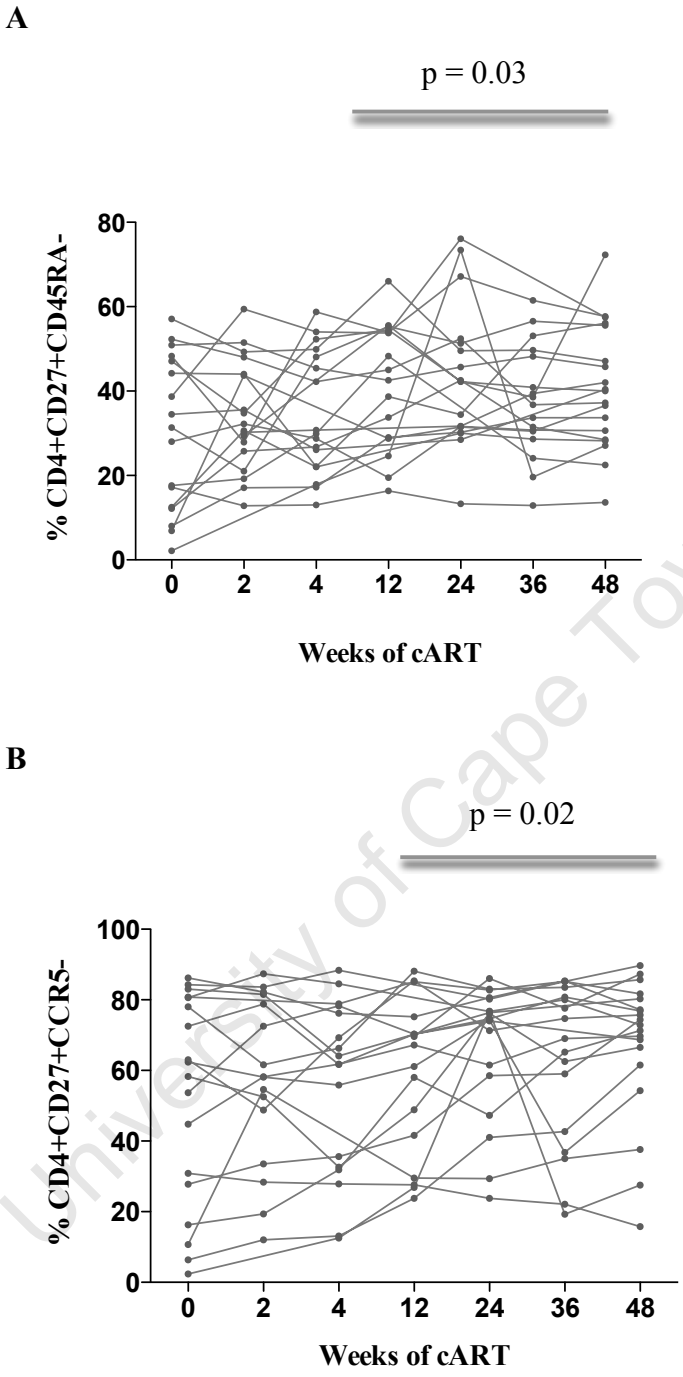

Figure 14. Changes observed in the mean expansion of the$CD4^+CD27^+CD45RA^-$ population during cART. Before and after plot **A,** shows the mean expansion of the $CD4^+CD27^+CD45RA^-$population, (n=19), which increased significantly by 12 weeks (p=0.001) and remained significantly higher until week 48 (one way ANOVA, p=0.03). Before and after plot **B,** shows the mean expansion of the $CD4^+CD27^+CCR5^-$ population, (n=19), which also proportionally increased by 12 weeks (p=0.01) and remained significantly higher until week 48 (p=0.02).

3.2.4.3. Effector $CD4^+$ T cells

The proportion of $CD4^+$ T cells expressing CCR5 (effector memory and terminally differentiated effector T cells) varied widely between the study participants as presented in **Figure 15A.** The median at week 0 was 5.8% (IQR 3-12). It steadily decreased during the study period and significantly by week 48 (2.7%, IQR 2.1-4.8, p=0.02 compared to week 0). Terminally differentiated effector T cells were also analysed by their lack of expression of CD27 and CCR7. The mean percentage of the $CD4^+CD27^-CCR7^-$ T cell population at week 0 was 50±29.1%. This decreased significantly to 38.2±20.4% (p=0.02) at week 12 and continued to decrease until week 48 (32±20.2%, p=0.02 compared to week 0) and supports the change observed in the $CD4^+CCR5^+$ T cell population.

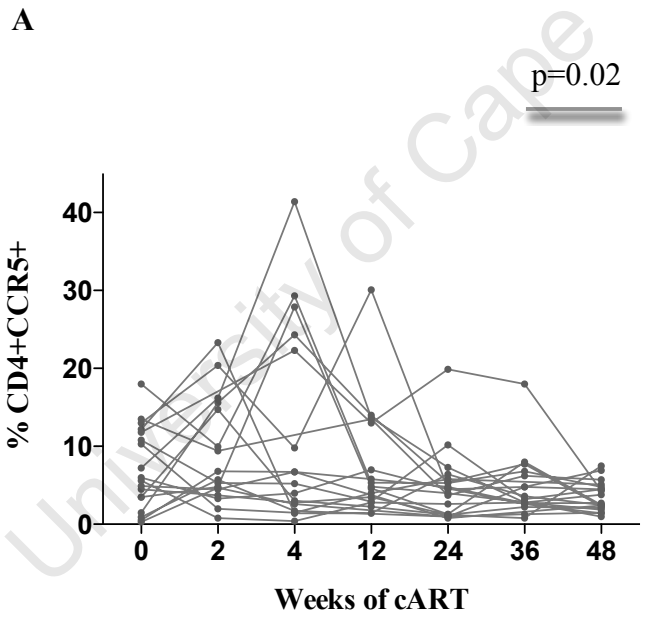

Figure 15A. **Changes observed in the median decrease in the proportion of the $CD4^+CCR5^+$ population during cART.** Before and after plot **A** shows the median decrease in the proportion of the $CD4^+CCR5^+$ population, (n=19). A significant change occurred at week 48 when it decreased to 2.7% (IQR 2.1-4.8, p=0.02) compared to 5.8% (IQR 3-12) at week 0.

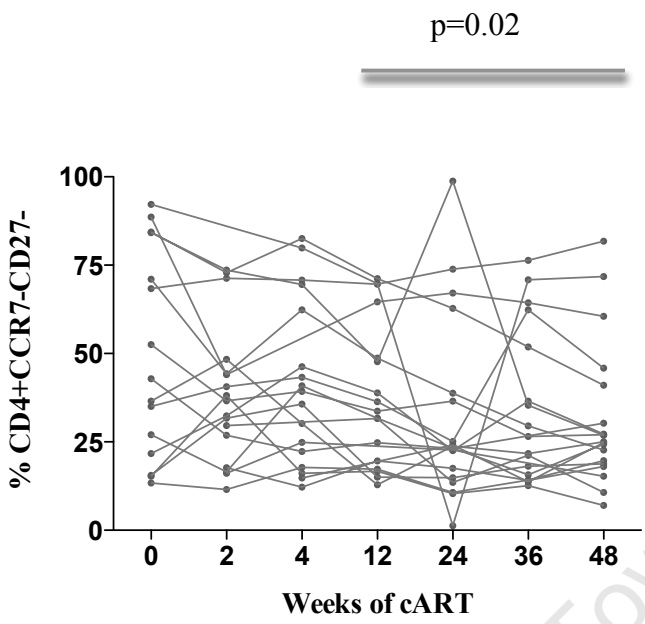

Figure 15B. Changes observed in the mean decrease of the percentage of the CD4$^+$CD27CCR7$^-$, terminally differentiated effector T cells during cART. Before and after plot **B** shows the mean decrease in the percentage of the CD4$^+$CD27$^-$CCR7$^-$, terminally differentiated effector T cells, (n=19). A significant decrease occurred at week 12 (p=0.02), which was sustained until week 48 (p=0.02).

3.2.4.3. Activated CD4$^+$ T cells

The PPD stimulated PBMC were also analysed for the expression of the activation markers CD69 and CD25, as presented in **Figure 16** (128).

The median proportion of the CD4$^+$CD69$^+$ T cells was 1.6% (IQR 1.4-3.8) at week 0 and 1.5% (IQR 1.0-2.1) at week 48. The majority of the CD4$^+$CD69$^+$ population also expressed CD45RO, a marker of memory cells. The median proportion of the CD4$^+$CD69$^+$CD45RO$^+$ population was 1.67% (IQR 1.2-3.3) at week 0 and 1.3% (IQR 0.8-1.6) at week 48, **Figure 17**. The expression of CD25 was also low. The median proportion of CD4$^+$CD25$^+$ T cells was 2.3% (IQR 0.85-6.55) at week 0 and 1.4% (IQR 0.91-3.67) at week 48, **Figure 18**. The expression of these activation markers did not change significantly during the study period.

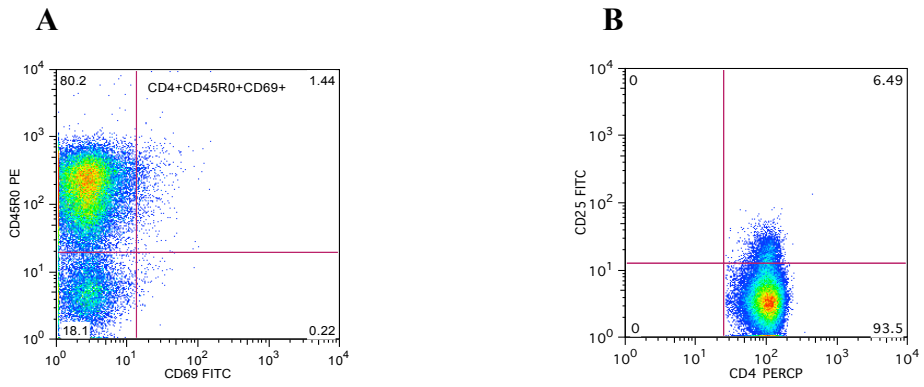

Figure 16. **The identification of the CD4$^+$CD45RO$^+$CD69$^+$ and the CD4$^+$CD25$^+$ T cells**. Scatter dot plot **A** shows the identification of the CD4$^+$CD45RO$^+$CD69$^+$ T cells using the FL2-CD45RO PE and FL1-CD69 FITC parameters, (n=1). Plot **B** shows the identification of the CD4$^+$CD25$^+$ T cells using the FL3-CD4 PerCP and FL1-CD25 FITC parameters, (n=1).

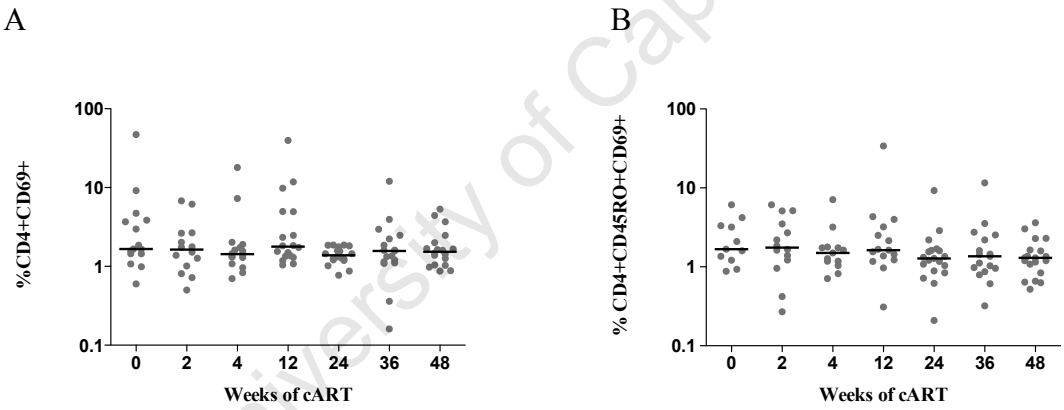

Figure 17. **The median proportions of the CD4$^+$CD69$^+$ T cells, and the CD4$^+$CD69$^+$ T cells expressing CD45RO**. Scatter dot plot **A** shows the median proportions of the CD4$^+$CD69$^+$ T cells, (n=19), during the study period, of which the majority also expressed a memory phenotype as determined by the expression of CD45RO, shown in plot **B**, (n=19). No significant change occurred.

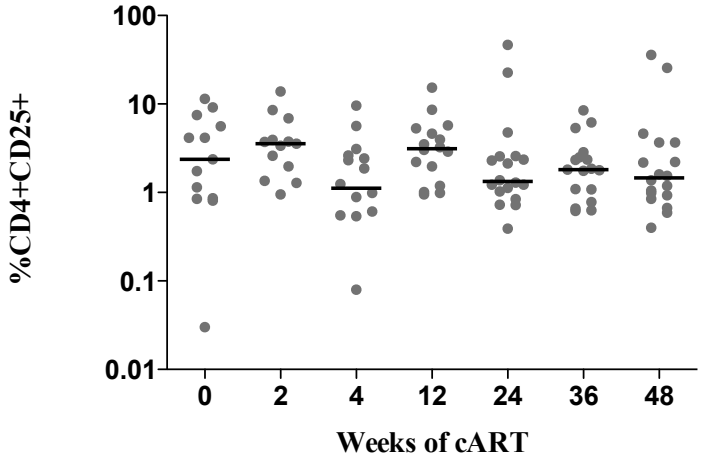

Figure 18. **The median proportions of the $CD4^+CD25^+$ T cells.** Scatter dot plot showing the median proportions of $CD4^+CD25^+$ T cells during the study period, (n=19). No significant change occurred.

3.2.4.4. Cytokine producing $CD4^+$ T cells

The median proportion of PPD specific $CD4^+$ IFN-γ producing cells was 0.92% (IQR 0.28-1.38) at week 0 and decreased significantly to 0.35% (IQR 0.17-0.52) at week 48 of the study period (p=0.021) as presented in **Figure 19A**. The majority of the $CD4^+$ IFN-γ producing cells were of a memory phenotype as >80% expressed CD45RO throughout the study period, as presented in **Figure 20**. Similarly, analysis of the $CD4^+$ $IL\text{-}2^+$ T cells revealed a significant decrease from a median of 0.43% (IQR 0.27-1.3) at week 0 to a median of 0.2% (IQR 0.14-0.36) at week 48, **Figure 19B.** The expression of IL-10 in the $CD4^+$ population was variable, showing a median of 0.36% (IQR 0.22-0.8) at week 0, which increased to 0.63% (IQR 0.21-3.12) at week 2 (p=0.06), and decreased to 0.31% (IQR 0.14-0.53) at week 48 resulting in no overall change during the study period as presented in **Figure 19C.**

The detection of the proportion of $CD4^+$ $CD25^+$ T cells producing IL-10 was extremely low, with a median of 0.09% (IQR 0.03-0.29) at week 0 and 0.02% (IQR 0.01-0.07) at week 48 (not shown). Analysis of TNF expression in the $CD4^+$ T cell population showed no significant change between week 0 (median 0.34%, IQR 0.16-1.1) and week 48 (median 0.31% IQR 0.15-0.63), **Figure 19D**.

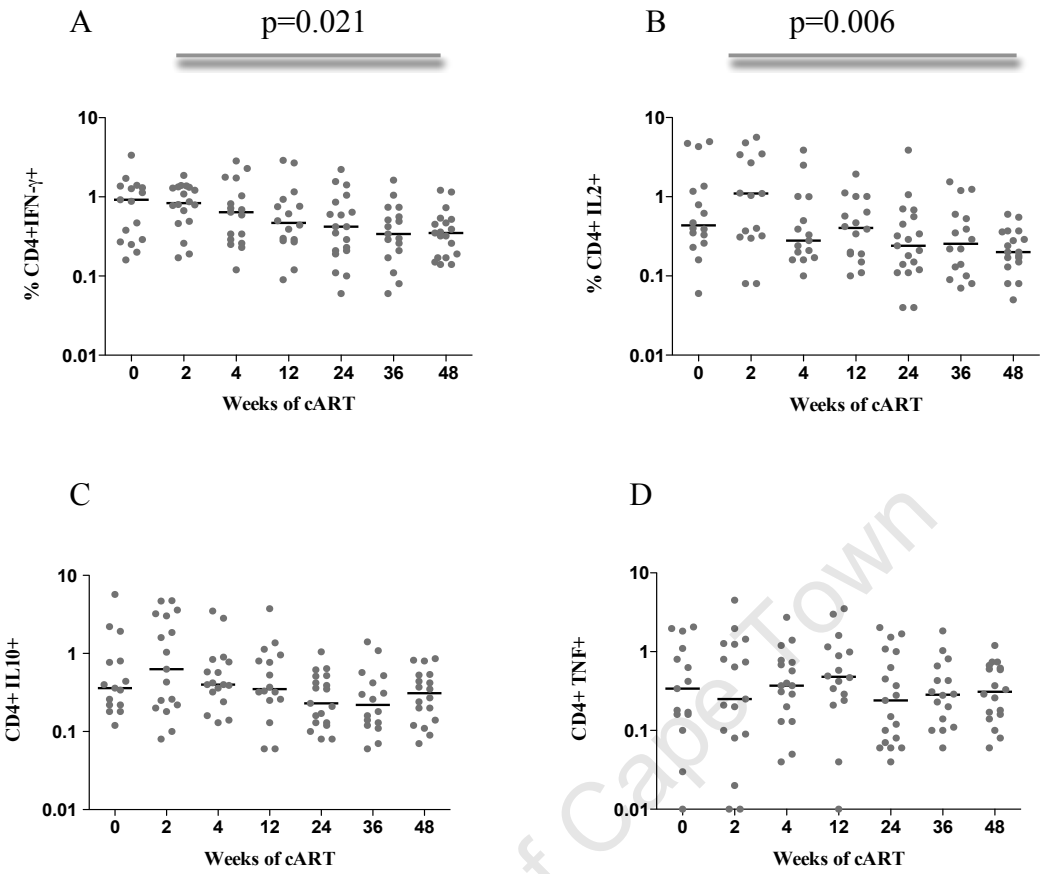

Figure 19. **The median proportions of the cytokine producing CD4$^+$ T cells.** Scatter dot plots showing the median proportions of cytokine producing CD4$^+$ T cells, (n=19). Plot **A** shows the significant decrease of the CD4$^+$ IFN-γ producing T cells from 0.92% (IQR 0.28-1.38) at week 0 0.35% (IQR 0.17-0.52) at week 48. Similarly, Plot **B** shows the significant decrease in the CD4$^+$ IL-2$^+$ T cells from a median of 0.43% (IQR 0.27-1.3) at week 0 to a median of 0.2% (IQR 0.14-0.36) at week 48. Plots **C** and **D** shows the CD4$^+$IL-10$^+$and the CD4$^+$TNF$^+$T cells, respectively, which showed no significant change during the study period.

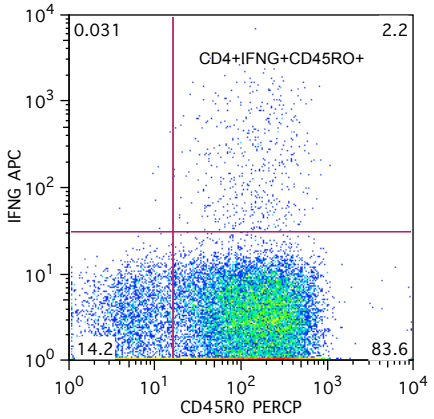

Figure 20. **The identification of the CD4$^+$IFN-γ$^+$CD45RO$^+$ T cells.** Scatter dot plot showing the identification of the CD4$^+$IFN-γ$^+$CD45RO$^+$ T cells using the FL4-IFN-γ APC and the FL3-CD45RO PERCP parameters, (n=1).

The expression of the $CD4^+$ IFN-γ^+, $CD4^+$ IL-2^+ and $CD4^+$ IL-10^+ T cells at 48 weeks of cART were compared to the expression of the same T cell populations in twelve HIV uninfected, MTB sensitized adults (**Section 2.1**). The cytokine secreting $CD4^+$ T cells detected in the HIV infected adults were significantly lower than those detected in the HIV uninfected controls from the same population. The HIV uninfected controls showed a median proportion of 0.73% (IQR 0.5-0.85) for $CD4^+$ IFN-γ^+ T cells, 0.6% (IQR 0.43-1) for $CD4^+$ IL-2^+ T cells and versus 0.84% (IQR 0.6-2.4) respectively for $CD4^+$ IL-$10+^+$ T cells, as presented in **Figure 21**.

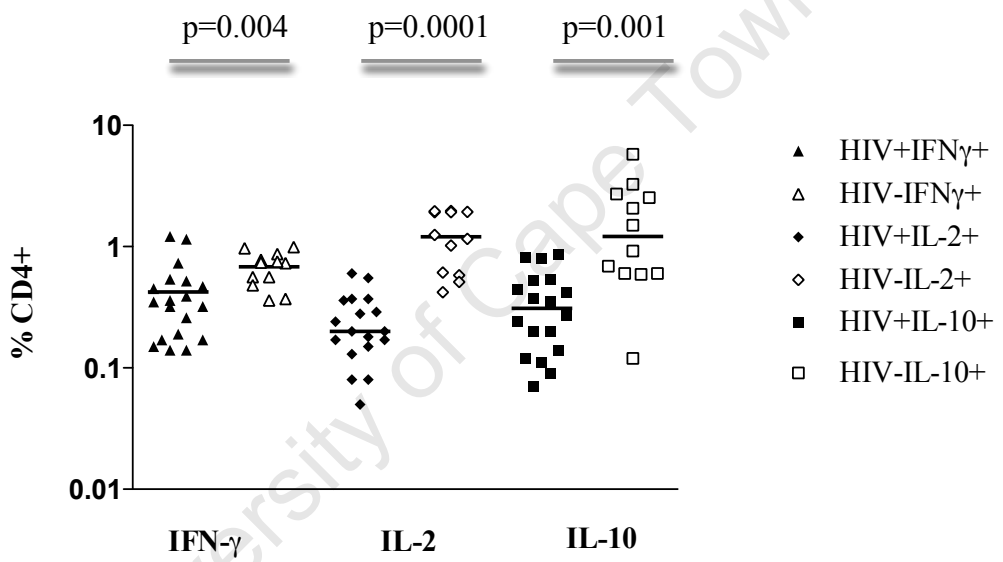

Figure 21. Comparison of cytokine production in HIV infected adults, (n=19), on cART for 48 weeks to HIV uninfected adults, (n=12), from the same community. The median proportion of $CD4^+$IFN-γ^+T cells was 0.35% (IQR 0.17-0.52) versus 0.73% (IQR 0.5-0.85) respectively. The medians of the $CD4^+$ IL2^+ T cells were 0.2% (IQR 0.15-0.36) versus 0.6% (IQR 0.43-1) respectively and those of the $CD4^+$ IL10^+ T cells were 0.31% (IQR 0.14-0.53) versus 0.84% (IQR 0.6-2.4) respectively.

3.2.5. CD8 T cells

$CD8^+$ T cells were identified using the SSC and FL3 (CD8 PerCP) parameters, and selected by gating as presented in **Figure 22**. The median proportion of $CD8^+$ T cells at week 0 was 55% (IQR 39-61). This did not change significantly over the study period, with the median proportion at week 48 being 53% (IQR 43-64, p=0.94), **Figure 23.**

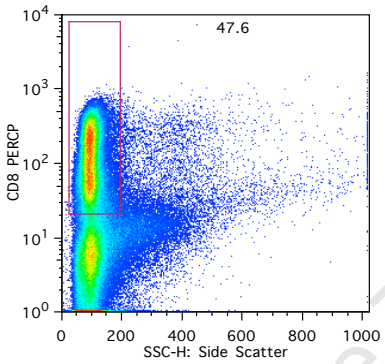

Figure 22. The gating strategy used for $CD8^+$ Tcells. Scatter dot plot showing the gating strategy for $CD8^+$ Tcells, (n=1), which were isolated using the SSC and FL3-PERCP parameters.

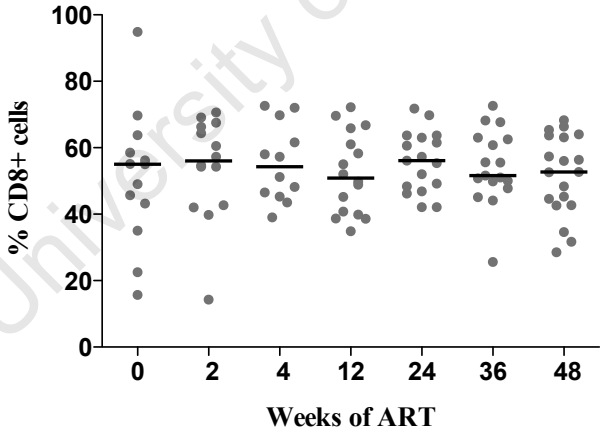

Figure 23. The gating strategy used for $CD8^+$ Tcells. Scatter dot plot showing the median proportions of the $CD8^+$ T cell population over the study period, (n=19). No significant change occurred.

3.2.6. B lymphocytes (B cells)

B cells were identified using a combination of anti-CD3 and anti-CD19. The lymphocyte population was selected by gating, using the FSC and SSC parameters as presented in **Figure 24**. The lymphocyte population was further analysed to identify the $CD3^{-}CD19^{+}$ B cell population using the FL4-APC and the FL3-PerCP parameters. The median proportion of the B cell population declined significantly from a median of 2.27% (IQR 1.3-5.7) at week 0 to 1.26% (IQR 0.6-2.3, p=0.012) at week 48, **Figure 25.**

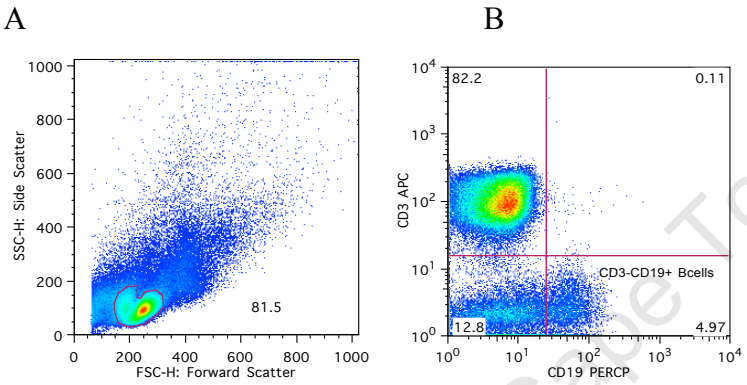

Figure 24. **The gating strategy used for B cells**. Scatter dot plots showing the gating strategy for B cells, (n=1). The lymphocyte population was identified using the SSC and FSC parameters as shown in plot **A**. Plot **B** shows the identification of the $CD3^{-}CD19^{+}$ B cells.

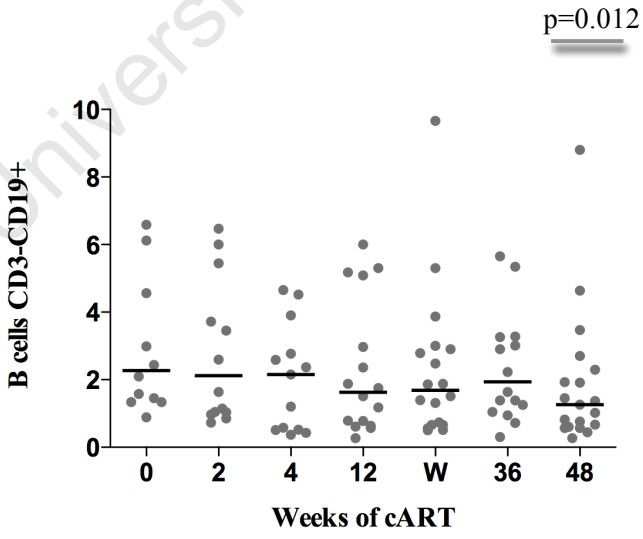

Figure 25. **B cells detected during the study period.** Scatter dot plot plot showing B cell detection during the study period, (n=19). The median proportion of B cells declined significantly from 2.27% (IQR 1.3-5.7) at week 0 to 1.26% (IQR 0.6-2.3, p=0.012) at week 48.

3.2.7. NK and NKT cells

NK and NKT cells were identified using a combination of anti-CD3 and anti-CD56. The lymphocyte population was gated as shown in **Figure 26**, and further analysed to identify NK cells as $CD3^{-}CD56^{+}$ and NKT cells as $CD3^{+}CD56^{+}$, using the FL4-APC and the FL2-PE parameters as presented in **Figure 27 A and B**. The median proportion of the NK cells at week 0 was 4.3% (IQR 2.8-15.2), which nearly doubled over the study period to 8.3% (IQR 3.6-12.10). The median proportion of the NKT population did not change significantly over the study period either, changing from 3.6% (IQR 2.5-5.2) at week 0 to 4.6% (IQR 3-5.7) at week 48, a difference that was not statistically significant, **Figure 27 A and B**.

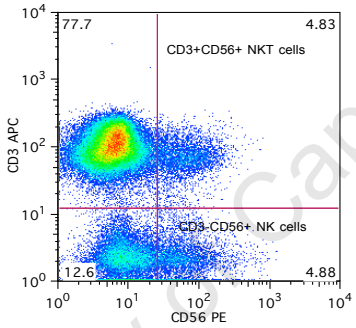

Figure 26. The detection of NK and NKT populations. Scatter dot plot showing detection of NK and NKT populations using the FL4-CD3 APC and FL2-CD56 PE parameters, (n=1). NK cells were identified as $CD3^{-}CD56^{+}$ and NKT cells as $CD3^{+}CD56^{+}$.

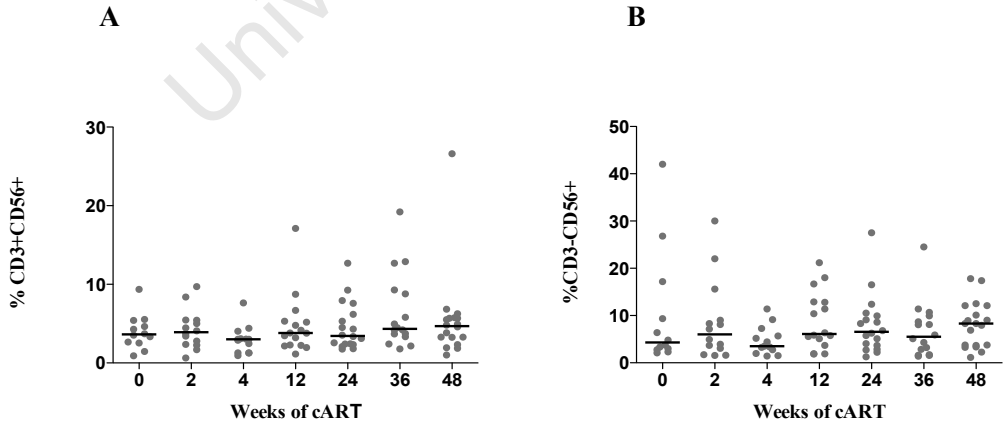

Figure 27. The median proportions of the NKT and NK cells. Scatter dot plots **A** and **B** shows the median proportions of the NKT (n=18), and NK cells (n=19), respectively, over the study period, which did not change significantly.

3.3. The CD4$^+$ T cell IFN-γ response to re-stimulation by MTB antigens

IFN-γ secretion in response to the antigens listed in **Section 2.4.4** was measured using the ELISpot assay described in **Section 2.4**. The ELISpot results were interpreted as stated in **Section 2.4.5.**

3.3.1. PBMC viability and function

The isolation of viable and functional PBMC may be affected by various factors in the isolation process, including cryopreservation (116). Following the thawing and resting process, the viability of the PBMC was assessed using Trypan blue as described in **Section 2.2.1**. The viability of all the PBMC used in the ELISpot assay was >80%.

The functional capability of the PBMC used in the ELISpot assay was also assessed using the flow cytometry, by comparison of its IFN-γ secretion in response to SEB stimulation, to that of freshly isolated PBMC (116). The PBMC were re-stimulated and stained as described in **Section 2.3.2.** The median proportion of the freshly isolated PBMC, secreting IFN-γ, was 13.2% (n=6) compared to a median proportion of 12.3% for the cryopreserved IFN-γ secreting PBMC of the same samples.

3.3.2. Controls

The PHA stimulated control well had a SFC of >5 spots per well, and twice the SFC of the negative control well, for each time point tested. The SFC of the unstimulated negative control wells, if any, were subtracted from the MTB antigen restimulated SFC. **Figure 28** is representative of the study PBMC ELISpot results obtained.

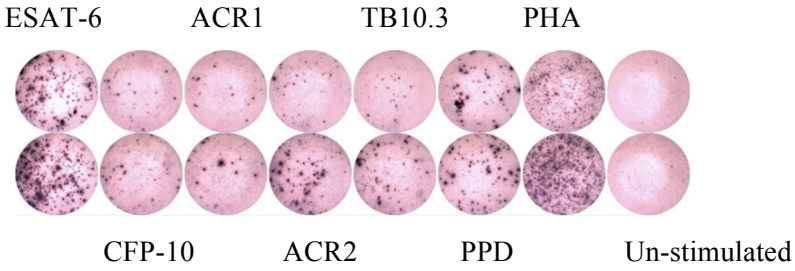

Figure 28. Representative PBMC ELISpot results. The restimulating antigen used is indicated above or beneath the appropriate duplicate wells.

3.3.3. Verification of the ELISpot $CD4^+$ T cell IFN-γ response

Verification of the $CD4^+$ T cell IFN-γ secretion in the ELISpot assay was performed as described in **Section 2.4.4**. Four cryopreserved samples (two from week 36 and two from 48 week) were used in the $CD4^+$ depletion experiments. The efficacy of the $CD4^+$ magnetic bead depletion, was assessed using the surface phenotype staining method described in **Chapter 2**, and was found to be 90 ± 5% efficient.

The depletion of the $CD4^+$ T cells resulted in a mean decrease in the secretion of INF-γ, in response to MTB specific antigen re-stimulation, as follows:

1. 82±11% for ESAT-6
2. 90±10% for CFP-10
3. 86±12% for ACR1
4. 75±7% for ACR2
5. 86±4% for TB10.3

The bar graph in **Figure 29**, presents the effect of $CD4^+$ T cell depletion on the IFN-γ secreting response detected in the ELISpot assay.

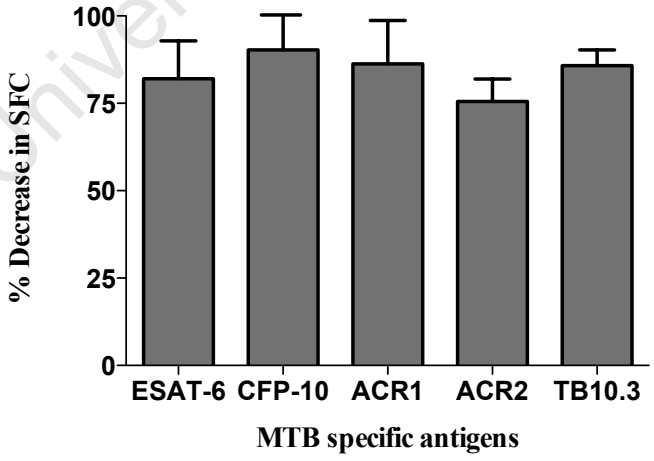

Figure 29. The mean decrease in the IFN-γ SFC, following $CD4^+$ T cell depletion. Bar graph showing the mean decrease in the IFN-γ SFC, following $CD4^+$ T cell depletion in the ELISpot assay, (n=4).

3.3.4. Detection of LTBI

LTBI was established on the basis of an IFN-γ response to the RD1 encoded antigens ESAT-6 and CFP-10, in the ELISpot assay (88,89). Participants, who were unable to be tested at week 0, were tested at either week 2 or week 4 of cART. Two participants did not show a detectable IFN-γ response at week 0, but developed a detectable IFN-γ response by 2 weeks into cART. Thus it was established, within the first month of starting cART, that all participants enrolled had LTBI. The summed response to ESAT-6 and CFP-10, at the time of starting cART, showed a mean of 376 (±482) SFC /10^6 PBMC.

3.3.5. MTB antigen specific IFN-γ ELISpot responses

The number of cryopreserved PBMC available determined the number of antigens tested in the ELISpot assay. Preference was given to the inclusion of PPD, ESAT-6 and CFP10 (as these are antigens currently used in the ascertainment of LTBI), as well as the PHA and negative control. Thus the data for TB10.3, ACR1, and ACR2 do not reflect all the time points. As stated in **Section 2.6**, means are shown for normally distributed data and medians are shown for data not normally distributed.

3.3.5.1. PPD

The median IFN-γ SFC/10^6 PBMC at week 0, in response to PPD re-stimulation, was 7 (IQR 1-50). A significant overall increase occurred by week 48, median SFC/10^6 PBMC 60 (IQR 17-168, p=0.02), **Figure 30**. The most significant increase occurred at week 12, median SFC/10^6 PBMC 192 (IQR 67-833, $p<0.05$ after correcting for multiple comparisons).

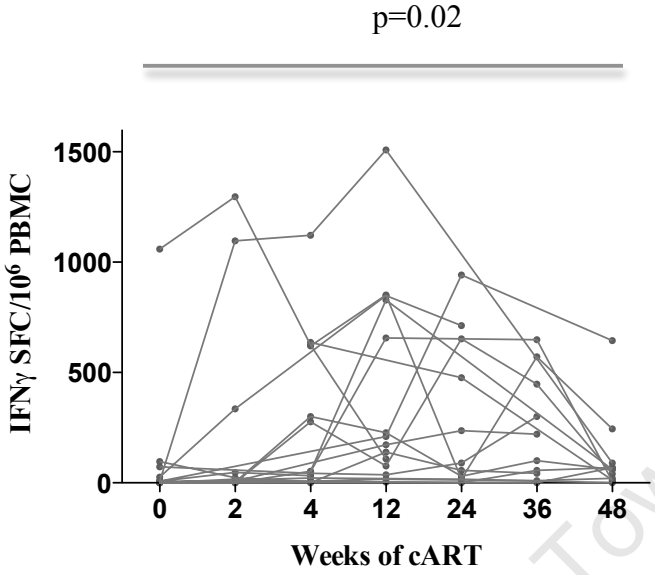

Figure 30. **Changes observed in the median IFN-γ SFC/10^6 PBMC in response to PPD re-stimulation, during cART.** Before and after plot showing the significant increase in the median IFN-γ SFC/10^6 PBMC in response to PPD re-stimulation, from 7 (IQR 1-50) at week 0, to 60 (IQR 17-168) at week 48, p=0.02 (Kruskal Wallis test), (n=15).

3.3.5.2. ESAT-6 and CFP-10

The summed IFN-γ SFC/10^6 PBMC, in response to ESAT-6 and CFP-10 re-stimulation, increased significantly from a mean of 376 (±482) SFC/10^6 PBMC at week 0, to 1077 (±738) SFC/10^6 PBMC at week 48, p=0.04, **Figure 31**.

The most significant increases, compared to week 0, occurred at weeks 36 and 48 weeks (p=<0.05 after correcting for multiple comparisons).

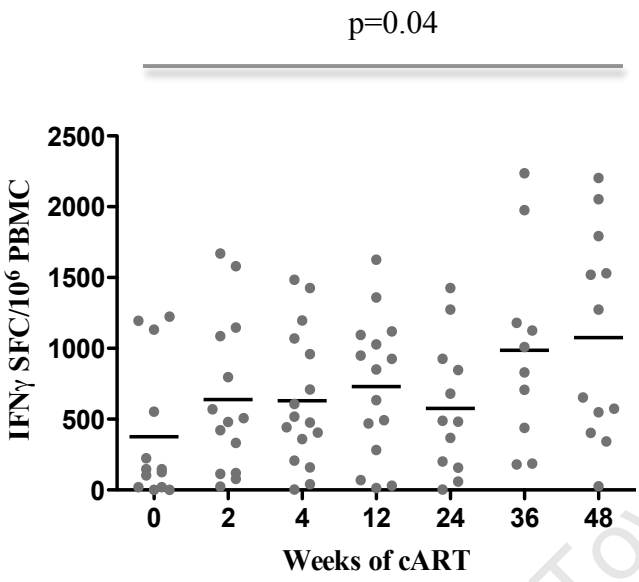

Figure 31. **The summed mean IFN-γ SFC/10^6 PBMC, in response to ESAT-6 and CFP-10 re-stimulation**. Scatter dot plot showing the significant increase in the summed mean IFN-γ SFC/10^6 PBMC, in response to ESAT-6 and CFP-10 re-stimulation, (n=16), from 376 (±482) at week 0, to 1077 (±738) at week 48, p=0.04, (one way ANOVA).

As as result of the heterogeneity introduced to the study, by the group who had previously been treated for TB, the summed IFN-γ response to ESAT-6 and CFP-10 restimulation was also analysed according to previous TB status, on the available samples at week 48, **Figure 32**. The summed response to ESAT-6 and CFP-10 was significantly higher, p=0.01, in the group of patients who did not previously receive TB therapy n=7, compared to those who did n=5. The medians were 1793 SFC/million PBMC (IQR 1397-2129), and 548 SFC/million PBMC (IQR 343-653), respectively at 48 weeks of cART.

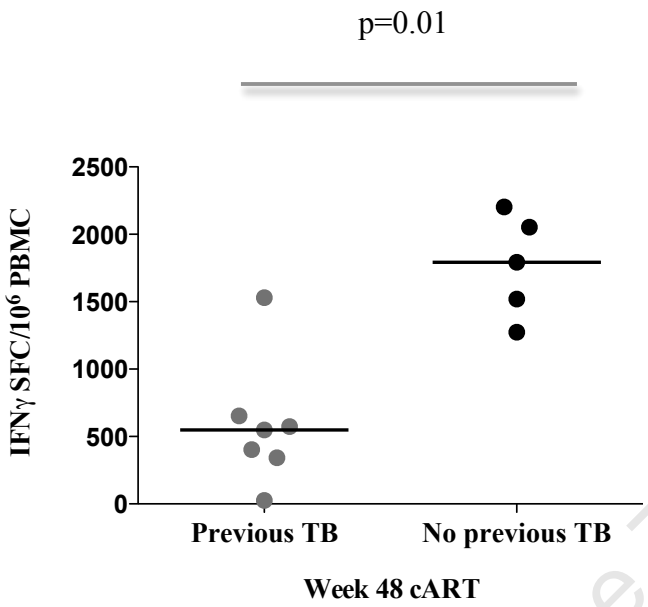

Figure 32. The summed response to ESAT-6 and CFP-10 of the group who had previous TB treatment and the group who did not. Scatter dot plot showing the comparison of summed response to ESAT-6 and CFP-10 between the group who had previous TB treatment, (n=7) and the group who did not, (n=5), at 48 weeks of cART. The difference was significantly higher, p=0.01, in the group who did not have previous TB treatment.

3.3.5.3. ACR1 and ACR2

The IFN-γ response to restimulation by ACR1 and ACR2, reflected an increase during the study period which was significant for ACR2, **Figure 33A** and **33B**. The median SFC/10^6 PBMC for ACR1 was 67 (IQR 22-1535) at week 0, and 864 (IQR 83-1313) at week 48. However, the increase was not statistically significant. The median SFC/10^6 PBMC for ACR2 was 23 (IQR 15-60) at week 0, and 577 (IQR 87-1387) at week 48, p=0.02.

A B p=0.02

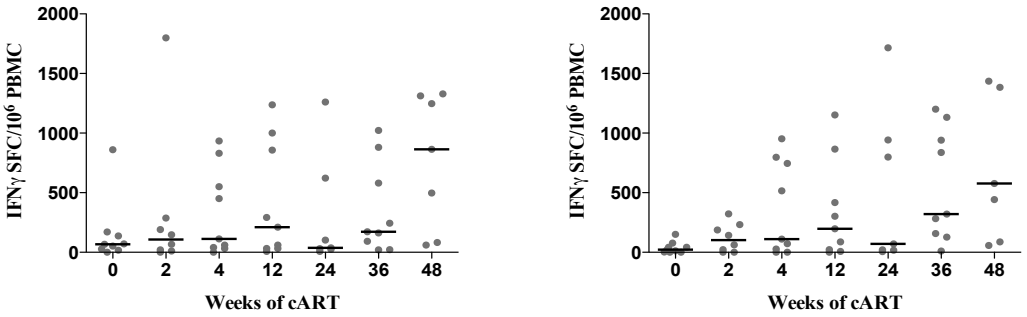

Figure 33A and 33B. **The IFN-γ response to ACR1 and ACR2.** Scatter dot plots showing the IFN-γ response to ACR1and ACR2. Plot **A** shows the median increase in the response to ACR1, (n=9), over the study period. No significant change occurred. Plot **B** shows the median increase in the response to ACR2, (n=9), which was significant at week 48, p=0.02.

3.3.5.4. TB10.3

The median IFN-γ response to TB10.3 showed a significant increase from 40 SFC/10^6 PBMC (IQR 30-975) at week 0, to 1296 SFC/10^6 PBMC (IQR 73-1387) p=0.04, at week 48, **Figure 34.**

p=0.04

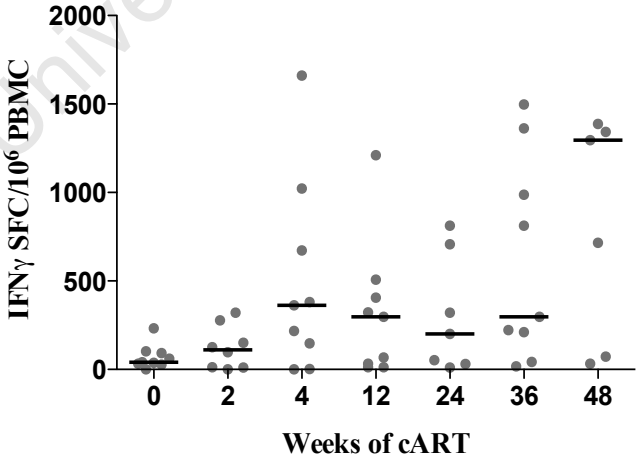

Figure 34. The median IFN-γ response to TB10.3. Scatter dot plot showing the significant increase in the median IFN-γ response to TB10.3 over the 48-week study period, (n=9).

Chapter 4. Discussion and concluding remarks

4.1. Discussion

Studies on cART associated restoration of PPD specific responses and qualitative changes in $CD4^+$ T cells have thus far been limited, to low incidence areas, in developed countries (109)(110)(111)(112,). Similar analyses in areas of high incidence are lacking. It has also been documented that the immune response to MTB is influenced by host genetics (129). Therefore previous studies may not reflect the changes that occur in a high incidence setting in South Africa.

This study describes the restoration of cART associated PPD and MTB specific responses, in a cohort, within a community currently experiencing one of the highest rates of TB incidence. During the 48-week study period, the significantly decreased viral load was accompanied by a statistically significant increase in the CD4 count and the percentage of the $CD4^+$T cell population, changes well associated with effective cART.

An *in vitro* response to the MTB antigens ESAT-6 and CFP-10, as measured in the ELISpot assay, was detected within the first 4 weeks of the study period in all of the 19 participants who had completed the study, indicating LTBI (86)(89). Since the prevalence of LTBI in this community has been documented at a rate of between 70% and 90%, this was not unexpected (130)(131)(132). The summed responses to ESAT-6 and CFP-10 progressively increased during the study period. An increase of 65% occurred over the 48-week study period, which was statistically significant. This data was supported by the parallel, statistically significant, increase in the PPD specific T cells detected by the ELISpot assay.

The summed response to ESAT-6 and CFP-10 restimulation was about 10 times higher than the reponse to PPD restimulation. This difference most likely reflects the difference in antigenic composition of these stimulants. PPD is a mixure of more than 200 proteins shared amongst MTB, *M. Bovis* BCG and other enviromental mycobacteria whereas ESAT-6 and CFP-10 each contain one purified antigen (85)(89)(90)(91). The higher responses to the RD1 antigens, in this group of people, most likely also refect true sensitisation to MTB, and that these responses are preserved even at low CD4 counts, in a high incidence environment.

Additionally, the absolute numbers of IFN-γ producing cells, responding to re-stimulation by the alpha crystallins ACR1 and ACR2, and the secreted Esx family protein, TB10.3, also increased. Despite considerable variability, these increased responses were statistically significant for ACR2 and TB10.3. The depletion of the $CD4^+$ T cells in the ELISpot assay, revealed this population as the main source of IFN-γ secretion.

The summed response to ESAT-6 and CFP-10 in the group who had not previously received TB therapy (n=10, median 1793 SFC/million PBMC), was significantly higher at 48 weeks of cART, when compared to that observed in the group of patients who had previously received TB therapy (n=9, median 548 SFC/million PBMC, p=0.01). The number of RD-1 antigen specific T cells detected by the ELISpot assay has been associated with bacterial load (133). Thus, the lower response detected in the group who had previously been treated for TB, may reflect a lower bacterial load consequent on beneficial antituberculous chemotherapy. Lawn and colleagues have reported similar findings in 2007 on a study performed in a high TB incidence setting in South Africa (134).

A comparison between the proportions of central memory T cells and cytokine secreting $CD4^+$ T cells, as determined by flow cytometry, revealed no differences at week 0 and week 48 of cART between the group who had received previous TB treatment and the group who had not. This suggests that treatment of prior TB did not have a negative influence on cART associated restoration of T cell function. These finding are significant

as they support recommendations on the implementation of isoniazid preventive therapy in HIV infected adults sensitized with MTB (135).

The ELISpot assay does not differentiate between specific T cell subsets. It measures IFN-γ secreted within 6 hours of antigen re-stimulation and therefore reflect the activity of the acquired immunity that is able to provide a rapid effector memory response (136).

The increase in PPD and MTB specific IFN-γ secreting $CD4^+$ T cell numbers, as detected by the ELISpot assay, most likely reflects the reconstitution of MTB specific immune function, influenced by the progressive cART associated reconstitution of the $CD4^+$ T cell pool (the percentage of $CD4^+$ T cells measured in the flow cytometry assay, increased significantly from 7.3% to 17.4%).

At the same time, the proportion of PPD specific IFN-γ secreting $CD4^+$ T cells (effectors) as measured by flow cytometry, showed a decline from 0.92% to 0.35% during the study period. By comparison to the detection of absolute numbers in the ELISpot assay, the effector IFN-γ secreting response detected in the flow cytometry assay, is a measure of a proportional subset within an expanding pool.

Coinciding with the significant decline in the effector population was a significant increase in the proportion of the central memory population at 12 weeks. The central memory T cells population was identified as $CD4^+CD27^+CD45RA^-$, as well as $CD4^+CD27^+CCR5^-$. Both combinations of surface phenotype molecules detected a significant expansion of the central memory population at 12 weeks. The dynamics detected in the central memory, effector memory and terminally differentiated effector, $CD4^+$ populations, most likely reflect cART associated reconstitution and restoration of immune function (137). Thus it could be expected that as the immune function qualitatively improves, the quantitative effort directed toward a specific antigen proportionally declines.

Figure 35, is a concept diagram reflecting the dynamics (corrected for CD4 count), detected within the reconstituting $CD4^+$ T cell pool. At week 0 the proportion of terminally differentiated effector $CD4^+$ T cells are similar to that of the $CD4^+$ $T_{CM.}$

This is a reflection of the rate at which the antigen specific T_{CM} are proliferating in order to generate effector T cells, as the immune response strives to maintain infection control. At week 48 the absolute numbers of each of the subtypes reflected have increased significantly. At the same time, as mentioned above, the proportion of the terminally differentiated effector $CD4^+$ T cells have decreased within the expanding pool. This is paralleled by a significant increase in the proportion of the central memory population. Again, this most likely reflects cART associated restoration of immune function and a consequent reduction in the numbers needed to generate an effective antigen specific response.

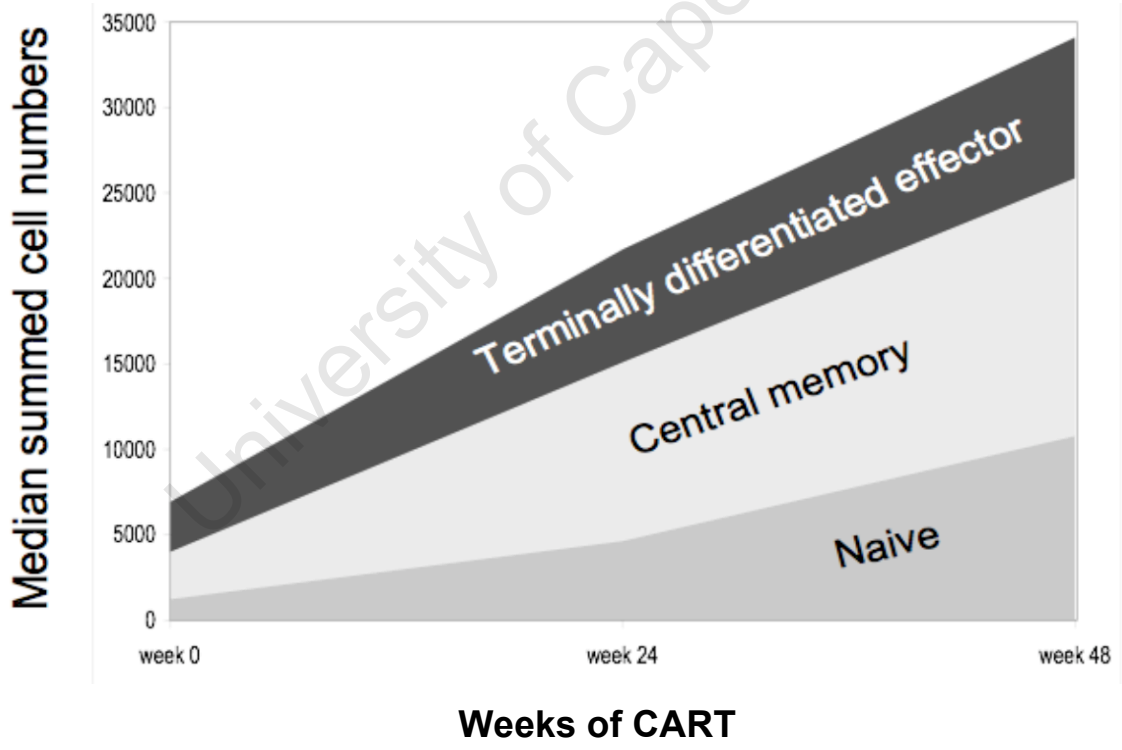

Figure 35. A concept diagram reflecting the cART associated dynamics observed within the reconstituting CD4+ T cell pool. The proportion of naïve ($CD4^+CD27^+CD45RA^+$), central memory ($CD4^+CD27^+CD45RA^-$) and terminally differentiated effector ($CD4^+CD27^-CCR7^-$) T cells were summed at each timepoint for each patient, normalised to 100% and multiplied by the CD4 count per 100 microliter, of each respective patient at that timepoint. The diagram illustrates that while effector T cells proportionally decline during cART, the actual numbers increase.

The proportion of naïve $CD4^+$ T cells ($CD4^+CD27^+CD45RA^+$), showed a significant expansion by 36 weeks of cART. The thymus is the primary supply of naïve T cells. Thymocytes express CXCR4, and are therefore a target for CXCR4 tropic HIV. The observed expansion most likely reflects recovery of thymic function as a result of decreased damage due to viral infection and replication.

Post bone-marrow transplant studies have revealed, that both thymic output, as well as peripheral expansion contributes to immune reconstitution following severe immunodepletion. Similarly it has been shown that thymic output and peripheral expansion contributes to T cell reconstitution in cART treated people (100). Deon *et al*, 2004, measured T cell receptor excision circles to determine the dynamics of recent thymic emigrants in the pheriphery of HIV infected people, who had received anti-retroviral treatment. Their study showed restoration of thymic function following anti-retroviral treatment (157). These observations are supported by the findings of this study.

MTB specific IFN-γ secretion, as a single measurement, may misrepresent the total cytokine response to PPD stimulation and may not be an optimal correlate of protection. Studies investigating the cytokine secreting, antigen specific phenotype of T cells responding to BCG vaccination in infants, and BCG vaccinated adults who had received a boosting recombinant MVA85A vaccine, detected the induction of antigen specific T cells secreting IL-2 and TNF (138)(139). IL-10 has been associated with the regulation of effector T cell responses against TB and is induced by BCG vaccination in newborns (140).

The proportion of $CD4^+IL\text{-}2^+$ T cells declined significantly during the study period, from 0.43% to 0.2% over 48 weeks of cART. This significant decrease in proliferation reflects the qualitative restoration of antigen specific immune function and therefore a lower requirement for quantity.

The variable changes observed in the proportion of $CD4^+IL\text{-}10^+$ cells, did not result in a significant overall change during 48 weeks. No significant change in the proportion of $CD4^+TNF^+$ cells occurred between week 0 and week 48.

The cytokine producing capacity of the HIV infected patients receiving cART for 48 weeks, was compared to that of HIV uninfected controls recruited from the same community. The comparison revealed that the reconstituted $CD4^+$ T cells secreting IFN-γ, IL-2 and IL-10 was significantly lower than that of the HIV uninfected controls ($p<0.01$ for all cytokines). The impaired restoration of functional MTB specific $CD4^+$ T cell responses, despite long-term antiretroviral treatment, has been documented (141). These results support those findings.

TB incidence rates amongst people receiving cART in Cape Town remains higher than the rate amongst HIV uninfected people living in the same community (142). Perhaps this difference in functional ability of the MTB specific $CD4^+$ T cells, contributes to the difference in TB incidence rates described.

The activation status of the $CD4^+$ T cells was determined by the expression of CD69 and CD25 (128). The level of CD69 and CD25 expression was low throughout the study period and showed an insignificant decrease at 48 weeks. The $CD4^+CD69^+$ population was also assessed for expression of CD45RO. The majority of the $CD4^+CD69^+$ population expressed CD45RO, indicating a memory phenotype, which supports previous observations made (112)(143).

The proportion of $CD8^+$ T cells did not change significantly over the 48 weeks of cART. A combination of the ethically approved volume of blood drawn and the limited PBMC available did not allow the detection of changes in activation of the $CD8^+$ T cells. Based on the results from previous studies, a decrease in $CD8^+$ T cell activation would have been expected (144).

Helper T cells contribute to the induction of B cell antibody production (48). HIV induced destruction of the helper $CD4^+$ T cell population would therefore contribute to the HIV infected host's ability to control infection by opportunistic pathogens, via antibody production. The phenotypical and functional alteration of B cells by HIV infection has been shown (145). Additionally, B cells have been shown to act as extracellular reservoirs for HIV, binding virions via CD21 and transporting them to T cells (146). The proportion of B cells identified as $CD3^-CD19^+$ cells showed a significant decline from week 0 to week 48 of cART. Again, this might reflect the cART associated, restoration of immune function and thus the improved quality of response would require fewer numbers. B cell numbers might be affected by viral load, as decreasing viral load would require less HIV specific antibody production.

The frequency and absolute numbers of $CD3^-CD56^+$ NK cells has been shown to decrease in HIV infection (147). A combination of antiretroviral treatment and IL2 therapy was documented to reconstitute the NK cell population. Antiretroviral treatment alone did not show significant change in the NK cell population during a 1-year period of follow up (148). Our study data indicated no significant change over 48 weeks of cART, in the proportion of $CD3^-CD56^+$ cells, supporting the finding above.

The depletion of NKT cells in HIV infection has also been documented (149). A previous study revealed that IL-2 therapy, in conjunction with anti-retroviral therapy, was associated with a significant increase in the reconstitution of NKT cells. Anti-retroviral therapy alone revealed an insignificant trend of 17% in the increase of NKT cells (150). Our study revealed a weak, statistically insignificant reconstitution of the NKT cell population, supporting the finding described above.

4.2. Concluding remarks

A limitation of the study is the lack of a control group of persons not sensitized by MTB. Verification that the MTB specific changes detected are related to the restoration of immunity to MTB infection would require performing the same study procedures, including restimulation by non-TB specific antigens, in appropriate control groups. Such control groups should include an equal number of HIV infected people with no prior sensitisation to MTB, as well as an equal number of HIV uninfected people with prior sensitisation to MTB.

However, the current statistics on prior sensitisation to MTB as well as the rate of HIV-TB co-infection in this high prevalence setting, as mentioned in the introduction, makes the recruitment of such control groups extremely difficult (4)(5)(130)(131)(132). This is confounded by the reality that no test is able to exclude prior sensitisation to MTB in HIV infected people. Previous work in a low incidence setting detected MTB specific T cell reconstitution in HIV infected people (137). Repeating the study in a low TB incidence setting might negate meaningful comparisons because findings in a genetically different population may not be comparable to the findings in Cape Town.

Also, Samri *et al*, 2007, found that in HIV infected people with advanced disease, T cell responses to TB and Cytomegalovirus, but not HIV specific proteins, were restored (151). It therefore seems unlikely that our studies findings are due to non-specific HIV antigen associated reconstitution.

The study aimed to determine the reconstitution of different T cell types in a TB endemic area, where infection pressure, and thus antigen pressure, is high. Therefore the PBMC used in the flow cytometry assay were PPD re-stimulated in an 18-hour incubation period, in an attempt to enhance MTB specific responses, as it is difficult to detect antigen specific responses in advanced HIV disease. This might have resulted in an *in vitro* up regulation of surface marker expression as well as activation induced apoptosis (152)(153).

However a control experiment measuring surface marker expression at various time points, in PPD stimulated as well as unstimulated PBMC, revealed no change in surface marker expression in response to the 18 hour PPD re-stimulation.

The evaluation of immunity to MTB is often measured via the rapid effector, IFN-γ secreting response. However this measure has shown poor correlation with protection to MTB in previous studies (154). Supporting this, a recent study in mice, on vaccine induced protection, revealed that IFN-γ secreting MTB specific $CD4^{+}$T cells correlated poorly with protection and was more likely a reflection of MTB antigen load rather than protection (155). The investigation of vaccine induced MTB specific T cells in human adults and infants have revealed T cells with complex phenotypic and polyfunctional cytokine secreting profiles (138)(139). These polyfunctional MTB specific T cells have been detected in HIV infected people, and were inversely correlated with HIV viral load (156).

Missed data, is a concern in longtitudinal studies. It results in reduction of sample size and possibly loss of power. In our setting, the most frequent cause of missed time points, was temporary relocation of the study participants. We analysed the available data using statistical measures designed to handles missing data, however, future longtitudinal studies planned for this setting should carefully consider this factor (158).

Despite the limitations, the results of this study provide insight into the reconstitution of the presumed protective immune responses, during cART, in MTB sensitised people. cART is associated with an absolute increase in effector function while the proportional measure declines. The correlate most strongly associated with increased cART mediated, MTB specific immunity, was the central memory response. This may contribute significant considerations to the design of new vaccines as well as the monitoring of MTB specific vaccine induced, protective responses.

4.3. Presentations and publications

The work contained in this dissertation was presented in the following presentations and manuscript:

Oral presentations

1. "The Effect of Antiretroviral Treatment on the T Cell Response of Patients With Latent *M. Tuberculosis* Infection (LTBI)."
   Ronnett Seldon, Graeme Meintjes, Priscilla Mouton, Willem A. Hanekom, Robert J. Wilkinson, Katalin A Wilkinson. Faculty of Health Sciences, IIDMM, University of Cape Town.
   Research Day 2006, School Of Biomedical Sciences, Faculty of Health Sciences, University of Cape Town."
2. "Phenotypic analysis of *M. tuberculosis* specific immune restoration during highly active antiretroviral treatment."
   Ronnett Seldon, Graeme Meintjes, Priscilla Mouton, Willem A. Hanekom, Robert J. Wilkinson, Katalin A Wilkinson. Faculty of Health Sciences, IIDMM, University of Cape Town.
   The Imperial College London Wellcome Centre for Clinical Tropical Medicine Annual Scientific Meeting, Lima, Peru, February 2007.
3. "Phenotypic analysis of M.tuberculosis specific immune restoraration during highly active antiretroviral treatment."
   Ronnett Seldon, Graeme Meintjes, Priscilla Mouton, Willem A. Hanekom, Robert J. Wilkinson, Katalin A. Wilkinson. Faculty of Health Sciences, IIDMM, University of Cape Town.
   University of Cape Town and Groote Schuur Hospital, Department of Medicine, 34th Annual Research Day, September 2007.
4. '"Phenotypical analysis of M.Tuberculosis specific CD4T cells that expand during combined antiretroviral therapy in people with latent Tuberculosis infection."
   Ronnett Seldon, **Institute of Infectious Diseases and Molecular Medicine.**
   University of Cape Town, Institute of Infectious Disease & Molecular Medicine, Immunology Seminar Series, September 2009.

Poster presentation

1. "Combined antiretroviral therapy and the restoration of protective T cell responses against tuberculosis in HIV infected people."
   Ronnett Seldon[*], Priscilla Mouton[†], Graeme Meintjes[*,†], Molebogeng X. Rangaka[*], Willem Hanekom[*], Robert John Wilkinson[*, †, ‡, §],Katalin Andrea Wilkinson[*,‡]
   *Institute of Infectious Diseases and Molecular Medicine and Department of Medicine, University of Cape Town, South Africa
   †Infectious Diseases Unit, GF Jooste Hospital, Cape Town, South Africa
   ‡National Institute for Medical Research, Mill Hill, London, NW7 1AA
   §Division of Medicine, Wright Fleming Institute, Imperial College London, W2 1PG UK
   Novartis Institute for Tropical Diseases Symposiun on Tuberculosis, Maputo, Mozambique, September 2008.

Publication

1. Wilkinson KA, Seldon R, Meinttjies G, Rangaka MX, Hanekon WA, Maartens G, Wilkinson RJ. Dissection of regenerating T cell responses against tuberculosis in HIV infected adults sensitized by *Mycobacterium tuberculosis*. *American Journal of respiratory and Critical Care Medicine* **(180,7)** 2009: 674-683.

Poster Abstracts

1. "Highly active antiretroviral therapy and the restoration of protective responses against tuberculosis in HIV infected people."
   Katalin A. Wilkinson, Ronnett Seldon, Graeme Meintjes, Priscilla Mouton, Willem A. Hanekom, Robert J. Wilkinson.
   Institute of Infectious Diseases and Molecular Medicine, Faculty of Health Sciences, University of Cape Town, South Africa.
   Keystone Challenges of global Vaccine Development, Cape Town, South Africa, October 8-13 2007.

2. "Combined antiretroviral therapy and the restoration of protective responses against tuberculosis in HIV infected people."
   Katalin A. Wilkinson[1,2], Ronnett Seldon[1], Graeme Meintjes[1], Priscilla Mouton[1], Willem A. Hanekom[1], Robert J. Wilkinson[1,2,3]
   1.Institute of Infectious Diseases and Molecular Medicine, Faculty of Health Sciences, University of Cape Town, South Africa
   2.National Institute for Medical research, Mill Hill, London NW7 1AA, UK
   3.Division of Medicine, Imperial College London W2 1PG UK.
   Seventh International Conference on thte Pathogenesis of Mycobacterial Disease, Saltsjobaden, Sweden, June 2008.

References

1. Thomas N. Daniel, "The history of tuberculosis", *Respiratory Medicine* **100** (2006): 1862-1870.
2. World Health Organisation, *Tuberculosis Fact Sheet N˚104*, (2007) [Online]. Available: http://www.who.int/mediacentre/factsheets/fs104/en/ **[2009, February 2]**.
3. Christopher Dye, Suzaan Scheele, Paul Dolin, Vikram Pathania, Mario C. Raviglione, "Global burden of tuberculosis: estimated incidence, prevalence, and mortality by country", *JAMA* **282** (1999): 677-686.
4. Candy Day, Andy Gray, "Health and related indicators", *Health Systems Trust Report* (2006): 417-420.
5. World Health Organisation, *Global tuberculosis control - surveillance, planning, financing,* (2008) [Online]. Available: http://www.who.int/tb/publications/globalreport/2008/en **[2009, February 2**].
6. Robin Wood, Gary Maartens, and Carl J.Lombard, "Risk Factors for Developing Tuberculosis in HIV-1-Infected Adult From Communities With a Low or Very High Incidence of Tuberculosis", *Journal of Acquired Immune Deficiency Syndromes* **23** (2000): 75-80.
7. Pam Sonnenberg, Judith R. Glynn, Katherine Fielding, Jill Murray, Peter Godfrey-Fausset, and Stuart Shearer, "How Soon After Infection With HIV Does The Risk Of Tuberculosis Start To Increase? A Retrospective Cohort Study in South African Gold Miners", *The Journal of Infectious Diseases* **191** (2005): 150-158.
8. Jill Murray, Pam Sonnenberg, Nelson G, Bester Andre, Stuart Shearer, and Judith R. Glynn, "Cause of death and presence of respiratory disease at autopsy in an HIV-1 seroconversion cohort of southern African gold miners", *AIDS* **21,6** (2007): 97-104.
9. Helmy Rachman, and Stefan H. E. Kaufmann, "Exploring functional genomics for the development of novel intervention strategies against tuberculosis", *International Journal of Medical Microbiology* **297** (2007): 559-567.

10. Thomas R. Frieden, Timothy R. Sterling, Sonal S. Munsiff, Catherine J. Watt and Christopher Dye, "Tuberculosis", *The Lancet* **362** (2003): 887-899.
11. Neil W. Schluger and William N. Rom, "The Host Immune response to Tuberculosis", *American Journal of Respiratory and Critical Care Medicine* **157** (1998): 679-691.
12. Arthur M. Dannenberg, "Immune Mechanisms in the Pathogenesis of Pulmonary Tuberculosis", *Reviews of Infectious Diseases* **11,2** (1989): 369-378.
13. Padmini Salgame, "Host innate and Th1 responses and the bacterial factors that control *Mycobacterium tuberculosis* infection", *Current Opinion in Immunology* **17** (2005): 374-380.
14. Reinout van Crevel, Tom H. M.Ottenhof, and Jos W. M. van der Meer, "Innate immunity to Mycobacterium tuberculosis", *Clinical Microbiology Reviews* **5,2** (2002): 294-309.
15. Dominic O. Co, Laura H. Hogan, Shin-Il Kim and Mayas Sander, "Mycobacterium Granulomas: keys to a long-lasting host-pathogen relationship", *Clinical Immunology* **113** (2004): 130-136.
16. Bernadette M. Saunders and Warwick J. Britton, "Life and death in the granuloma: immunopathology of tuberculosis", *Immunology and Cell Biology* **85** (2007): 103-111.
17. Matthew J. Fenton and Mary W. Vermeulen, "Immunopathology of Tuberculosis: Roles of Macrophages and Monocytes", *Infection and Immunity* **64,3** (1996): 683-690.
18. Peter Anderson, "Vaccine strategies against Latent tuberculosis infection", *TRENDS in Microbiology* **15,1** (2006): 7-13.
19. Karel Styblo, "Recent advances in epidemiological research in tuberculosis", *Advances in Tuberculosis Research* **20** (1980): 1-63.
20. JoAnn M. Turfariello, John Chan, and JoAnne Flynn, "Latent tuberculosis: mechanisms of host and bacillus that contribute to persistent infection", *The Lancet Infectious Diseases* **3** (2003): 578-590.
21. JoAnne L. Flynn and John Chan, "Immunology of tuberculosis", *Annual Reiew of Immunology* **19** (2001): 93-129.

22. Troels Lillebaek, Asger Dirksen, Inga Baess, Benedicte Strunge, Vibeke O. Thomsen, and Ase B. Andersen, "Molecular Evidence of Endogenous Reactivation of Mycobacterium tuberculosis after 33 years of Latent Infection", *The Journal of Infectious Diseases* **185** (2002): 401-404.

23. Peter A. Selwyn, Diana Hartel, Victoria A. Lewis, Ellie E. Schoenbaum, Sten H. Vermund, Robert S. Klein, Andrew T. Walker, and Gerald H. Friedland, " A prospective study of the risk of tuberculosis among intravenous drug users with human immunodeficiency virus infection", *The New England Journal of Medicine* **320,9** (1989): 545-550.

24. Sally Blower and Virginie Supervie, "Predicting the future of XDR tuberculosis", *The Lancet 7* (2007): 443.

25. Stephen E. Weis, Philip C. Slocum, Francis X. Blais, Barbara King, Mary Nunn, G. Burgis Matney, Enriqueta Gomez, and Brian H. Foresma, "The Effect of Directly Observed Therapy on the Rates of Drug Resistance and Relapse in Tuberculosis", *The New England Journal of Medicine* **330** (1994): 1179-1184.

26. Mario C. Raviglione, and Ian M. Smith, "XDR Tuberculosis: Implications for Global Public Health", *The New England Journal of Medicine* (2007): 356-357.

27. World Health Organisation, *Global tuberculosis control - surveillance, planning, financing,* (2003) [Online]. Available: http://www.who.int/tb/gtb **[2009, February 2].**

28. Matteo Zignol, Mehran S. Hosseini, Abigail Wright, Catharina Lambregt-van Weezenbek, Paul Nunn, Catherine J. watt, Brian G. Williams, and Christopher Dye, "Global Incidence of Multidrug-Resistant Tuberculosis", *The Journal of Infectious diseases* 1**94** (2006): 479-485.

29. Neel R Gandhi, Anthony Moll, A Willem Sturm, Robert Pawinski, Thiloshini Govender, Umesh Lalloo, Kimberly Zeller, Jason Andrews, Gerald Friedland, "Extensively drug-resistant tuberculosis as a cause of death in patients co-infected with tuberculosis and HIV in a rural area of South Africa," *The Lancet* **368** (2006): 1575-1580.

30. Richard J. O'Brien, and Mel Spigelman, "New drugs for tuberculosis: current status and future prospects", *Clinics in Chest Medicine* **26** (2005): 327-340.
31. Marc P. Gerard, Uli Fruth, and Marie-Paule Kieny, "A review of vaccine research and development: Tuberculosis", *Vaccine* **23** (2005): 5725-5731.
32. Paul E.M. Fine, "Variation in protection by BCG: implications of and for heterologous immunity", *The Lancet* **346** (1995): 1339-1345.
33. Stephen H.E. Kaufmann, "Is the development of a new tuberculosis vaccine possible?" *Nature Medicine* **6,9** (2000): 955-960.
34. Anil K. Tyagi, and Aparna Khera, "Protection against tuberculosis: How close are we to a perfect vaccine?" *Current Science* **86,1** (2004): 154-166.
35. Peter J. Delves, and Ivan M. Roit, "The Immune System", *The New England Journal of Medicine* **343,1** (2000): 37-49.
36. Charles A. Janeway, Paul Travers, Mark Walport, Mark J. Shlomchik, "Basic concepts in Immunology: The components of the immune system," in *Immunobiology 6th Edition* (Garland Science Publishing 2005), 2-11.
37. Ruslan Medzhitotv, and Charles Janeway, " Innate Immunity", *The New England Journal of Medicine* **343,3** (2000): 338-344.
38. Ulrich H. von Adrian, and Charles R. Mackay, " T-cell Function and Migration", *The New England Journal of Medicine* **343,14** (2000): 1020-1034.
39. Eun-Kyeong Jo, " Mycobacterial interaction with innate receptors: TLRs, C-type lectins, and NLRs", *Current Opinion in Infectious Diseases* **21** (2008): 279-286.
40. Carl Nathan, and Michael U. Shiloh, " Reactive oxygen and nitrogen intermediates in the relationship between mammalian hosts and microbial pathogens", *Proceedings of the National Academy of Sciences USA* **97,16** (2000): 8841-8848.
41. JoAnne L.Flynn, and John Chan, "Immune evasion by Mycobacterium tuberculosis", *Current Opinion in Immunology* **15** (2003): 450-455.
42. Ronald N. Germaine, "MHC-dependant antigen processing and peptide presentation: providing legends for T lymphocyte activation", *Cell* **76,2** (1994): 287-299.

43. Florian Winau, Guido Hegasy, Stefan H.E. Kaufmann, Ulrich E. Schaible, " No life without death-apoptosis as prerequisite for T cell Activation", *Apoptosis* **10,4** (2005): 707-715.

44. Ulrich E. Schaible, Florian Winnau, Peter A. Sieling, Karsten Fisher, Helen L. Collins, Kristine Hagens, Robert L. Modlin, Volker Brinkmann, and Stefan H. Kaufmann, "Apoptosis facilitates antigen presentation to T lymphocytes through MHC-1 and CD1 in tuberculosis", *Nature Medicine* **9** (2003): 1039-1046.

45. Kenneth M. Murphy, Steven L. Reiner, "The lineage decisions of helper T cells", *Nature Reviews Immunology* **2** (2002): 933-944.

46. Anne O'Garra, and Leslie M. McEvoy, and Albert Zlotnik, " T-cell subsets: chemokine receptors guide the way", *Current Biology* **8,18** (1998): 646-649.

47. Chen Dong, " Diversification of T-helper-cell lineages: finding the family root of IL-17 producing cells", *Nature Reviews Immunology* **6** (2006): 329-333.

48. Randolph J. Noelle, Meenakashi Roy, David M. Shepherd, Ivan Stamenkovic, Jeffrey A. Ledbetter, and Alejandro Aruffo, " A 39-kDa protein on activated helper T cells binds CD40 and transduces the signal for cognate activation of B cells", *Proceedings of the National Academy of Sciences USA* **89,14** (1992): 6550–6554.

49. Christophert Caux, Catherine Massacrier, Beatrice Vanbervliet, Bertrand Dubois, Cees Van Kooten, Isabelle Durand, and Jacques Banchereau, "Activation of human dendritic cells through CD40 cross-linking", *The Journal of Experimental Medicine* **180,4** (1994): 1263-1272.

50. Uno Shu, Mamoru Kiniwa, Chang You Wu, Charles Maliszewski, Nadia Vezzio, John Hakimi, Maurice Gately, and Guy Delespesse, "Activated T cells induce interleukin-12 production by monocytes via CD40-CD40 ligand interaction", *European Journal of Immunology* **25,4** (1995): 1125-1128.

51. Mark R. Alderson, Richard J. Armitage, Teresa W. Tough, Laura Strockbine, William C. Fanslow, and Melanie K. Spriggs, "CD40 expression by human monocytes: regulation by cytokines and activation of monocytes by their ligand for CD40", *The Journal of Experimental Medicine* **178,2** (1993): 669-674.

52. Charles A. Janeway, Paul Travers, Mark Walport, Mark J. Shlomchik, "T Cell-Mediated Immunity: T cell-mediated cytotoxicity", in *Immunobiology 6th Edition* (Garland Science Publishing 2005), 351-356.

53. Charles A. Janeway, Paul Travers, Mark Walport, Mark J. Shlomchik, "Innate Immunity: Induced innate responses to infection", in *Immunobiology 6th Edition* (Garland Science Publishing 2005), 75-95.

54. W.Henry Boom, David H. Canaday, Scott A. Fulton, Adam J. Gehring, Roxana E. Rojas, Marta Torres, " Human immunity to *M. tuberculosis*: T cell subsets and antigen processing", *Tuberculosis Edinburgh* **83** (2003): 98-106.

55. Bernadette M. Saunders, Anthony A. Frank, Ian M. Orme, and Andrea M. Cooper, "CD4 is required for the development of a protective granulomatous response to pulmonary tuberculosis", *Cellular Immunology* **216** (2002): 65-72.

56. Melanie J. Newport, Clare M. Huxley, Sara Huston, Catherine M. Hawrylowicz, Ben A. Oostra, Robert Williamson, and Michael Levin, "A mutation in the interferon-gamma-receptor gene and susceptibility to mycobacterial infection", *The New England Journal of Medicine* **335,26** (1996): 1941-1949.

57. Dyana K. Dalton, Sharon Pitts-Meek, Satish Keshav, Irene S. Figari, Allan Bradley, and Timothy A. Stewart, " Multiple defects of immune cell function in mice with disrupted interferon-gamma genes", *Science **259,5102*** (1993): 1739-1742.

58. Irene S Leal, Birgitte Smedegard, Peter Anderson, and Ruiu Appelberg, "Failure to induce enhanced protection against tuberculosis by increasing T-cell-dependant interferon-γ generation", *Immunology* **104** (2001): 157-161.

59. Daniel Elias, Hanna Akuffo, and Sven Britton." PPD induced *in vitro* interferon gamma production is not a reliable correlate of protection against Mycobacterium tuberculosis", *Transactions of the Royal Society of Tropical Medicine and Hygiene* **99** (2005): 363-368.

60. Charles A. Janeway, Paul Travers, Mark Walport, Mark J. Shlomchik, "T Cell-mediated Immunity: General properties of armed effector T cells", in *Immunobiology 6th Edition* (Garland Science Publishing 2005), 343-351.

61. Joseph Keane, Sharon Gershon, Robert P. Wise, Elizabeth Mirabile-Levens, John Kasznica, William D. Schwieterman, Jeffrey N. Braun, and M. Miles Braun, " Tuberculosis associated with infliximab, a tumor necrosis factor alpha-neutralizing agent", *The New England Journal of Medicine* **345,15** (2001): 1098-1104.

62. Joanna Turner, Mercedes Gonzalez-Juarrerog, Debo L. Ellis, Randy J. Basaraba, Andre Kipnis, Ian M. Orme, and Andrea M. Cooper, "In Vivo IL-10 Production Reactivates Chronic Pulmonary Tuberculosis in C57BL/6 Mice", *The Journal of Immunology* **169** (2002): 6343-6341.

63. Vassiliki A. Boussiotis, Eunice Y. Tsai, Edmond J. Yunis, Sok Thim, Julio C. Delgado, Christopher C. Dascher, Alla Berezovskaya, Dominique Rousset, Jean-Marc Reynes, and Anne E. Goldfeld, " IL-10-producing T cells suppress immune responses in anergic tuberculosis patients", *The Journal of Clinical Investigation* ***105*** (2000): 1317-1325.

64. Stephen D. Lawn, Donna Rudolp, Alain Ackah, Doulhourou Coulibaly, Stefan Wiktor, and Renu B. Lal, "Lack of induction of interleukein-2-receptor- α in patients with tuberculosis and human immunodeficiency virus co-infection: implications for pathogenesis", *Transactions of The Royal Society of Tropical Medicine and Hygiene* **95** (2001): 449-452.

65. JoAnne L. Flynn, Marsha M. Goldstein, Karla J. Triebold, Beverley Koller, Barry R. Bloom, " Major histocompatibility complex class I-restricted T cells are required for resistance to Mycobacterium tuberculosis infection", *Proceedings of the National Academy of Sciences USA* **89** (1992): 12013-12017.

66. Ajit Lalvani, Roger Brookes, Robert J. Wilkinson, Adam S. Malin, Ansar A. Pathan, Peter Andersen, Hazel Dockrell, Geoffrey Pasvol, and Adrian V. S. Hill, "Human cytolytic and interferon γ-secreting CD8 T lymphocytes specific for Mycobacterium tuberculosis", *Proceedings of the National Academy of Sciences USA* **95** (1998): 270-275.

67. Sugata Roy, Peter F. Barnes, Ankita Garg, Shiping Wu, David Cosman, and Ramakrishna Vankayalapati, "NK Cells Lyse T Regulatory Cells That Expand in Response to an Intracellular Pathogen", *The Journal of Immunology* **180** (2008): 1729-1736.

68. Jayne S. Sutherland, David J. Jeffries, Simon Donkor, Brigitte Walther, Philip C. Hill, Ifedayo M.O. Adetifa, Richard A. Adegbola, Martin O.C. Ota, " High granulocyte/lymphocyte ratio and paucity of NKT cells defines TB disease in a TB-endemic setting", *Tuberculosis Edinburgh* epub ahead of print (2009): 1-7.

69. Katsuhiko Tsukaguchi, Kithiganahalli N. Balaji, and W. Henry Boom, " $CD4^+$ αβ T cell and γδ T cell responses *to Mycobacterium tuberculosis*: similarities and differences in antigen recognition, cytotoxic effector function and cytokine production", *The Journal of Immunology* **154** (1995): 1786-1796.

70. Francesco Dieli, Marita Troye-Blomberg, Juraj Ivanyi, Jean Jacques Fournie, Alan M. Krensky, Marc Bonneville, Marie A. Peyrat, Nadia Caccamo, Guido Sireci, and Alfredo Salerno, " Granulysin-dependant killing of intracellular and extracellular Mycobacterium tuberculosis by Vgamma9/Vdeltta2T lymphocytes", *The Journal of Infectious Diseases* **184** (2001): 1082-1085.

71. Julian K. Hickling, "Measuring human T-lymphocyte function", *Expert Reviews in Molecular Medicine* (1998): 1-20.

72. Laura L. Carter and Susan L. Swain, "Single cell analyses of cytokine production", Current Opinion in Immunology **9** (1997): 177-182.

73. Lance Hultin and Patricia Hultin, "Flow Cytometry-Based Immunophenotyping Method and Applications", in Barbara Detrick, Robert G. Hamilton and James D. Folds, Editors, *Manual of Molecular and Clinical Laboratory Immunology 7th Edition* (American Society for Microbiology Press 2006), 147-157.

74. Misha Rahman, "Principles of the flow cytometer", in *Introduction to Flow Cytometry* (Serotec Ltd. 2006), 4-7.

75. Kim Gautho, Editor, "Optimizing Instrument Electronics", in *BD CellQuest ProSoftware User's Guide* (Becton Dickson Biosciences 2002), 77-103.

76. Calman Prussin, Dean D. Metcalfe, "Detection of intracytoplasmic cytokine using flow cytometry and directly conjugated anti-cytokine antibodies", *Journal of Immunological Methods* **188** (1995): 117-128.

77. Smita A. Ghanekar, Holden T. Maecker, and Vernon C. Maino, "Monitoring of Immune Response Using Cytokine Flow cytometry", in Barbara Detrick, Robert G. Hamilton and James D. Folds, Editors, *Manual of Molecular and Clinical Laboratory Immunology 7th Edition* (American Society for Microbiology Press 2006), 353-360.

78. Shar L. Waldrop, Christine J. Pitcher, Dolores M. Peterson, Vernon C. Maino and Louis J. Picker, "Determination of Antigen-specific Memory/Effector $CD4^+$ T Cell Frequencies by Flow Cytometry", *Journal of Clinical Investigation* **99** (1997): 1739-1750.

79. Catherine Barbey, Estelle Pradervand, Nathalie Barbier, and Francois Spertini, "Ex Vivo Monitoring of Antigen-Specific $CD4^+$ T Cells after Recall Immunizattion with Tetanus Toxoid", *Clinical and Vaccine Immunology* **14,9** (2007): 1108-1116.

80. Cecil C. Czerkinsky, L A. Nilsson, H Nygren, O Ouchterlony, A Tarkowski, "A solid-phase enzyme-linked immunospot (ELISPOT) assay for enumeration of specific antibody-secreting cells", *Journal of Immunological Methods* **65** (1983): 109-121.

81. Barbara L. Shacklet and Douglas F. Nixon, "Methods for Detection of Antigen-Specific T Cells by Enzyme-Linked Immunospot Assay (ELISPOT)", in Barbara Detrick, Robert G. Hamilton and James D. Folds, Editors, *Manual of Molecular and Clinical Laboratory Immunology 7th Edition* (American Society for Microbiology Press 2006), 245-248.

82. Ajit Lalvani, Ansar A.Pathan, Helen McShane, Robert J. Wilkinson, Mohammed Latif, Christopher P. Conlon, Geoffrey Pasvol, and Adrian V. S. Hill, "Rapid Detection of Mycobacterium tuberculosis Infection by Enumeration of Antigen-specific T Cells", *American Journal of Respiratory and Critical Care Medicine* **163** (2001): 824-828.

83. Annika C. Karlsson, Jeffrey N. Martin, Sophie R.Younger, Barry M. Bredt, Lorrie Epling, Rollie Ronquillo, Arjun Varma, Steven G. Deeks, Joseph M. McCune, Douglas F. Nixon, Elizabeth Sinclair, " Comparison of the ELISPOT and cytokine flow cytometry assays for the enumeration of antigen-specific T cells", *Journal of Immunological Methods* **282** (2003): 141-153.

84. Sally A. Clark, Stephen L. Martin, Anton Pozniak, A Steel, Brian Ward, Jake Dunning, Donald C. Henderson, Mark Neslon, Brian Gazzard, and Peter Kelleher, " Tuberculosis antigen-specific immune responses can be detected using enzyme-linked immunospot technology in human immunodeficiency virus (HIV)-1 patients with advanced disease", *Clinical and Experimental Immunology* **150** (2007): 238-244.

85. Philip C. Hill, Roger H. Brookes, Annette Fox, Dolly Jackson-Sillah, Moses D. Lugos, David J. Jeffries, Simon A. Donkor, Richard A. Adegbola, Keith P. W. J. McAdam. " Surprisingly High Specificity of the PPD Skin Test for M. tuberculosis Infection from Recent Exposure in The Gambia", *PLoS* **1** (2006): 1-8

86. Ajit Lalvani, "Diagnosing Tuberculosis infection in the 21st Century: New Tools To Tackle an Old enemy," *CHEST* 1**31** (2007): 1898-1906.

87. Stewart T. Cole, "Comparative mycobacterial genomics", *Current* Opinion *in Microbiology* **1** (1998): 567–571.

88. Sandra M. Arend, Anrik C. F. Engelhard, Gertjan Groot, Kirsten de Boer, Peter Andersen, Tom H. M. Ottenhoff, and Jaap T. van Dissel, "Tuberculin Skin Testing Compared with T-Cell Responses to Mycobacterium tuberculosis-Specific and Nonspecific Antigens for Detection of Latent Infection in Persons with Recent Tuberculosis Contact", *Clinical and Diagnostic Laboratory Immunology* **8,6** (2001): 1089-1096.

89. Madhukar Pai, Lee W. Riley, and John M. Colford Jr, "Interferon-γ assays in the immunodiagnosis of tuberculosis: a systemic review", *The Lancet Infectious Diseases* **4** (2004): 761-775.

90. Katalin A. Wilkinson, O M. Kon, Sandra M. Newton, Graeme M. Meintjies, R N. Davidson, Geoffrey Pasvol, "Effect of treatment of latent tuberculosis infection on the T cell response to *Mycobacterium tuberculosis* antigens", *The Journal of*

Infectious Diseases **193** (2006): 354-359.

91. Delia Goletti, Ornella Buttera, Federica Bizzoni, Rita Casetti, Enrico Girardi, and Fabrizio Poccia, "Region of Difference 1 Antigen Specific $CD4^+$ Memory T Cells Correlate with a Favourable Outcome of Tuberculosis", *The Journal of Infectious Diseases* **194** (2006): 984-992.
92. Thierry Garnier, Karin Eiglmeier, Jean- Christophe.Camus, Nadine Medina, Hima Mansoor, Melinda Pryor, Stephanie Duthoy, Sophie Grondin, Celine Lacroix, Christel Monsempe, Sylvie Simon, Barbara Harris, Rebecca Atkin, Jon Doggett, Rebecca Mayes, Lisa Keating, Paul R. Wheeler, Julian Parkhill, Bart G. Barrell, Stewart T. Cole, Stephen V. Gordon, and R. Glyn Hewinson", "The complete genome sequence of *Mycobacterium bovis*", *Proceedings of the National Academy of Sciences USA* **100,13** *(*2003): 7877–7882.
93. Philip J. Hogarth, Karen E. Logan, H. Martin Vordermeier, Mahavir Singh, R. Glyn Hewinson, Mark A. Chambers, "Protective immunity against *Mycobacterium bovis* induced by vaccination with Rv3109c—a member of the *esat-6* gene family", *Vaccine* **23** (2005) 2557–2564.
94. Graham R. Stewart, Sandra M. Newton, Katalin A. Wilkinson, Ian R. Humphreys, Helen N. Murphy, Brian D. Robertson, Robert J. Wilkinson, and Douglas B. Young", The stress-responsive chaperone α-crystallin 2 is required for pathogenesis of Mycobacterium tuberculosis", *Molecular Microbiology* **55,4** (2005): 1127-1137.
95. Katalin A. Wilkinson, Graham R. Stewart Sandra M. Newton, H. Martin Vordermeier, John R. Wain, Helen N. Murphy, Katherine Horner, Douglas B. Young, and Robert J. Wilkinson, " Infection Biology of a Novel Crystallin of *Mycobacterium tuberculosis*: Acr2", *The Journal of Immunology* **174** (2005): 4237-4243.
96. Charles R. Mackay, "Dual personality of memory T cells", *Nature* **401** (1999): 659-660.
97. Frederica Sallusto, Danielle Lenig, Reinhold Forster, Martin Lipp and Antonio Lanzavecchia, "Two subsets of memory T lymphocytes with distinct homing potentials and effector functions", *Nature* **40**1 (1999): 708-712.

98. Michael D. Roth, "Interleukin 2 induces the expression of CD45RO and the memory phenotype by CD45RA$^+$ peripheral blood lymphocytes", *Journal of Experimental Medicine* **179** (1994): 857-864.

99. Elisabeth Amyes, Andrew J. McMichael, and Margaret Callan, " Human CD4 T Cells Are Predominantly Distributed among Six Phenotypically and Functionally Distinct Subsets", The Journal of Immunology **175** (2005): 7565-5773.

100. Daniel C Douek, Louis J. Picker, and Richard A. Koup, "T Cell Dynamics in HIV-1Infectiton", *The Annual Review of Immunology* **21** (2003): 265-304.

101. Steven M. Schnittman, H Clifford Lane, Jack Greenhouse, Jesse S. Justement, Michael Baseler, and Anthony S. Fauci, "Preferential infection of CD4+ memory Tcells by human immunodeficiency virus type 1: evidence for a role in the selective T-cell functional defects observed in infected individuals", *Proceedings of the National Academy of Sciences USA* **87,16** (1990): 6058-6062.

102. Joseph J. Mattapallil, Daniel C.Douek, Brenna Hill, Yoshiaki Nishimura, Malcolm Martin, and Mario Roederer, "Massive infection and loss of memory CD4+T cells in multiple tissues during acute SIV infection", *Nature* **434** (2005): 1093-1097.

103. Jason M. Brenchley, Timothy W. Schacker, Laura E. Ruff, David A. Price, Jodie H. Taylor, Gregory J. Beilman, Phuong L. Nguyen, Alexander Khoruts, Matthew Larson, Ashley T. Haase, and Daniel C. Douek, "CD4+ T Cell Depletion during all Stages of HIV Disease Occurs Predominantly in the Gastrointestinal Tract", *The Journal of Experimental Medicine* **200,6** (2004): 749-759.

104. Enrico Girardi, Giorgio Antonucci, Paola Vanacore, Marco Libanore, Isabella Errante, Alberto Matteelli, Giuseppe Ippolito, and the Gruppo Italiano di Studio Tubercolosi e AIDS (GISTA), "Impact of combination antiretroviral therapy on the risk of tuberculosis among persons with HIV infection", *AIDS* **14,13** (2000): 1985-1991.

105. Guilherme Santoro-Lopes, Ana Maria Felix de Pinho, Lee H. Harrison, and Mauro Schechter, "Reduced Risk of Tuberculosis among Brazilian Patients with Advanced Human Immunodeficiency Virus Infection Treated with highly Active Antiretroviral Therapy", *The Journal of Clinical Infectious Diseases* **34** (2002): 543-546.

106. Ole Kirk, Jose M. Gatell, Amanda Mocroft, Court Pedersen, Rui Proenca, Ray P. Brettle, Simon E. Barton, Philippe Sudre, Andrew N. Phillips, and Jens D. Lundgren for the EuroSIDA Study Group, "Infections with *Mycobacterium tuberculosis* and *Mycobacterium avium* among HIV-infected Patients after the Introduction of Highly Active Antiretroviral Therapy", *American Journal of Respiratory and Critical Care Medicine* **162** (2000): 865-872.

107. Jeffrey L. Jones, Deborah L Hanson, Mark S. Dworkin, Kevin M. De CocK, and The Adult/Adolescent Spectrum of HIV Disease Group, " HIV-associated tuberculosis in the era of highly active antiretroviral therapy*", The International Journal of Tuberculosis and Lung Disease* **4,11** (2000): 1026-1031.

108. Motasim Badri, Douglas Wilson, Robin Wood, "Effect of highly active antiretroviral therapy on incidence of tuberculosis in South Africa: a cohort study", *The Lancet* **359** (2002): 2059-2064.

109. Tao Sheng Li, Roland Tubiana, Christine Katlama, Vincent Calvez, Hocine Ait Mohand, Brigitte Autran, " Long-lasting recovery in CD4 T-cell function and viral-load reduction after highly active antiretroviral therapy in advanced HIV-1 disease", *The Lancet* **351** (1998): 1682-1686.

110. Michael M. Lederman, "Immune restoration and $CD4^+$ T-cell function with antiretroviral therapies", *AID*S **15,2** (2001): S11-S15.

111. Alan L. Landay, Daniel Bettendorf, Ellen Chan, John Sprittzler, John L. Schmitz, R. Pat Bucy, Charles J. Gonzalez, Carol T. Schnizlein-Bick, Tom Evans, Kate E. Squires, and John P. Phair, "Evidence of Immune reconstitution in Antiretroviral Drug-Experienced Patients with Advanced HIV Disease", *AIDS RESEARCH AND HUMAN RETROVIRUSES* **18,2** (2002): 95-102.

112. Richard L.Hengel, Maria C. Allende, Robin L. Dewar, Julia A. Metcalf, JoAnn M. Mican, and H. Clifford Lane, " Increasing $CD4^+$ Cells Specific for Tuberculosis Correlate witth Improved Clinical Immunity after Highly Active Antiretroviral Therapy", *AIDS RESEARCH AND HUMAN RETROVIRUSES* **18,13** (2002): 969-975.

113. Beate Kampmann, Gwen N. Tena-Coki, Mark P. Nicol, Michael Levin and Brian Eley, " Reconstitution of antimycobacterial immune responses in HIV-infected children receiving HAART", *AID*S 20 (2006): 1011-1018.

114. Arne Boyum, "Isolation of Lymphocytes, Granulocytes and Macrophages", *Scandinavian Journal of Immunology* **5** (1976): 9-15.

115. Warren Strober, "Trypan Blue Exclusion Test of Cell Viability", in *Current Protocols in Immunology: Appendix 3B* (John Wiley & Sons 1997), A.3B.1-A.3B.2.

116. Adriana Weinberg, "Cryopreservation of Peripheral Blood Mononuclear Cells", in Barbara Detrick, Robert G. Hamilton and James D. Folds, Editors, *Manual of Molecular and Clinical Laboratory Immunology 7th Edition* (American Society for Microbiology Press 2006), 241-24.

117. Adriana Weinberg, Li Zhang, Darby Brown, Alejo Erice, Bruce Polsky, Martin S. Hirsch, Susan Owens, And Karan Lamb, "Viability and Functional Activity of Cryopreserved Mononuclear Cells ", *Clinical and Diagnostic Laboratory Immunlogy* 7,4 (2000): 714-716.

118. David Ernst, Editor, " Immunofluorescent Staining of Intracellular Molecules for Flow Cytometric Analysis"' in *Techniques for Immune Function Analysis: Application Handbook, 1st Edition* (Becton Dickson Biosciences 2003), 61-82.

119. Holden T. Maecker, "Cytokine Flow Cytometry", in Teressa S. Hawley and Robert G. Hawley, Editors, *Methods in Molecular Biology: Flow Cytometry Protocols, 2nd Edition* (Humuna Press Inc. 2004), 95-107.

120. Stefanie Kuerten, Tobias R. Schlingmann, Tarvo Rajasalu, Doychin N. Angelov, Paul V. Lehmann, and Magdelana Tary-Lehman, " Lack of Disease Specificity Limits the Usefulness of In Vitro Costimulation in HIV- and HCV-Infected Patients", *Clinical and Developemental Immunology* (2008): 1-10.

121. Joseph E. Alouf, Heide Muller-Alouf, "Staphylococcal and streptococcal superantigens: molecular, biological and clinical aspects", *International Journal of Medical Microbiology* **292** (2003): 429-440.

122. Becton Dickson Biosciences, *BD Calibrite Beads Technical Data Sheet* (3/2003) [Online]. Available: http://www.bdbiosciences.com/ptProduct.jsp?prodId=70022 **[2009,August 23].**

123. David Ernst, Editor, " Immunofluorescent Staining of Cell Surface Molecules for Flow Cytometric Analysis of Immune Function", in *Techniques for Immune Function Analysis: Application Handbook, 1st Edition* (Becton Dickson Biosciences 2003), 9-32.

124. Christian R. Kreher, Markus T. Dittrich, Robert Guerkov, Bernhard O. Boehm, Magdalena Tary-Lehmann, "$CD4^+$ and $CD8^+$ cells in cryopreserved human PBMC maintain full functionality in cytokine ELISPOT assays", *Journal of Immunological Methods* **278** (2003): 79-93.

125. John W. Sleasman, Beatriz H. Leon, Lucia F. Aleixo, Mabel Rojas, and Maureen Goodenow, "Immunomagnetic Selection of Purified Monocyte and Lymphocyte Populations from Peripheral Blood Mononuclear Cells following Cryopreservation", *Clinical and Diagnostic Laboratory Immunology* **4,6** (1997): 653-658.

126. Axl A. Neurauter, Mark Bonyhadi, Eli Lien, Lars Nokleby, Erik Ruud, Stephanie Camacho, Tanja Aarvak, " Cell Isolation and Expansion using Dynabeads®", *Advances in Biochemical Engineering/Biotechnology* **106** (2007): 41-73.

127. Sharon Shalekoff, Leisl Page-Shipp, and Caroline T. Tiemessen, " Effects of Anticoagulants and Temperature on Expression of Activation Markers CD11b and HLA-DR on Human Leukocytes", *Clinical and Diagnostic Laboratory Immunology* **5,5** (1998)" 695-702.

128. Arnoldo Caruso, Stefano Lecenziati, Maria Corulli, Angelo D. Canaris, Maria A. De Francesco, Simona Fiorentini, Laura Peroni, Francesca Fallacara, Francesco Dima, Andrea Balsari, and Adolfo Turano, " Flow Cytometric Analysis of Activation Markers on Stimulated T Cells and Their Correlation With Cell Proliferation", *Cytometry* **27** (1997): 71-76.

129. Paramasivam Selvaraj, "Host genetics and tuberculosis sensitivity", *Current Science* **86,1** (2004): 115-121.

130. Molebogeng Xheeda Rangaka, Katalin A.Wilkinson, Ronnett Seldon, Gilles van Cutsem, Graem Ayton Meintjies, Chelsea Morroni, Priscilla Mouton, Lavanya Diwakar, Tom G. Connell, Gary Maartens, and Robert J. Wilkinson, "Effect of HIV-1 Infection on T-Cell-based and Skin Test Detection of Tuberculosis Infection", *American Journal of Respiratory and Critical Care Medicine* **175** (2007): 514-520.

131. Tom G. Connell, Muki S. Shey, Ronnett Seldon, Molebogeng X. Rangaka, Gilles van Cutsem, Marcella Simsova, Zuzana Marcekova, Peter Sebo, Nigel Curtis, Lavanya Diwakar, Graem A. Meintjies, Claude Leclerc, Robert J. Wilkinson, Katalin A. Wilkinson, "Enhanced ex vivo stimulation of mycobacterium tuberculosis-specific Tcells in HIV-infected persons via antigen delivery by the Bordetella Pertussis adenylate cyclase vector", *Clinical and Vaccine Immunology* **14** (2007): 847-854.

132. Molebogeng X. Rangaka, Lavanya Diwakar, Ronnett Seldon, Gilles van Cutsem, Graem A. Meintjties, Chelsea Morroni, Priscilla Mouton, Muki S. Shey, Gary Maartens, Katalin A. Wilkinson, and Robert J. Wilkinson, "Clinical, Immunological, and epidemiological importance of antituberculosis T cell responses in HIV-infected Africans", *Journal of Clinical Infectious Disease*s **44** (2007): 1639-1646.

133. Ansar A. Pathan, Katalin A. Wilkinson, Paul Klenerman, Helen McShane, Robert N. Davidson, Geoffrey Pasvol, Adrian V.S. Hill, and Ajit Lalvani, "Direct Ex Vivo Analysis of Antigen-Specific IFN-γ-Secreting CD4 T Cells in Mycobacterium tuberculosis-Infected Individuals: Associations with Clinical Disease State and Effect of Treatment", *The Journal of Immunology* **167** (2001): 5217-5225.

134. Stephen D. Lawn, Nonzwakazi Bangani, Monica Vogt, Linda-Gail Bekker, Motasim Badri, Marjorie Ntobongwana, Hazel M. Dockrell, Robert J. Wilkinson, and Robin Wood, " Utility of interferon-γ ELISPOT assay responses in highly tuberculosis exposed patients with advanced HIV infection in South Africa", *BMC Infectious Diseases* **7,99** (2007): 1639-1646.

135. Marcus A. Bachhuber, Robert Gross, "Mortality benefit of isoniazid preventative therapy in HIV-positive persons: a simulation study", *The International Journal of Tuberculosis and Lung Disease* **13,8** (2009): 1038-1040.

136. Ajit Lalvani, Roger Brooks, Sophie Hambleton, Warwick J. Britton, Adrian v. S. Hill, and Andrew J. McMichael, " Rapid Effector Function in $CD8^+$ Memory T cells", *The Journal of Experimental Medicine* **186** (1997): 859-865.

137. Brigitte Autran, Guislaine Carcelain, Tao Sheng Li, Catherine Blanc, Dominique Mathez, Roland Tubiana, Christine Katlama, Patrice Debre, Jacques Leibowitch, "Positive effects of combined antiretroviral therapy on $CD4^+$T cell homeostasis and function in advanced HIV disease", *Science* **277** (1997): 112-116.

138. Andreia P. Soares, Thomas J. Scriba, Sarah Joseph, Ryhor Harbacheuski, Rose Ann Murray, Sebastian Gelderbloem, Anthony Hawkridge, Gregory D. Hussey, Holden Maecker, Gilla Kaplan, and Willem A. Hanekom, "Bacillus Calmette-Guerin Vaccination of Human Newborns Induces T cells with Complex Cytokine and Phenotypic Profiles", *The Journal of Immunology* **180** (2008): 3569-3577.

139. Natalie E. Beveridge, David A. Price, Joseph P. Casazza, Ansar A. Pathan, Clare R. Sander, Tedi E. Asher, David R. Ambrozak, Melissa L. Precopio, Phillip Scheinberg, Nicola C. Alder, Mario Roederer, Richard A. Koup, Daniel C. Douek, Adrian V.S. Hill, Helen McShane," Immunisation witth BCG and recombinant MVA85A induces long-lasting, polyfunctional Mycobacterium tuberculosis-specific CD4+ memory T lymphocye populations", *European Journal of Immunology* **37,11** (2007): 3089-3100.

140. Willem A.Hanekom, "The immune response to BCG vaccination of newborns", *Annals of the New York Academy of Sciences* **1062** (2005): 69-78.

141. Rebecca Sutherland, Hongbing Yang, Thomas J. Scriba, Beatrice Ondondo, Nicola Robinson, Christopher Conlon, Annie Suttil, Helen McShane, Sarah Fidler, Andrew McMichael, and Lucy Dorrell, "Impaired IFN-γ-secreting capacity in mycobacterial antigen-specific CD4 T cells during chronic HIV-1 infection despite long-term HAART", *AIDS* **20** (2006): 821-829.

142. Stephen D. Lawn, Motasim Badri, and Robin Wood, "Tuberculosis among HIV-infected patients receiving HAART: Long term incidence and risk factors in a South African cohort", *AID* **19** (2005): 2109-2116.

143. Thomas Wendland, Hansjakob Furrera, Pietro L. Vernazzab, Karin Frutig, Anna Christena, Lukas Matterc, Raffaele Malinvernia, and Werner J. Pichler, "HAART in HIV-infected patients: restoration of antigen-specific CD4 T-cell responses in vitro is correlated with CD4 memory T-cell reconstitution, whereas improvement in delayed type hypersensitivity is related to a decrease in viraemia", *AIDS* **13** (1999): 1857-1862.

144. Evans, T. G., W. Bonnez, H. R. Soucier, T. Fitzgerald, D. C. Gibbons, and R. C. Reichman, "Highly active antiretroviral therapy results in a decrease in CD8+ T cell activation and preferential reconstitution of the peripheral CD4+ T cell population with memory rather than naive cells", *Antiviral Research* **39** (1998): 163-173.

145. Susan Moir, Angela Malaspina, Kisani M. Ogwaro, Eileen T. Donoghue, Claire W. Hallahan, Linda A. Ehler, Shuying Liu, Josepj Adelsberger, Rejean Lapointe, Patrick Hwu, Michael Baseler, Jan M. Orenstein, Tae-WooK Chun, Jo Ann Mican, and Anthony S. Fauci, "HIV-1 induces phenotypic and functional perturbations of B cells in chronically infected individuals", *Proceedings of the National Academy of Sciences USA* **98** (2001): 10362-10367.

146. Susaan Moir, Angela Malaspina, Yuexia Li, Tae-Wook Chun, Tomeka Lowe, Joseph Adelsberger, Michael Baseler, Linda A. Ehler, Shuying Liu, Richard T. Davey, Jr., Jo AnnMican, and Anthony. S. Fauci, " B cells of HIV-1-infected patients bind virions through CD21-complement interactions, and transmit infectious virus to activated T cells", *The Journal of Experimental Medicine* **192** (2000): 637-646.

147. Raquel Tarazona, Javiar G. Casado, Olga Delarosa, J. Torre-Cisneros, Julian L. Villanueva, Berta Sanchez, Maria D. Galiani, Rafael Gonzalez, Rafael Solana, and Jose Pena, "Selective depletion of CD56 (dim) NK cell subsets and maintenance of CD56 (bright) NK cells in treatment-naive HIV-1-seropositive individuals", *The Journal of Clinical Immunology* **22** (2002): 176-183.

148. Jakob Michaelsson, Brian R. Long, Christopher P. Loo, Lanier L. Lanier, Gerald. Spots, Frederick M. Hecht, and Douglas F. Nixon, "Immune reconstitution of CD56 (dim) NK cells in individuals with primary HIV-1 infection treated with interleukin-2", *The Journal of Infectious Diseases* **197** (2008): 117-125.

149. Hans van der Vliet, B. Mary von Blomberg, Mette D. Hazenberg, Nobusuke Nishi, Sigrid A. Otto, Birgit H. van Benthem, Maria Prins, Frans A. Claessen, Alfons J. van den Eertwegh, Giuseppe Giaccone, Frank Miedema, Rik J. Scheper, and Herbert M. Pinedo, " Selective decrease in circulating V alpha 24+V beta 11+ NKT cells during HIV type 1 infection", *The Journal of Immunology* **168** (2002): 1490-1495.

150. Markus Moll, Jennifer Snyder-Cappione, Gerald Spotts, Frederick M. Hecht, Johan K. Sandberg, and Douglas F. Nixon, "Expansion of CD1d-restricted NKT cells in patients with primary HIV-1 infection treated with interleukin-2", *Blood* **107** (2006): 3081-3083.

151. Assia Samri, Ruth Goodall, Catherine Burton, Nesrima Imami, Guiseppe Pantaleo, Anthony Kelleher, Guido Poll, Frances Gotch, Brigitte Autran, "Three-year immune reconstitution in PI-sparing and PI-containing antiretroviral regimens in advanced HIV-1 disease", *Antiviral Therapy* **12** (2007): 553-558.

152. Sharon Shalekoff, Liesl Page-Shipp, and Caroline T. Tiemessen, " Effects of Anticoagulants and Temperature on Expression of Activation Markers CD11b and HLA-DR on Human Leukocytes", *Clinical and Diagnostic Laboratory Immunology* (1998): 695-702.

153. Chihiro Terai, Richard S. Kombuth, C. David Pauza, Douglas D. Richman, and Dennis A. Carson, "Apoptosis as a Mechanism of Cell Death in Cultured T Lymphoblasts Acutely Infected with HIV-1", *The Journal of Clinical Investigation* **87** (1991): 1710-1715.

154. Helen A. Fletcher, "Correlates of Immune Protection from Tuberculosis", *Current Molecular Medicine* **7** (2007): 319-325.

155. Hans-Willi Mittrucker, Ulrich Steinhoff, Anne Kohler, Marion `Krause, Doris Lazar, Peggy Mex, Delia Miekley, and Stefan H. E. Kaufmann, " Poor correlation between BCG vaccination-induced T cell responses and protection against tuberculosis", *Proceedings of the National Academy of Sciences USA* **104** (2007): 12434-12439.

156. Cheryl L. Day, Nompumelelo Mkhwanazi, Sharon Reddy, Zenele Mncube, Mary van der Stok, Paul Klenerman, and Bruce D. Walker, " Detection of Polyfunctional Mycobacterium tuberculosis-Specific T cells and Association with Viral Load in HIV-1-Infected Persons", *The Journal of Infectious Diseases* **197** (2008): 990-999.

157. Marie-lise Deon, Jean-Francois Poulin, Rebeka Bordi, Myriam Sylvestre, Rachel Corsini, Nadia Kettaf, Ali Dalloul, Mohamed-Rachid Boulassel, Patrice Debre, Jean-Peirre Routy, Zvi Grossman, Rafick-Pierre Sekaly, and Remi Cheynier, " HIV Infection Rapidly Induces and Maintains Suppression of Thymocyte Proliferation", *Immunity* **21** (2004): 757-768.

158. Jean Mundahl Engels and Paula Diehr, "Imputation of missing longtitudinal data: a comparison of methods", *Journal of Clinical Epidemiology* **56** (2003): 968-976.

Appendix 1. Representative flow cytometer, calibration report.

4-Color Lyse/Wash FACSComp Report

Institution: SATVI LAB IIDMM
Director: willem
Operator: ronnett

Date: Thu, Oct 6, 2005 3:09 PM
Software: FACSComp 4.2
Cytometer: FACSCalibur E3530

Parameter	High	Low	Separation	Minimum	Result	Lot ID
FSC	163	56	107	70	Pass	09209M
SSC	234	0	234	180	Pass	09209M
FL1	205	62	143	108	Pass	09208M
FL2	210	50	160	135	Pass	09962H
FL3	220	47	173	135	Pass	08665L
FL4	198	132	66	34	Pass	00453O

Parameter	Detector	Amplifier	Threshold
FSC	E00	2.00	52
SSC	446	1.00	
FL1	722	Log	
FL2	612	Log	
FL3	642	Log	
FL4	782	Log	

Blue Laser Current 5.76 Amps
Blue Laser Power 15.00 mWatts

Compensation	FL1-%FL2	FL2-%FL1	FL2-%FL3	FL3-%FL2	FL3-%FL4	FL4-%FL3
	1.2	19.4	0.0	17.8	3.0	2.4

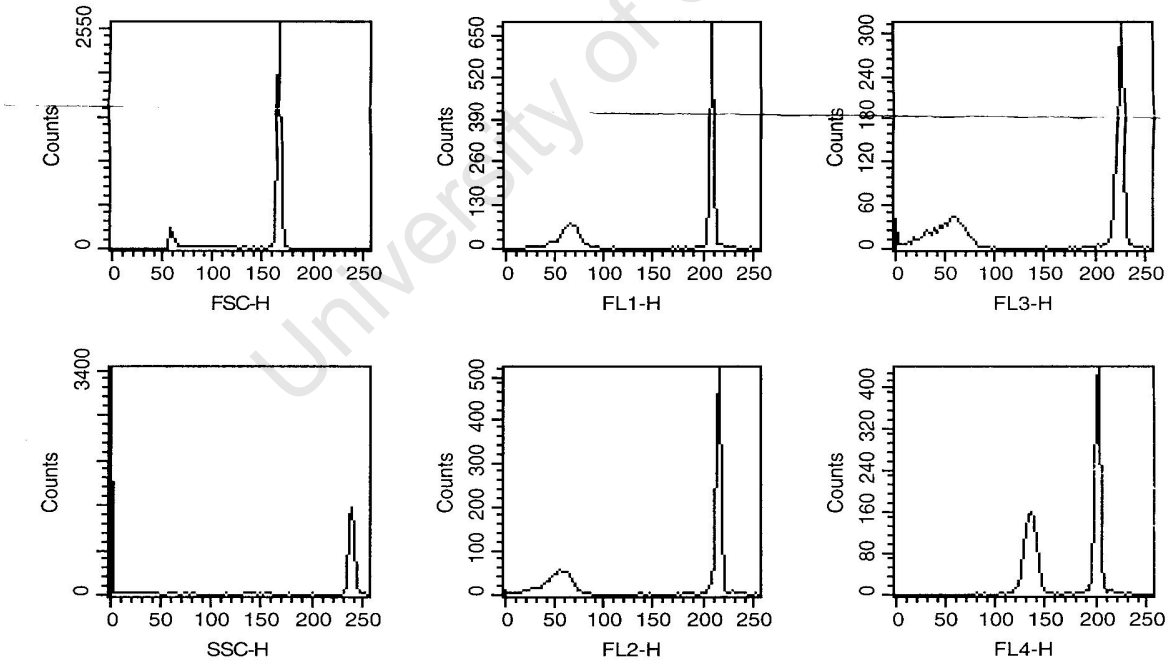

Comments:

Time Delay Calibration Passed.

Appendix 2. Representative report of optomised flow cytometer settings used.

Cytometer Type: FACSCalibur

Detectors/Amps:

Param	Detector	Voltage	AmpGain	Mode
P1	FSC	E00	2.00	Lin
P2	SSC	443	1.00	Lin
P3	FL1	607	1.00	Log
P4	FL2	562	1.00	Log
P5	FL3	575	1.00	Log
P6	FL1-A		1.00	Lin
P7	FL4	650		Log

Threshold:
Primary Parameter: FSC
Value: 52

Secondary Parameter: None

Compensation:
FL1 - 0.3 % FL2
FL2 - 33.8 % FL1
FL2 - 0.0 % FL3
FL3 - 15.8 % FL2
FL3 - 5.8 % FL4
FL4 - 2.1 % FL3

Appendix 3. Individual tables of flow cytometry and ELISpot results.

Table 11. CD4 Counts (cells/µl) (**Figure 7**).

Study number	Week 0	Week 2	Week 4	Week 12	Week 24	Week 36	Week 48
1	141	NA	NA	NA	183	234	209
2	161	NA	NA	NA	302	362	413
3	63	NA	NA	NA	353	NA	302
4	23	NA	NA	NA	295	358	472
5	147	NA	NA	NA	567	418	439
6	22	NA	NA	NA	126	145	270
7	309	NA	NA	NA	356	489	NA
8	93	NA	NA	165	179	NA	293
10	108	NA	154	NA	104	239	232
11	131	NA	360	341	535	NA	552
13	86	212	230	261	295	261	357
14	103	159	178	251	336	NA	323
17	61	NA	NA	160	117	206	162
20	118	132	318	236	248	278	323
21	99	NA	NA	511	194	276	429
22	90	188	148	158	140	121	89
24	11	48	63	107	209	257	253
25	40	NA	41	165	115	126	240
28	3	NA	NA	175	312	330	531

NA= Not available

Table 12. $CD4^+$ T cells (% of PBMC) (**Figure 12**).

Study number	Week 0	Week 2	Week 4	Week 12	Week 24	Week 36	Week 48
1	NA	51	49	NA	38	39	32
2	51	44	60	NA	51	56	49
3	28	34	38	NA	36	NA	43
4	6	3	4	7	14	32	40
5	33	33	41	41	41	39	39
6	8	10	34	7	36	14	15
7	24	20	17	17	17	27	33
8	NA	36	NA	11	31	40	36
10	11	9	14	14	18	14	14
11	23	15	14	21	25	28	30
13	20	17	19	28	28	33	44
14	12	15	17	19	21	NA	15
17	7	17	NA	1	3	3	3
20	13	7	10	11	8	13	12
21	13	21	14	24	27	35	39
22	14	14	12	11	10	8	5
24	1	3	1	3	NA	34	42
25	1	NA	1	2	1	2	2
28	8	6	5	3	4	10	20

Table 13. Naïve $CD4^+$T cells (% of PBMC) (**Figure 14**).

Study number	Week 0	Week 2	Week 4	Week 12	Week 24	Week 36	Week 48
1	8	10	15	NA	22	28	25
2	10	12	16	NA	14	15	15
3	13	21	21	NA	25	NA	29
4	2	6	10	16	15	22	24
5	9	12	11	9	28	33	31
6	2	3	4	5	8	14	15
7	15	13	9	12	23	24	26
8	NA	7	NA	15	10	9	14
10	12	14	13	17	24	29	16
11	9	16	18	15	19	19	20
13	4	6	15	7	12	9	14
14	13	15	15	18	21	NA	19
17	2	21	NA	8	7	8	8
20	14	19	19	14	15	13	11
21	5	8	9	9	9	14	9
22	9	9	9	9	8	7	7
24	3	6	7	10	10	20	20
25	2	NA	6	6	8	8	9
28	0	2	4	8	11	14	18

Table 14. Central memory $CD4^+$T cells, $CD4^+CD27^+CD45RA^-$ (% of PBMC) (**Figure 15A**).

Study number	Week 0	Week 2	Week 4	Week 12	Week 24	Week 36	Week 48
1	NA	38	38	NA	42	50	49
2	16	38	29	NA	35	32	39
3	47	48	32	NA	42	NA	45
4	21	31	31	39	44	41	41
5	41	45	37	40	41	53	51
6	50	47	25	43	46	59	61
7	53	32	65	68	75	67	63
8	NA	46	NA	52	62	48	49
10	49	51	47	49	57	48	41
11	61	53	57	71	64	57	58
13	NA	38	38	NA	42	50	49
14	16	38	29	NA	35	32	39
17	47	48	32	NA	42	NA	45
20	21	31	31	39	44	41	41
21	41	45	37	40	41	53	51
22	50	47	25	43	46	59	61
24	53	32	65	68	75	67	63
25	NA	46	NA	52	62	48	49
28	49	51	47	49	57	48	41

Table 15. Central memory $CD4^+$T cells, $CD4^+CD27^+CCR5^-$ (% of PBMC)(**Figure 15B**).

Study number	Week 0	Week 2	Week 4	Week 12	Week 24	Week 36	Week 48
1	81	87	85	NA	77	80	73
2	84	84	88	NA	80	85	82
3	83	82	64	NA	76	NA	80
4	28	34	36	42	59	59	74
5	86	82	76	75	81	85	77
6	58	53	33	49	76	63	67
7	81	NA	79	85	83	85	90
8	NA	NA	NA	70	86	78	87
10	62	58	56	61	74	37	54
11	78	62	66	88	83	84	86
13	63	49	69	85	71	75	76
14	54	73	78	70	74	NA	69
17	11	55	NA	30	29	35	38
20	45	58	62	67	62	69	70
21	73	79	62	70	75	81	77
22	31	28	28	28	24	22	16
24	16	19	32	58	47	65	71
25	2	NA	13	27	77	19	28
28	6	12	13	24	41	43	62

Table 16. Effector $CD4^+$T cells, $CD4^+CCR5^+$ (% of PBMC) (**Figure 16A**).

Study number	Week 0	Week 2	Week 4	Week 12	Week 24	Week 36	Week 48
1	0	5	3	NA	1	5	5
2	1	6	2	NA	1	1	2
3	1	7	7	NA	1	NA	2
4	2	16	24	14	5	8	2
5	4	5	28	5	4	3	4
6	18	10	29	5	5	7	5
7	4	15	3	2	1	2	2
8	NA	NA	NA	5	1	8	3
10	5	4	3	4	1	1	8
11	6	1	0	3	3	3	1
13	12	23	1	1	6	4	3
14	10	2	2	4	6	NA	5
17	14	9	NA	14	4	6	6
20	11	5	5	3	10	3	5
21	5	5	7	6	5	3	3
22	6	3	4	7	5	5	7
24	13	20	10	30	5	3	1
25	12	NA	22	13	20	18	4
28	7	16	41	14	7	3	2

Table 17. Effector $CD4^+$T cells, $CD4^+CCR7^-CD27^-$ (% of PBMC) (**Figure 16A**).

Study number	Week 0	Week 2	Week 4	Week 12	Week 24	Week 36	Week 48
1	NA	NA	15	NA	24	14	25
2	NA	18	12	20	18	14	18
3	NA	16	25	NA	23	NA	15
4	71	44	62	49	39	30	23
5	13	12	18	17	11	14	20
6	22	32	46	39	23	37	27
7	15	38	16	17	10	13	7
8	NA	30	NA	32	14	21	11
10	35	41	43	36	25	62	46
11	16	32	36	15	15	18	19
13	37	48	30	13	24	22	25
14	43	27	22	25	23	NA	30
17	89	44	NA	65	67	64	61
20	53	37	39	34	37	27	27
21	27	17	41	32	23	16	24
22	68	71	71	70	74	76	82
24	84	74	70	48	99	35	27
25	92	NA	80	70	1	71	72
28	84	73	83	71	63	52	41

Table 18. $CD4^+CD69^+$ T cells, (% of PBMC) (**Figure 18A**).

Study number	Week 0	Week 2	Week 4	Week 12	Week 24	Week 36	Week 48
1	2	NA	NA	12	1	2	NA
2	1	NA	1	10	1	0	2
3	NA	NA	2	NA	2	NA	1
4	NA	NA	1	1	1	3	1
5	NA	1	1	2	1	1	1
6	1	2	18	1	2	4	4
7	2	1	1	1	1	2	1
8	NA	1	NA	1	2	2	2
10	47	3	2	2	1	2	2
11	5	1	2	2	1	1	1
13	4	2	2	2	1	1	2
14	2	2	1	2	1	NA	1
17	3	2	NA	2	2	2	1
20	1	1	1	40	2	1	2
21	2	1	1	1	2	1	4
22	1	3	1	2	1	2	2
24	1	6	1	1	1	1	1
25	4	NA	2	5	NA	12	1
28	9	7	7	5	2	0	5

Table 19. $CD4^+CD45RO^+CD69^+$ T cells (% of PBMC) (**Figure 18B**).

Study number	Week 0	Week 2	Week 4	Week 12	Week 24	Week 36	Week 48
1	NA	NA	NA	NA	9	1	1
2	NA	NA	NA	NA	1	0	2
3	NA	NA	NA	NA	1	NA	1
4	NA	NA	1	1	1	3	1
5	NA	3	2	NA	1	1	1
6	6	4	NA	3	2	3	2
7	2	0	3	3	2	1	1
8	NA	1	NA	1	1	1	1
10	NA	5	2	1	1	2	1
11	4	1	2	2	1	1	1
13	3	2	2	2	3	1	1
14	2	2	1	2	1	NA	1
17	2	2	NA	1	2	1	1
20	1	1	1	34	1	2	2
21	1	0	1	1	2	1	4
22	1	2	1	2	1	4	2
24	1	6	1	0	1	1	1
25	3	NA	2	4	0	12	1
28	NA	5	7	4	2	1	3

Table 20. $CD4^+CD25^+$ T cells, (% of PBMC) (**Figure 19**).

Study number	Week 0	Week 2	Week 4	Week 12	Week 24	Week 36	Week 48
1	NA	NA	NA	NA	9	1	1
2	NA	NA	NA	NA	1	0	2
3	NA	NA	NA	NA	1	NA	1
4	NA	NA	1	1	1	3	1
5	NA	3	2	NA	1	1	1
6	6	4	NA	3	2	3	2
7	2	0	3	3	2	1	1
8	NA	1	NA	1	1	1	1
10	NA	5	2	1	1	2	1
11	4	1	2	2	1	1	1
13	3	2	2	2	3	1	1
14	2	2	1	2	1	NA	1
17	2	2	NA	1	2	1	1
20	1	1	1	34	1	2	2
21	1	0	1	1	2	1	4
22	1	2	1	2	1	4	2
24	1	6	1	0	1	1	1
25	3	NA	2	4	0	12	1
28	NA	5	7	4	2	1	3

Table 21. $CD4^+IFN\text{-}\gamma^+$ T cells, (% of PBMC), (**Figure 20A**).

Study number	Week 0	Week 2	Week 4	Week 12	Week 24	Week 36	Week 48
1	NA	1.2	0.3	NA	0.2	0.1	0.1
2	1.3	0.8	1.0	NA	0.1	0.1	0.2
3	1.4	1.1	0.3	NA	0.2	NA	0.3
4	3.4	0.5	1.8	0.4	1.4	0.7	0.5
5	13.8	1.9	2.9	1.2	0.4	0.7	0.4
6	0.9	1.3	1.7	0.9	2.2	0.5	0.5
7	0.4	1.4	0.7	0.8	0.2	0.1	0.2
8	NA	1.4	NA	0.5	1.6	1.1	1.2
10	0.3	0.8	0.3	0.1	0.1	0.2	0.5
11	0.2	0.2	0.1	0.1	0.2	0.3	0.2
13	0.2	0.2	0.2	0.4	0.4	0.3	0.2
14	0.3	0.3	0.3	0.3	0.6	NA	0.3
17	0.3	1.3	NA	0.6	0.4	0.3	0.5
20	1.4	1.3	2.3	2.7	1.1	0.4	0.3
21	0.5	0.5	0.3	0.3	0.9	0.3	0.4
22	1.3	0.9	0.6	0.8	0.6	0.5	0.4
24	1.1	0.8	0.6	0.3	0.6	0.6	0.7
25	0.9	NA	0.7	2.9	0.1	1.6	1.2
28	1.7	0.7	0.8	0.3	0.3	0.2	0.1

Table 22. $CD4^+IL2^+$ T cells, (% of PBMC) (**Figure 20B**).

Study number	Week 0	Week 2	Week 4	Week 12	Week 24	Week 36	Week 48
1	0.8	1.0	0.3	NA	0.2	0.3	0.3
2	1.2	0.1	0.1	NA	0.1	0.4	0.4
3	0.4	0.4	0.2	NA	0.1	NA	0.2
4	4.7	2.7	2.5	1.9	3.9	1.5	0.4
5	0.6	0.3	0.2	0.5	0.1	NA	0.1
6	1.4	0.4	1.0	1.0	0.7	1.2	0.4
7	0.5	3.4	0.5	0.4	0.1	0.1	0.2
8	NA	1.1	NA	0.4	0.6	0.2	0.1
10	4.3	10.7	0.3	0.2	0.0	0.1	0.2
11	NA	0.1	0.4	0.6	0.2	0.1	0.2
13	0.4	0.3	0.2	0.3	0.2	0.5	0.1
14	0.2	5.6	0.2	0.1	0.3	NA	0.2
17	0.2	1.1	NA	0.1	0.3	0.1	0.2
20	0.3	0.3	1.0	1.0	0.5	0.2	NA
21	0.1	15.0	0.2	0.2	0.2	0.1	0.2
22	NA	NA	13.9	0.2	0.7	0.4	0.1
24	0.4	3.5	0.0	0.2	0.0	0.1	0.3
25	5.0	NA	0.2	1.1	1.1	1.2	0.6
28	0.3	4.8	3.9	0.6	0.3	0.6	0.6

Table 23. $CD4^{+}IL10^{+}$ T cells, (% of PBMC) **(Figure 20C**).

Study number	Week 0	Week 2	Week 4	Week 12	Week 24	Week 36	Week 48
1	NA	1.0	0.3	NA	0.1	0.1	0.5
2	0.3	0.2	0.2	NA	0.2	0.1	0.4
3	0.1	0.3	0.2	NA	0.1	NA	0.2
4	2.2	4.8	2.8	1.4	1.1	0.6	0.5
5	0.4	0.1	0.4	0.3	0.2	NA	0.1
6	0.4	0.1	0.9	1.0	0.1	0.4	0.4
7	0.8	1.6	0.4	0.8	0.1	0.3	0.2
8	NA	1.9	NA	0.3	0.2	0.1	0.1
10	1.9	3.0	0.1	0.1	0.4	0.1	0.4
11	NA	0.6	0.6	0.8	0.1	0.1	0.4
13	0.2	0.4	0.1	1.1	0.5	0.3	0.1
14	0.2	4.7	0.4	0.3	0.4	NA	0.1
17	0.3	0.2	NA	0.1	0.4	0.2	0.2
20	0.2	0.3	0.6	0.1	0.4	0.1	NA
21	0.2	0.2	0.8	0.3	0.2	0.3	0.8
22	NA	NA	0.4	0.5	0.5	0.5	0.9
24	0.4	3.6	0.4	0.3	0.1	0.2	0.3
25	5.7	NA	0.8	0.4	0.6	1.4	0.1
28	0.8	3.2	3.5	3.7	0.6	1.1	0.8

Table 24. $CD4^{+}TNF^{+}$ T cells, (% of PBMC) (**Figure 20D**).

Study number	Week 0	Week 2	Week 4	Week 12	Week 24	Week 36	Week 48
1	NA	1.2	0.1	NA	0.1	0.1	0.1
2	0.0	0.0	0.3	NA	0.1	0.3	0.2
3	0.2	0.1	0.1	NA	0.6	NA	0.1
4	0.0	0.0	0.8	0.5	2.0	1.0	0.6
5	0.6	0.2	0.4	0.3	0.4	NA	0.4
6	0.8	0.8	1.2	1.0	1.5	0.8	0.6
7	0.2	4.5	1.4	1.2	0.1	0.1	0.2
8	NA	1.4	NA	0.5	0.0	0.7	0.7
10	1.8	0.0	0.7	0.0	0.1	0.1	0.1
11	NA	0.1	0.2	0.0	0.1	0.1	0.7
13	0.4	0.3	0.0	1.6	0.2	0.4	0.1
14	0.3	0.7	0.4	0.2	0.1	NA	0.3
17	0.2	2.0	NA	0.3	0.2	0.2	0.2
20	1.1	1.3	2.7	3.5	1.1	0.4	NA
21	0.1	0.2	0.4	0.6	1.0	0.2	0.3
22	NA	NA	0.6	0.2	0.3	0.1	0.3
24	0.2	0.6	0.1	0.4	0.5	0.3	0.7
25	2.0	NA	0.3	3.0	1.7	1.8	1.2
28	2.1	0.1	0.7	0.9	0.1	0.3	0.6

Table 25. $CD8^+$ T cells (% of PBMC), (**Figure 24**).

Study number	Week 0	Week 2	Week 4	Week 12	Week 24	Week 36	Week 48
1	NA	NA	NA	NA	42	26	32
2	NA	NA	NA	NA	63	63	63
3	NA	NA	NA	NA	46	NA	29
4	NA	69	62	50	57	52	45
5	NA	NA	48	41	47	50	56
6	23	14	NA	35	70	45	35
7	43	40	47	49	49	48	45
8	NA	64	NA	40	72	63	65
10	70	68	73	67	56	68	64
11	55	57	51	52	52	56	56
13	49	66	45	66	62	73	53
14	46	61	44	39	64	NA	43
17	16	42	NA	45	42	44	43
20	59	54	57	58	NA	68	64
21	95	71	72	72	NA	61	68
22	56	54	58	61	61	50	48
24	64	55	70	70	64	56	53
25	35	NA	39	39	48	51	66
28	55	43	NA	55	55	51	57

Table 26. B cells $CD3^-CD19^+$ (% of Lymphocytes), (**Figure 26**).

Study number	Week 0	Week 2	Week 4	Week 12	Week 24	Week 36	Week 48
1	NA	NA	NA	NA	9.7	11.4	8.8
2	NA	NA	NA	NA	3.9	3.3	1.5
3	NA	NA	NA	NA	0.7	NA	0.6
4	NA	NA	2.8	0.8	0.5	0.3	0.5
5	NA	6.0	3.9	6.0	5.3	5.4	3.5
6	10.4	15.9	NA	5.3	1.4	2.9	2.7
7	6.6	1.1	1.2	1.5	2.9	2.2	1.9
8	NA	1.2	NA	5.1	3.0	1.6	1.4
10	1.3	0.7	0.6	0.6	1.9	1.1	0.6
11	0.9	1.0	0.5	0.6	0.7	0.7	0.6
13	6.1	6.5	4.7	0.6	1.3	1.3	1.0
14	2.1	3.5	4.5	1.9	1.9	NA	0.7
17	NA	5.5	NA	1.8	0.7	1.4	1.3
20	3.0	2.6	2.6	5.2	NA	5.7	4.6
21	4.6	3.7	2.2	3.0	2.8	3.3	2.3
22	2.4	1.6	2.4	2.4	2.5	3.0	1.9
24	1.5	0.9	0.4	1.2	1.5	1.4	0.8
25	1.6	NA	0.4	0.3	0.5	NA	0.3
28	1.3	1.0	0.5	0.8	0.6	1.0	0.8

Table 27. NK cells $CD3^{-}CD56^{+}$ (% of Lymphocytes), (**Figure 27A**).

Study number	Week 0	Week 2	Week 4	Week 12	Week 24	Week 36	Week 48
1	NA	NA	NA	NA	17	10	17
2	NA	NA	NA	NA	3	2	4
3	NA	NA	NA	NA	9	NA	9
4	NA	NA	11	13	8	5	8
5	NA	9	4	5	4	6	4
6	42	30	NA	18	5	9	3
7	3	2	3	2	3	2	2
8	NA	4	NA	13	6	2	8
10	5	7	7	6	7	8	7
11	9	8	3	17	4	11	12
13	2	2	5	2	1	4	3
14	6	4	6	6	6	NA	9
17	NA	16	NA	21	28	25	18
20	4	3	2	4	NA	3	8
21	3	5	2	2	2	3	1
22	3	2	4	10	11	1	12
24	17	8	3	6	9	11	13
25	2	NA	1	11	12	NA	10
28	27	22	9	6	10	8	4

Table 28. NKT cells $CD3^{+}CD56^{+}$ (% of Lymphocytes), (**Figure 27A**).

Study number	Week 0	Week 2	Week 4	Week 12	Week 24	Week 36	Week 48
1	NA	NA	NA	NA	17	10	17
2	NA	NA	NA	NA	3	2	4
3	NA	NA	NA	NA	9	NA	9
4	NA	NA	11	13	8	5	8
5	NA	9	4	5	4	6	4
6	42	30	NA	18	5	9	3
7	3	2	3	2	3	2	2
8	NA	4	NA	13	6	2	8
10	5	7	7	6	7	8	7
11	9	8	3	17	4	11	12
13	2	2	5	2	1	4	3
14	6	4	6	6	6	NA	9
17	NA	16	NA	21	28	25	18
20	4	3	2	4	NA	3	8
21	3	5	2	2	2	3	1
22	3	2	4	10	11	1	12
24	17	8	3	6	9	11	13
25	2	NA	1	11	12	NA	10
28	27	22	9	6	10	8	4

Table 29. IFN-γ SFC/10^6 PBMC in response to PPD restimulation (**Figure 30**).

Study number	Week 0	Week 2	Week 4	Week 12	Week 24	Week 36	Week 48
1	NA	NA	637	NA	477	NA	13
2	1	NA	7	NA	1	57	68
3	NA	13	22	NA	17	NA	1
4	1	1	277	77	653	447	40
5	73	NA	43	37	90	300	NA
6	7	7	NA	173	237	220	NA
7	1	3	300	227	30	100	60
8	7	NA	NA	210	942	NA	644
10	1	1	3	3	NA	1	69
11	1	17	7	17	NA	10	20
13	97	23	1	139	56	43	NA
14	7	47	33	NA	NA	NA	NA
17	26	335	NA	848	713	NA	NA
20	NA	1	53	828	NA	NA	60
21	7	1096	1122	1508	NA	NA	90
22	1059	1297	624	109	NA	NA	NA
24	NA	NA	620	851	17	571	245
25	NA	NA	50	657	NA	648	7
28	NA	203	83	43	100	NA	250

Table 30. Summed IFN-γ SFC/10^6 PBMC in response to ESAT-6 and CFP-10 restimulation (**Figure 31**).

Study number	Week 0	Week 2	Week 4	Week 12	Week 24	Week 36	Week 48
1	NA	NA	40	NA	157	NA	653
2	127	NA	1427	NA	3	1010	2204
3	NA	1580	607	NA	60	NA	27
4	223	507	1197	493	1273	830	343
5	103	NA	160	70	483	1180	NA
6	20	113	NA	30	680	187	NA
7	1	23	3	13	200	707	573
8	1223	NA	NA	927	847	NA	548
10	147	333	443	470	NA	181	1274
11	1133	1147	960	1120	NA	439	1531
13	553	570	477	950	927	1126	NA
14	147	1087	517	NA	NA	NA	NA
17	20	120	NA	634	488	NA	NA
20	NA	79	406	1095	NA	NA	1519
21	1	422	1069	1360	NA	NA	2054
22	1195	1670	709	852	NA	NA	NA
24	NA	480	208	1029	1426	2237	1793
25	NA	NA	1485	1627	NA	1976	NA
28	NA	797	360	283	367	NA	403

Table 31. IFN-γ SFC/10^6 PBMC in response to ACR1 restimulation (**Figure 33A**).

Study number	Week 0	Week 2	Week 4	Week 12	Week 24	Week 36	Week 48
2	70	0	830	NA	7	173	864
4	170	287	450	210	103	880	83
5	67	NA	113	60	30	93	NA
6	27	20	NA	33	37	20	NA
7	0	10	0	7	25	23	60
10	53	147	40	33	NA	162	1313
11	137	190	60	293	NA	244	1247
13	17	67	33	1000	1261	1023	NA
21	861	1799	551	858	NA	NA	1329
24	NA	NA	934	1238	623	581	497

Table 32. IFN-γ SFC/10^6 PBMC in response to ACR2 restimulation (**Figure 33B**).

Study number	Week 0	Week 2	Week 4	Week 12	Week 24	Week 36	Week 48
2	0	0	797	NA	17	127	1384
4	43	233	953	303	943	1200	57
5	77	NA	73	23	20	283	NA
6	23	63	NA	7	70	157	NA
7	0	0	0	0	5	10	87
10	43	143	27	87	NA	320	2313
11	150	187	110	417	NA	1132	1436
13	3	23	0	1152	1716	941	NA
21	13	323	515	198	NA	NA	443
24	NA	NA	746	865	799	838	577

Table 33. IFN-γ SFC/10^6 PBMC in response to TB10.3 restimulation (**Figure 3**4).

Study number	Week 0	Week 2	Week 4	Week 12	Week 24	Week 36	Week 48
2	27	0	673	NA	10	210	1296
4	103	277	1023	297	707	987	33
5	40	NA	380	33	30	223	NA
6	37	10	NA	13	53	43	NA
7	0	13	3	13	320	17	73
10	33	150	217	67	NA	297	2030
11	233	320	147	323	NA	812	1343
13	60	97	0	1211	201	1363	NA
21	92	125	363	406	NA	NA	716
24	NA	NA	1660	508	813	1498	1387

Appendices